Fall 2009

Synthesis and Physicochemical Characterization of Diamond-Like Semiconductors and Intermetallic Compounds Using High Temperature Solid-State Synthesis, Polychalcogenide Flux Synthesis and the Solid-State Microwave Synthetic Method

Jonathan Lekse

SYNTHESIS AND PHYSICOCHEMICAL CHARACTERIZATION OF DIAMOND-LIKE SEMICONDUCTORS AND INTERMETALLIC COMPOUNDS USING HIGH TEMPERATURE SOLID-STATE SYNTHESIS, POLYCHALCOGENIDE FLUX SYNTHESIS AND THE SOLID-STATE MICROWAVE SYNTHETIC METHOD

A Dissertation

Submitted to the Bayer School of

Natural and Environmental Sciences

Duquesne University

In partial fulfillment of the requirements for

the degree of Doctor of Philosophy

By

Jonathan W. Lekse

December 2009

SYNTHESIS AND PHYSICOCHEMICAL CHARACTERIZATION OF DIAMOND-LIKE SEMICONDUCTORS AND INTERMETALLIC COMPOUNDS USING HIGH TEMPERATURE SOLID-STATE SYNTHESIS, POLYCHALCOGENIDE FLUX SYNTHESIS AND THE SOLID-STATE MICROWAVE SYNTHETIC METHOD

By

Jonathan W. Lekse

Approved September 10, 2009

Jennifer A. Aitken Professor of Chemistry (Dissertation Director)	Jeffry D. Madura Professor of Chemistry (Committee Member)
H. M. “Skip” Kingston Professor of Chemistry (Committee Member)	Charles E. Taylor Division Director NETL (Outside Reader)
David W. Seybert Dean, Bayer School Professor of Chemistry	Jeffry D. Madura Chair, Department of Chemistry Professor of Chemistry

ABSTRACT

SYNTHESIS AND PHYSICOCHEMICAL CHARACTERIZATION OF DIAMOND-LIKE SEMICONDUCTORS AND INTERMETALLIC COMPOUNDS USING HIGH TEMPERATURE SOLID-STATE SYNTHESIS, POLYCHALCOGENIDE FLUX SYNTHESIS AND THE SOLID-STATE MICROWAVE SYNTHETIC METHOD

By

Jonathan W. Lekse

December 2009

Dissertation Supervised by Professor Jennifer A. Aitken

Diamond-like semiconductors are interesting materials to study due to the wide variety of technologically useful properties that these materials possess. These normal valence compounds have structures that are based on that of diamond, either the cubic or hexagonal polymorph. Though there are a finite number of possible compounds, due to isovalent and isoelectronic principles, the total number of potential compounds is quite extensive. Quaternary diamond-like semiconductors provide a unique opportunity, because much of the previous research has focused on binary and ternary systems leaving quaternary systems, relatively unexplored. Additionally, quaternary diamond-like semiconductors possess a greater degree of compositional flexibility compared to binary and ternary materials, which could result in the ability to more carefully tune desired physical properties.

In order to prepare the new materials, Li_2ZnGeS_4, Li_2ZnSnS_4, Li_2CdGeS_4, Li_2CdSnS_4 and Ag_2MnSnS_4, several synthetic methods have been employed, including high-temperature solid-state synthesis, polychalcogenide flux synthesis and solid-state microwave synthesis. The solid-state microwave synthetic method was itself studied using a number of target systems such as the ternary diamond-like semiconductor, $AgInSe_2$. Additionally, several intermetallic compounds, such as Ag_3In, $AuIn_2$ and Bi_2Pd were prepared using this procedure. Solid-state microwave synthesis is not as well known as some of the other synthetic methods that were employed in this work possibly due to a lack of understanding of the method, training and equipment. Despite these problems, the method has the potential to save time, energy and cost due to the unique nature of microwave heating. In an attempt to gain a better understanding of this synthetic method and its capabilities, the solid-state microwave synthetic method was used to prepare diamond-like semiconductors and intermetallic compounds.

ACKNOWLEDGEMENTS

I would first like to thank my family for all of their support. Without them I would never have made it to this point. I would like to thank Amanda Peppler for her endless support and understanding. It is because of you that I want to be a better man. I would also like to thank my advisor, Dr. Jennifer Aitken, for inspiring me to always strive for the best. Thanks also go to my committee for always finding time for me and for supporting me during this experience.

A very special thanks to my friend and labmate, Nathan Takas, for many fruitful, and not so fruitful discussions, and for helping me start out in the lab. Thanks to Jin Lei Yao, Carl Brunetta, Erin Divito and Johanna Burnett for all of their help. I would also be remiss if I did not thank all of the undergraduate and high school students that have contributed to this work; Meghann Moreau, Kate McNerny, Tristan Stagger, Anna Pischera and Beth Leverett. I would also like to thank Christine Mastrovito for always reminding me of my place and helping to keep me almost sane.

I would also like to thank my friends, especially, Chris McClintock, Benjamin Bachman, Joe Mzyanski, John Casale and Christopher Damich. I would also like to thank the friends that I have made within the department, particularly, Dr. Brian Kail, Dr. Paul Kolesar and Rachelle Palchesko. Your support and humor over the years have been invaluable. In addition, I would like to thank Dr. Mitchell Johnson for his sagely advice.

Thanks to Dr. Charles Lake (Indiana University of Pennsylvania) for his assistance with some of the more difficult structures in this work and for helping me to truly understand crystallography. Thank you to Dr. P. Shiv Halasyamani, Dr. Kang Min Ok and Jeongho Yeon (University of Houston) for SHG measurements.

Thank you to the Bayer School of Natural and Environmental Sciences and the National Science Foundation (DMR-06-45304) for funding. The Panalytical X'Pert Pro diffractometer was purchased with funds from the National Science Foundation (DUE-0511444). The Bruker Apex 2 diffractometer was purchased with funds from the National Science Foundation (CRIF-02-34872).

TABLE OF CONTENTS

Page

LIST OF FIGURES

Figure # Page

LIST OF TABLES

Table # Page

1: An Introduction to Diamond-Like Semiconductors

1.1 Introduction

One of the major components of this work involves semiconductors, an integral part of our modern world with numerous applications including communications, computing, medicine, transportation, and many others. The advance of technology can be carried out in several ways; new applications can be found for existing materials, existing materials can be enhanced and/or used in new ways or new materials with improved, and potentially undiscovered properties, can be prepared and characterized. In order to pursue this last option, it is a good idea to have a starting point. Beginning with a type of semiconductors that sees a wide variety of applications would be an ideal launching pad for future research. A careful examination of the literature shows that one class of semiconductors that has found a wide variety of uses are those known as diamond-like semiconductors (DLS).

1.2 Normal Valence Compounds

DLS are normal valence compounds that have structures based upon either the cubic or hexagonal forms of diamond.[1,2] They are known as normal valence compounds because the elements will accept, donate and/or share electrons to obtain an octet. The bonding in these cases can range from ionic to covalent or somewhere in between. The degree to which a bond is considered ionic can be determined by the differences in the

electronegativities of the atoms participating in the bond. In addition to being normal valence compounds, DLS abide by a set of four rules.

1.3 Rules for Diamond-Like Semiconductors

The rules for DLS can be broken down into two categories. The first two rules can be thought of as the valence electron rules and the final two rules are based on Linus Pauling's influential paper detailing rules for bonding in crystalline solids.[4] The first rule is that the average valence electron concentration must equal four. For example, let us take the compound Cu_2CdGeS_4, it has 2 copper atoms, each with 1 valence electron, one cadmium atom with 2 valence electrons, one germanium atom with 4 valence electrons and four sulfur atoms, each with 6 valence electrons. When summed, there are a total of 32 valence electrons in one formula unit. The number of electrons is then divided by the total number of atoms per formula unit (8) to yield an average of 4 electrons per atom. This rule can be generalized for each type of DLS, below is the formula for a binary compound:

$$\text{Average Number of Valence Electrons} = (ve_{cation}+ve_{anion})/(n_{cation}+n_{anion})$$

Where ve_{cation} and ve_{anion} are the number of valence electrons per cation and anion, respectively and n_{cation} and n_{anion} are the number of cations and anions in the formula unit.

The second rule is that the average valence electron concentration per anion must equal eight. If we again use Cu_2CdGeS_4 as an example, we have 32 valence electrons and 4 anions. Division results in 8 electrons per anion. Similarly to the first rule, we can generalize this rule for each type of DLS. An example for a binary compound follows:

$$\text{Valence Electrons per Anion} = (ve_{cation}+ve_{anion})/(n_{anion})$$

It also follows from this rule, that each compound must have an equal number of cations and anions.

During his career, Pauling was greatly interested in the bonding between atoms.[3] Early in his life this led him to study crystallography and crystal structures. After years of research, he developed a set of rules to explain the trends in the known crystal structures of the time and to assist in the determination of structures in the future.[4] The first of his rules also happens to be the third rule for diamond-like semiconductors. This rule states that the coordination sphere of the ions in an ionic compound can be determined by the ratio of the radius of the cation to the radius of the anion. This is due to a coordination sphere becoming unstable if the geometry and the size of the cation are such that the anions come into close proximity and/or touch. This results in stable ratio ranges for each geometry, such as tetrahedron, octahedron and cube, that are listed in Pauling's paper.[4]

In diamond, the carbon atoms are tetrahedrally coordinated, so it follows that the atoms in a diamond-like semiconductor should also have this coordination geometry. Based upon Pauling's paper, the radius ratio should fall between 0.225 and 0.414, in order for an ion to have tetrahedral coordination. Some of the compounds in this work have crystal structures that have been solved and whose ions exhibit tetrahedral coordination despite having ratios that lie slightly outside of Pauling's range. This is due to the fact that there can be deviation from this rule especially in the presence of "soft" anions where the bonding has a greater covalent character and deviates from purely ionic bonds. One must remember that Pauling devised his rules based on the crystal structures known at the time, which included primarily oxides and highly ionic compounds.

The fourth and final rule that diamond-like semiconductors must obey is Pauling's second rule.[4] This rule is also known as the electrostatic valence sum rule and there are two ways in which to describe this rule. The first approach states that the cations will be arranged so that the octet of each anion is satisfied by the cations in the local coordination sphere. The second view is to examine the electrostatic charges. Whether or not a compound will follow this rule can be calculated in this approach by first defininig a valence bond (s) as:

$$s = z/v$$

where z is the charge of a cation and v is its coordination number. The electrostatic valence principle then postulates that in a stable coordination structure, the electric charge of each anion tends to compensate the strength of these electrostatic valence bonds. Thus we can sum all of the valence bonds, ζ, to an anion and it should equal the charge of that particular anion, as expressed below:

$$\zeta = \Sigma_i s_i = \Sigma_i z_i/v_i$$

It is important to observe that Pauling notes that not all compounds will rigorously satisfy this rule; but, as of the writing of his paper, most compounds satisfied this condition. Since the publication of his rules, new compounds have been synthesized and been found to deviate from Pauling's second rule. In these compounds, when the charge of the anion does not compensate for the electrostatic valence bonds, the structure is distorted in some way. The distortion is normally a contraction or elongation of bonds. If the anion charge is greater than the electrostatic valence bonds, then it will attracted the cations around it closer and if the anion charge is smaller than the electrostatic bonds, then the cations will

repel one another and be pushed further from the anion. This will result in distortions in a structure that deviates from this rule.

1.4 Structure

In both forms of diamond, every carbon atom is tetrahedrally coordinated to four other carbon atoms. In order to obtain a DLS, one could imagine performing an ordered substitution of a cation for half of the carbon atoms and an anion for the other half, such that each cation is coordinated to four anions and so on. These cationic and anionic substitutions should follow the four rules for DLS. Further substitutions can then be made on either the cationic or anionic sites resulting in ternary and quaternary compounds, Figure 1. These substitutions are limited, and due to the restrictions placed upon DLS by the rules stated above, the possible formulae are limited as well, Table 1. Though limited, the number of possible compounds is large enough that there is still a lot of room for exploration.

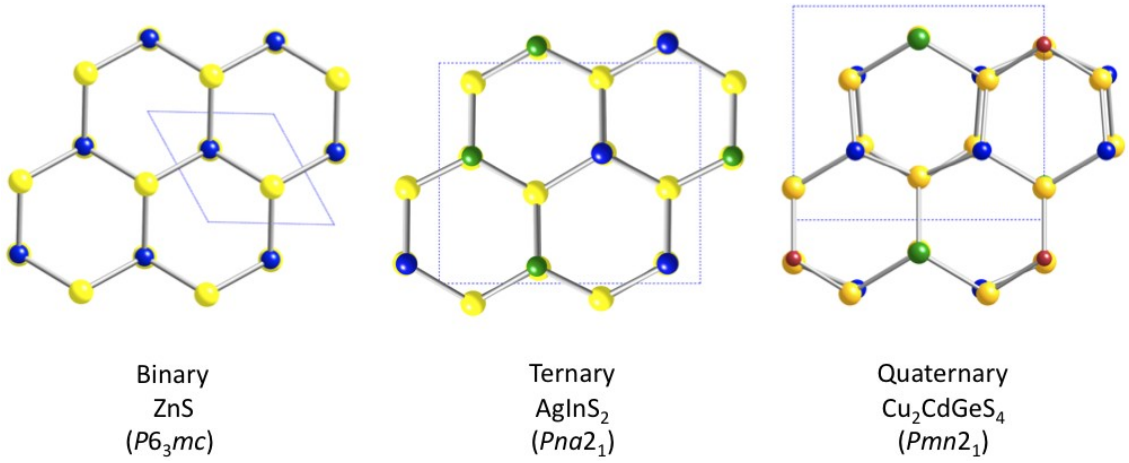

Figure 1.1. Structural progression beginning with binary ZnS and moving through ternary compounds, such as $AgInS_2$, to quaternary compounds represented by Cu_2CdGeS_4.

Table 1. Formulae for DLS compounds. The compounds in this work fall into two categories, denoted in red.

Binary	Ternary (1 cation)	Ternary (2 cations)	Quaternary (2 cations)	Quaternary (3 cations)
17	3_3427	14_253	1456	134_254
26	3_246	245_2	2356	23_245_4
35	2_257	136_2	2347	12_236_4
44	2_347_2	1_246_3	1357	1_2246_4
	2_437_3	1_356_4	1267	

1.5 Previous Research

Much of the previous research has focused on binary DLS. For example, there have been numerous studies with CdS,[5] particularly nanoparticles of CdS,[6,7] which are known as quantum dots and can be used for a variety of applications, including the tagging of biomolecules.[8,9] These compounds are normally quite thermodynamically stable and as a result are normally relatively easy to synthesize. There has also been a sizeable amount of research performed on several ternary DLS. Some of the more well-known ternary DLS are $CuInSe_2$, $CuGaSe_2$, $CuInS_2$, and $CuGaS_2$. [10] Solid solutions of these compounds are among the best photovoltaic materials known.[11]

There has been less focus on quaternary DLS, most likely due to the difficulty involved in the synthesis of these compounds. Early work was performed with copper-containing compounds because they are found as naturally occurring minerals. One particularly well known compound is stannite, Cu_2FeSnS_4.[12] The structure of stannite is derived from sphalerite; however, due to the substitutions on the cationic site, the symmetry of the system is reduced, resulting in a new structure type, which was termed stannite. This compound led researchers to experiment with other copper-containing compounds, such as Cu_2CdGeS_4.[13] It was discovered that Cu_2CdGeS_4 was a new structure type related to stannite, but with a structure derived from wurtzite instead of sphalerite. In 1974, a several new quaternary DLS compounds with this structure type were synthesized and the structure type was named wurtz-stannite.[14] Most of this early research focused on synthesis of new compounds and structural characterization, but few property measurements. The structural studies typically used powder data. Researchers

refined the crystal structure from powder data for a single compound and then refined the unit cell parameters for the rest of the compounds in the study.[15,16]

Following the 1960s, there are a few scattered reports of quaternary compounds such as the report of 20 new compounds of the formula Cu_2-II-IV-S_4(Se_4) (with II=Mn, Fe, Co, Ni, Zn, Cd, Hg and IV=Si, Ge, Sn) in 1974.[17] This general formula results in a total of 42 compounds, of which 22 were previously known. The remaining compounds were synthesized and their structure determined. All of the compounds fell into one of three structure types; stannite, wurtz-stannite or a new structure type based on a sphalerite-sized cell with either tetragonal, orthorhombic or monoclinic symmetry. There were also studies of Cu_2ZnGeS_4 performed in the 1980s. The first study focused on the structure of two polymorphs of Cu_2ZnGeS_4,[18] the compound was found to crystallize in either a pseudo-rhombohedral or tetragonal (stannite) structure depending on the heat treatment. For the second study, researchers doped the compound with manganese on the zinc site and studied the subsequent magnetic properties, specifically an anti-ferromagnetic interaction.[19] This was followed by the study of the magnetic properties of Ag_2MnGeS_4, which is important for a number of reasons, first the compound is a ferromagnetic semiconductor with a T_c = 64 K and second this is one of the first reports of a non-copper containing quaternary DLS.[20] In the mid-to-late 1990s, the interest in quaternary DLS and the subsequent research began to increase.

Through the late 1990s and early 2000s, a number of systems were more thoroughly studied including quaternary copper-containing selenides that had previously been reported,[17] such as $Cu_2FeSnSe_4$[21] and $Cu_2CoGeSe_4$,[22] magnetic measurements of Cu_2MnSnS_4[23] and new silver-containing compounds, such as Ag_2CdSnS_4[24,25] and

Ag_2CdGeS_4.[26] There have also been two reports of quaternary compounds that contain lithium as the 1^+ cation.[27,28] One of the reports was a study of the lithium-germanium-sulfide system looking for ionic conductors. During the research, several new compounds were discovered including the quaternary, DLS Li_2ZnGeS_4.[28] The primary focus of the paper was ionic conductivity, not a structural study, as a result, powder diffraction was used only to determine the crystal system, orthorhombic, and lattice parameters; a=7.83 Å, b=6.53 Å and c=6.21 Å. The second report describes the synthesis of three new sulfides, one of which follow the rules for DLS, Li_2CdSnS_4.[27] This report contains numerous questionable conclusions in the structural studies as well as in the band gap energy measurements. For example, Li_2CdSnS_4 is reported to be a layered compound with disorder between cationic sites, which should not occur in a true DLS, because disorder would lead to violations of Pauling's second rule. Additionally, there was no band gap observed in the optical absorption spectrum of Li_2CdSnS_4; despite the fact that the compound is a yellow color, which indicates a band gap in the visible region. Neither study of the lithium-containing compounds contained detailed physical property analysis, for example second harmonic generation response. The small number of known lithium-containing DLS combined with the minimal property measurements that have been performed, provide a great opportunity for additional research.

In addition to the small amount of research that has been performed on these compounds, there is another reason to study quaternary DLS. This is the additional compositional flexibility that could potentially allow for a greater ability to tune the physical properties of these materials. There are several areas that are of interest to this

work including photovoltaics and spin-based electronics; but, the greatest emphasis has been placed on non-linear optics.

1.6 Properties

1.6.1 Photovoltaics

Over the past 50 years, photovoltaics have been well established for supplying power in remote locations, powering small electronic devices such as calculators and for a variety of space vehicles and satellites.[29] Currently photovoltaic cells are being used for other applications such as large scale power generation in either power stations or in 'building integrated photovoltaics.'[29] Crystalline silicon has been the basis for this industry for much of its past; however, there are new materials that have come to rival silicon in one of two areas; cost of production and efficiency. Thin films of some ternary DLS and III-V binary DLS have band gap energies that lie close to the optimum band gap energy for solar energy conversion, 1.5 eV.[29,30] There are two primary goals with new photovoltaic materials. The first is to keep production costs to 1 $/peak Watt in order to keep costs competitive with other forms of power generation.[29] The second goal is to have acceptable energy payback times. In other words, how long will it take the device to produce the amount of energy that was consumed during production of the device.[29]

Chalcopyrite-based devices offer an interesting alternative to silicon devices. The first chalcopyrite solar cells were created using $CuInSe_2$ (CIS), which has a band gap of 0.96 eV.[31] It was then discovered that the band gap of the material could be widened, to 1.3 eV, by doping with Ga resulting in a solid solution with the general formula

$Cu(In,Ga)Se_2$ (CIGS). The wider gap of these materials and an improvement in material quality improved the efficiencies of these devices. The efficiencies of these devices reach 19.5%,[32] while crystalline silicon devices have reported efficiencies of 24.7%.[33] The advantage of CIGS comes in the high optical absorption coefficient for photons with energies greater than the band gap energy. Additionally, silicon has an indirect band gap, while CIGS have a direct gap, another property of ideal photovoltaic materials. This allows devices to consist of a very thin layer of material, which cuts production costs.

Other DLS need to be studied to determine if they posses similar or better efficiencies than existing compounds. One advantage that quaternary compounds posses is their compositional flexibility. This would be extremely valuable for tuning of the band gap energy.

1.6.2 Spintronics

In the 1970s electronic micro-processors and resistors were combined on an integrated circuit in a semiconductor chip. Since then the number of transistors and resistors that each chip possesses has increased dramatically. Moore's Law states that the number of resistors and transistors per unit area will double every 18 to 24 months.[34] The increasing number of resistors and transistors per unit area means that each individual transistor must become smaller and smaller. However, there are two obstacles to this continued advancement. The first obstacle is that though transistors continue to shrink, they can never become smaller than a single atom.[35] The second obstacle is Joule heating. Joule heating occurs when a current passes through any device.[35] The device has an inherent resistance that will result in energy losses to heat.

The solution to both obstacles may lie in the electron's spin. Over eighty years ago Paul A.M. Dirac combined the theories of quantum mechanics and relativity to establish relativistic quantum mechanics. One consequence of this theory is that an electron possesses an intrinsic angular momentum that is called spin. Current electronic devices completely ignore this quantity.[36] If this property could be exploited, it could lead to a new generation of devices.

There are three important processes for spintronics: spin generation, transport and detection.[37] Initially, ferromagnetic metals were used as sources of polarized spins. The problem with using metals occurs when the electrons are transferred to semiconductors. The large differences between the resistances of the metals and the semiconductors result in very low efficiencies for spin injection.[37,38] The efficiency of the spin injection process may be increased, if the spin generating material were a ferromagnetic semiconductor.[39]

One way to prepare ferromagnetic semiconductors is to dope a small amount of a magnetic ion, such as Mn^{2+}, into an otherwise non-ferromagnetic semiconductor. These materials are known as dilute magnetic semiconductors (DMS).[40] To date, the most popular and successful DMS is Mn-doped GaAs with a Curie temperature of 173 K.[41,42,43,44] GaN and ZnO have also been studied extensively due to the theoretical predictions of ferromagnetism above room temperature.[45] The second alternative is to incorporate the magnetic ion into the compound instead of doping. One particular possibility is to pursue quaternary DLS of the I_2-II-IV-VI_4 formula, where Mn or Fe are the II metal.

1.6.3 Non-Linear Optics

Non-linear optics began in 1961, when a quartz crystal was illuminated using a laser and observed to double the frequency of the incident light.[46] This phenomenon was descriptively named second harmonic generation (SHG) and was the birth of the field of nonlinear optics (NLO). Frequency doubling occurs when two incident photons are combined while passing through a medium. The energy of the resulting photon is double that of either incident photons and as a result has double the frequency. This can occur in a variety of orientations which leads to different polarizations for the exiting photons. The polarization of the exiting photons with respect to the incident photons determines the type of phase matchability of the material.

Since this discovery, scientists have been finding uses for NLO materials in a variety of applications including spectroscopy, laser medicine and others.[47] Applications for NLO materials can be organized in regions of the electromagnetic spectrum. Of the known materials, $KTiOPO_4$ (KTP),[48] $LiNbO_3$[49,50,51] and LiB_3O_5 (LBO)[52] have found uses in either the ultraviolet or visible regions of the electromagnetic spectrum. Diamond-like compounds have instead found uses in the IR region. These materials include $AgGaS_2$,[53,54,55] $CuGaS_2$[56] and $AgGaSe_2$.[57] The metal-chalcogen bonds in these materials typically lead to larger nonlinear optical responses due to their highly polarizable nature. Despite the promising nonlinear optical properties of these materials, these compounds are limited in their applications, due to low laser damage thresholds resulting from their small band gap energies.[56]

1.7 Synthesis

Quaternary diamond-like semiconductors can prove more difficult to synthesize than binary and ternary compounds. It is sometimes necessary to use multiple synthetic methods to obtain both single crystals for structural studies and phase-pure powders for property measurements. In order to obtain both for the materials in this work, several different synthetic strategies have been employed. These include high-temperature solid-state synthesis, polychalcogenide flux synthesis and solid-state microwave synthesis.

1.7.1 High-Temperature Solid-State Synthesis

The first synthetic method that was used is traditional, high-temperature solid-state synthesis. This method involves grinding the reagents in an argon-filled glovebox, sealing the reaction mixture in a fused-silica tube, and heating the tube in a furnace. The primary synthetic variables of this method are temperature, dwell times, and cooling rates. These variables can normally be optimized for the synthesis of either single crystals or phase-pure powders. For most syntheses the temperature needs to be carefully selected. Using a temperature that is too low can be detrimental to the synthesis of these quaternary compounds as there will be insufficient energy to result in complete reaction of the starting materials. Conversely, using a temperature that is too high can result in the synthesis of the most thermodynamically stable phases, which are typically binary compounds, instead of the desired quaternary phases, i.e. phase separation.

1.7.2 Polychalcogenide Flux Synthesis

The second synthetic method used is a polychalcogenide, specifically a lithium-polysulfide, flux, which is a type of molten salt flux. Molten salt syntheses have been used for over 100 years as a recrystallization and reaction medium.[58,59,60] This synthetic method utilizes an excess of a low melting component in the reactionto act like a solution. The flux, usually formed *in-situ*, assists the synthesis of extended structures in two ways. The first way is to enhance diffusion of the reactants.[58] The diffusion of reactants is one of the most difficult energetic barriers to be overcome in order to synthesize solid-state compounds. The energetic barrier to diffusion is typically large, requiring a great deal of energy in order to be overcome. Traditionally the barrier has been overcome by using a very high reaction temperature. Flux reactions provide a way to lower the activation barrier by enhancing diffusion. The end result is that lower reaction temperatures can be used and lower reaction temperatures provide the opportunity to obtain not only less thermodynamically stable but also metastable phases. The second advantage of this synthetic method is the mineralizing effect provided by the flux.[58] A mineralizing effect is loosely defined as something that helps to either solubilize the reagents or aids in crystal growth, of course a mineralizing agent could also aid in both.

The extension of the molten salt flux method to include a polychalcogenide reactants has been instrumental in the discovery of several new chalcogenides and was first developed due to the technological importance of several metal chalcogenide compounds.[60] Polychalcogenide and metal chalcogenide materials have been used for

applications such as the hydrodesulfurization of crude oil,[61,62,63] nonlinear optics,[64,65,66,67] photoconductivity,[68,69,70] and battery materials.[71,72,73]

The particular flux that was used for this work was a lithium polysulfide flux, which was formed from Li_2S and S. While the exact composition of the flux during heating is not well characterized, there are several ideas that are supported by the results of these reactions. Polychalcogenides are known to form chains, identified as $(Q_x)^{2-}$ where Q is the chalcogen, that can undergo complex oxidation/reduction reactions in solution.[58] It is reasonable to assume that these reactions will also occur in the molten flux state. The end members of these chains have a formal oxidation state of -1, while the internal atoms are zero valent. This combination of valence states makes these chains very reactive towards metals. Metal atoms are oxidized by the internal atoms of the chains, resulting in the now metal ion moving into the solution. This also breaks the chains into smaller fragments. The solubilized metal ions can then form an intermediate with the basic chains to form a site for crystal nucleation to occur.[58]

The chains are basic in nature with the pH of a given flux determined by the chain length. The shorter a chain is the more basic, and less oxidizing, the flux becomes. Therefore, increasing the amount of chalcogen will in effect dilute the basicity of the flux, increasing the acidity and resulting in a more oxidizing medium. Manipulating the composition of the flux is thus vital to obtaining the desired phases from flux syntheses by controlling the chalcogen salt to chalcogen ratio, Li_2S:S in this work, we can control the products of flux syntheses.

1.7.3 Solid-State Microwave Synthesis

The third synthetic method that was employed is solid-state microwave synthesis. This method was used for the synthesis of ternary DLS as well as a variety of other materials and will be discussed in greater detail in chapter 2.

1.8 Conclusion

We identified diamond-like semiconductors as a promising family of materials to study for numerous potential applications. The scope of this work was narrowed to focus of ternary and quaternary compounds with the general formulae, I-III-VI_2 and I_2-II-IV-VI_4. In the ternary system we turn our focus to the known compound $AgInSe_2$. Several new quaternary compounds were targeted with I=Li or Ag, II=Zn, Cd or Mn, IV=Sn or Ge and VI=S. In order to synthesize known and new compounds we decided to make use of three distinct synthetic techniques that will provide paths to these materials. Due to the current applications and interesting properties of related DLS, the new compounds will be thoroughly characterized to determine their potential for incorporation into real-world device applications.

1.9 References

[1] N.A. Goryunova *The Chemistry of Diamond-Like Semiconductors*; J.C. Anderson ed.; The MIT Press: Cambridge, U.K. 1965.

[2] E. Parthé *Crystal Chemistry of Tetrahedral Structures*, Gordon and Breach Science Publishers: New York, 1964.

[3] T. Goertzel, B. Goertzel *Linus Pauling: A Life in Science and Politics*, Basic Books: New York, 1996

[4] L. Pauling *J. Am. Chem. Soc.* **1929**, *51*, 1010.

[5] B. Ray, J.W. Brightwell, R.A. Herring, I.V.F. Viney *Lumin.: Phenom. Mater., Devices, [CECRI Res. Conf.], 3rd*, **1992**, 155.

[6] I. Willner, B. Willner *Pure and Applied Chemistry*, **2002**, *74*, 1773.

[7] W. Li, I. Shah *Encyclopedia of Nanoscience and Nanotechnology*, **2004**, *9*, 669.

[8] J. Netterwald *Drug Discovery & Development*, **2008**, *11*, 20.

[9] Q. Ma, C. Wang, X. Su *J. Nanosci. Nanotechno.* **2008**, *8*, 1138.

[10] H. Hahn, G. Frank, W. Klingler, A.D. Meyer, G. Stoeger *Z. Anorg. Allg. Chem.* **1953**, *271*, 153.

[11] A. Goetzberger, C. Hebling, H.-W. Schock *Mater. Sci. Eng.* **2003**, *R40*, 1.

[12] L.O. Brockway *Z. Kristallogr. Krist.* **1934**, *89*, 434.

[13] E. Parthé, K. Yvon, R.H. Dietch *Acta Crystallogr., Sect. B* **1969**, *25*, 1164.

[14] W. Schäfer, R. Nitsche *Mater. Res. Bull.* **1974**, *9*, 645.

[15] E. Parthé, K. Yvon, R.H. Dietch *Acta Crystallogr., Sect. B* **1969**, *25*, 1164.

[16] R. Kanno, T. Hata, Y. Kawamoto, M. Irie *Solid State Ionics* **2000**, *130*, 97.

[17] W. Schäfer, R. Nitsche *Mater. Res. Bull.* **1974**, *9*, 645.

[18] A.F. Moodie, H.J. Whitfield *Acta Crys. B* **1986**, *B42*, 236.

[19] Y. Shapira, E.J. McNiff Jr., N.F. Illivera Jr., E.D. Honig, K. Dwight, A. Wold *Phys. Rev. B* **1988**, *B37*, 411.

[20] M. Quintero, A. Willsher, J.C. Woolley, *J. Magn. Magn. Mater.* **1990**, *89*, 185.

[21] Infante, E. Roque, J.M. Delgado, Rivera, S.A. Lopez *Mater. Lett.* **1997**, *33*, 67.

[22] L.D. Gulay, O.P. Nazarchuk, I.D. Olekseyuk *J. Alloy Compd.* **2002**, *334*, 143.

[23] T. Fries, Y. Shapira, F. Palacio, C.M. Moron, G.J. McIntyre, R. Kersgaw, A. Wold, E.J. Mcniff Jr. *Phys. Rev. B* **1997**, *56*, 5424.

[24] O.V. Parasyuk, L.V. Piskach *Polish J. Chem.* **1998**, *72*, 966.

[25] O.V. Parasyuk, L.V. Olekseyuk, S.V. Volkov, V.I. Pakhnyo *J. Alloy Compd.* **2005**, *399*, 173.

[26] O.V. Parasyuk, L.V. Piskach, I.D. Olekseyuk, V.I. Pekhnyo *J. Alloy Compd.* **2005**, *397*, 95.

[27] M.S. Devi, K. Vidyasagar *J. Chem. Soc., Daltron Trans.* **2002**, *9*, 2092.

[28] R. Kanno, T. Hata, Y. Kawamoto, M. Irie *Solid State Ionics* **2000**, *130*, 97.

[29] R.W. Miles, G. Zoppi, I. Forbes *Mater. Today* **2007**, *10*, 20.

[30] L.D. Partain *Solar Cells and Their Applications* John Wiley & Sons: Hoboken, 1995.

[31] J.L. Shay, B. Tell, H.M. Kasper, L.M. Shiavone *Phys. Rev. B* **1973**, *7*, 4485.

[32] M.A. Contreras *Prog. Photovolt. Res. Appl.* **2005**, *13*, 209.

[33] J. Zhao *Appl. Phys. Lett.* **1998**, *73*, 1991.

[34] G.E. Moore *Electronics* **1965**, *38*, 4.

[35] S.-Q. Shen *AAPPS Bull.* **2008**, *18*, 29.

[36] M. Ziese, M.J. Thornton *Spin Electronics*, Springer-Verlag: Berlin, 2001.

[37] I. Žutić, J. Fabian, S. Das Sarma *Rev. Mod. Phys.* **2004**, *76*, 323.

[38] G. Schmidt, L.W. Molenkamp *Semicond. Sci. Technol*. **2002**, *17*, 310.

[39] D. Wu, Q.Y. Xu, F.M. Zhang, X.S. Liu, Y.W. Du *AAPS Bull.* **2008**, *18*, 52.

[40] H. Ohno *Science*, **1998**, *281*, 951.

[41] T. Jungwirth, K.Y. Wang, J. Mašek, K.W. Edmonds, J. König, J. Sinova, M. Polini, N.A. Goncharuk, A.H. MacDonald, M. Sawicki, A.W. Rushforth, R.P. Campion, L.X. Zhao, C.T. Foxon, B.L. Gallagher *Phys. Rev.* **2004**, *B72*, 165204.

[42] Y. Ohno, D.K. Young, B. Beschoten, F. Matsukura, H. Ohno, D.D. Awschalom *Nature* **1999**, *402*, 790.

[43] H.X. Tang, R.K. Kawakami, D.D. Awschalom, M.L. Roukes *Phys. Rev. Lett.* **2003**, *90*, 107201.

[44] R. Mattana, J.-M. George, H. Jaffrès, F. Nguyen Van Dau, A. Fert *Phys. Rev. Lett.* **2003**, *90*, 166601.

[45] T. Dietl, H. Ohno, F. Matsukura, J. Cibert, D. Ferrand *Science* **2000**, *287*, 1019.

[46] P.A. Franken, A.E. Hill, C.W. Peters, G. Weinrich *Phys. Rev. Lett.* **1961**. *7*, 118.

[47] Y. Kim, S.W. Martin, K.M. Ok, P.S. Halasyamani *Chem. Mater.* **2005**. *17*, 2046.

[48] K. Kato *IEEE J. Quantum Electron.* **1991**, *27*, 1137.

[49] R.C. Miller, W.A. Nordland *Phys. Rev.* **1970**, *B2*, 4896.

[50] S.J. Brosnan, R.L. Byer *IEEE J. Quantum Electron.* **1979**, *15*, 415.

[51] V.G. Dmitriev, G.G. Gurzadyan, D.N. Nikogosyan *Handbook of Nonlinear Optical Crystals*, Springer: New York, 1999.

[52] C. Chen, Y. Wu *J. Opt. Soc. Am.* **1989**, *B6*, 616.

[53] W. Ruderman, J. Maffetone, D. Zelman, D. Poirier *Mater. Res. Soc. Symp. Proc.* **1998**, *484*, 519.

[54] G.C. Bhar, R.C. Smith *Phys. Status Solidi* **1972**, *13*, 157.

[55] D.S. Chemla, P.J. Kupecek, D.S. Robertson, R.C. Smith *Opt. Commun.* **1971**, *3*, 29.

[56] A.G. Jackson, M.C. Ohmer, S.R. LeClair *Infrared Phys. Technol.* **1997**, *38*, 233.

[57] G.C. Catella, D Burlage *MRS Bull.* **1998**, *23*, 28.

[58] M. G. Kanatzidis, A.C. Sutorik *Prog. Inorg. Chem. Vol. 43*, K.D. Karlin, ed., John Wiley & Sons, Inc.:Hoboken, 1995.

[59] D. Elwell, H.J. Scheel *Crystal Growth from High-Temperature Solutions*, Academic: New York, 1975.

[60] H.J. Scheel *J. Cryst. Growth* **1974**, *24/25*, 669.

[61] R.R. Chianelli, T.A. Pecoraro, T.R. Halbert, W.-H. Pan, E.I. Stiefel *J. Catal.* **1984**, *86*, 226.

[62] T.A. Pecoraro, R.R. Chianelli *J. Catal.* **1981**, *67*, 430.

[63] S. Harris, R.R. Chianelli *J. Catal.* **1984**, *86*, 400.

[64] H. Eckert *Angew. Chem. Int. Ed. Engl.* **1989**, *28*, 1723.

[65] R. Zallen *Physics of Amorphous Solids* Wiley: New York, 1983.

[66] D. Strand, D. Adler *Proc. SPIE Int. Soc. Opt. Eng.* **1983**, *420*, 200.

[67] N. Yamada, N. Ohno, N. Akahira, K. Nishiuchi, K. Nagata, M. Takeo *Proc. Int. Symp. Opt. Memory 1987, J. Appl. Phys.* **1987**, *26 (Suppl. 26-4)*, 61.

[68] J.H. Armstrong, C.O. Pistole, M.S. Misra, V.K. Kapur, B.S. Basol *Space Photovoltaics Research and Technology 1991*, NASA Conference Publication 3121, NASA: Washington, D.C., 1991.

[69] K. Zweibel *Basic Photovoltaic Principles and Methods* Van Nostrand-Reinhold: New York, 1984.

[70] H.J. Möller *Semiconductors for Solar Cells*, Artech House: Boston, 1993.

[71] M.S. Whittingham *Solid State Ionic Devices July 18-23 1988 Singpore* B.V.R. Chowdari and S. Radhakrishna, eds., World Scientific: Singapore, 1988.

[72] W.L. Bowen, L.H. Burnette, D.L. DeMuth *J. Electrochem. Soc.* **1989**, *136*, 1614.

[73] D.W. Murphy, F.A. Trumbore *J. Electrochem. Soc.* **1976**, *123*, 960.

2 An Introduction to Solid-State Microwave Synthesis

2.1 A Brief History of Microwaves

The history of the study of microwaves began in 1864 when James Clerk Maxwell became the first individual to predict the existence of microwaves and by extension all electromagnetic waves.[74] He developed a series of equations that today bear his name and were able to incorporate all of the known observations about light, electricity, and magnetism into one cohesive theory. This theory postulated that light, electricity, and magnetism were all manifestations of the same fundamental phenomenon, the electric field. This was just theory without definitive proof until Heinrich Hertz became the first individual to produce and detect electromagnetic radiation during the 1880's.[75,76,77,78] He accomplished this by building a device that produced and measured UHF or VHF radio waves. UHF waves lie on the border between the radio and microwave regions of the electromagnetic spectrum, so it can be argued that microwaves were used by Hertz to confirm Maxwell's theory. Though they were known and in use for research into electromagnetic radiation well before, the actual term "microwave" was first used to describe this frequency range in 1931,[79] microwaves were predominantly investigated by physicists until the 1950s. Around this time, chemists began to make use of the heating ability that microwaves exhibit.

2.2 Definition and Applications

Microwaves are defined as electromagnetic radiation with wavelengths ranging from 0.3 to 300 GHz. This range can be broken into three regions known as the ultra-high frequency (UHF), super-high frequency (SHF) and extremely-high frequency (EHF). Microwaves in the UHF range (0.3 to 3 GHZ) are used for HAM radio, wireless internet, mobile phones, television and microwave ovens. The SHF range (3-30 GHZ) is used for radar and some wireless local area networks. The EHF range of microwaves (30-300 GHz) is mostly underdeveloped, but has a few uses such as radio astronomy and atmospheric monitoring. In order to avoid complications resulting from interference with telecommunications, two frequencies are reserved for conventional use in microwave ovens, 2.45 GHz and 0.9 GHz. Microwave devices are required to operate at one of these two frequencies, unless the apparatus is shielded and tested such that no microwave losses occur. The majority of conventional microwave ovens, and most research-grade microwaves, operate at 2.45 GHz, unless they are specially shielded.

2.3 Microwaves and Matter

The interactions between microwaves and matter fall into one of three categories. The first class of materials reflect microwave radiation. Typical examples are bulk metals and alloys such as steel and copper. These materials are used in the construction of microwave heating apparatus. The second class of materials are transparent to microwave radiation; that is, they transmit the electromagnetic waves without absorbing any of the energy of the waves. Microwave transparent materials such as alumina and quartz are

used as reaction vessels. The final class of compounds are able to absorb energy from microwaves. This class of materials includes polar liquids, such as water, and powdered metals. This class of materials is used as either the reactants or the reaction medium for chemical reactions.

There are several ways in which materials can absorb energy from microwaves but, it is first important to understand the difference between microwave dielectric heating and microwave spectroscopy. In microwave spectroscopy sharp peaks that correspond to transitions between quantized rotational energy levels are observed for molecules in the gas phase. In microwave reactions the materials that are absorbing microwave energy are typically in either a liquid or solid phase. In contrast to the gas phase, molecules in the liquid and/or solid phases are generally not free to rotate, resulting in the broadening of peaks in the microwave spectra to such an extent that they are not observable.[80] In these phases, dielectric heating effects are more important. Several mechanisms by which microwave irradiation can result in the heating of materials have been postulated by numerous scientists.[81-86] A thorough explanation of which is beyond the scope of this introduction; however, a brief discussion of the important points will be presented.

The basis for the multiple modes of dielectric heating is the ability of an electric field to exert a force on a charged particle. The first heating model is known as dipolar polarization and is due to the reorganization of molecules with a dipole moment.[81-86] Each microwave has an associated oscillating electric field. When a microwave passes through a medium that consists of molecules with dipole moments, the molecules will attempt to align with the electric field. As the field oscillates, so does the molecule. When

the frequency is long, the oscillation of the field is slower than the time it takes the molecules to reorganize. This leads to minimal heating because there is very little energy transferred due to random motion. When the frequency is shorter than the time it takes for the molecules to realign, there is no heating because the molecules do not rotate. In the microwave region the frequency corresponds approximately to the time realignment time of the molecules. The reorganization of the molecules lags slightly behind the electric field resulting in random motion as the molecules attempt, in vain, to stay in phase with the field. The random motion is what we perceive as heating in the medium.

The second method of heating is referred to as conduction.[81-86] This mechanism occurs when the sample is an electrical conductor. In electrical conductors the charge carriers, most likely electrons or ions, are moved through the material as a result of the electric field. The induced currents will result in heating due to electrical resistance, in the case of electrons, or collisions with other atoms or molecules, in the case of ions. This is the primary method for heating powdered metals in solid-state microwave synthesis. With all metals, there is a very thin layer in which some of the microwaves are attenuated resulting in induced currents that will give rise to heating. In bulk metals this heating effect is very small and hardly noticeable; however, in powdered metals most of the volume of the particles can be characterized as the surface layer. This allows powdered metals to be heated in a microwave field.

There is also a third proposed mechanism for microwave heating known as interfacial polarization.[81-86] The mechanism is important for systems that consist of two or more components with at least one conducting material and one non-conducting material. This effect can be thought of as a combination of dipole polarization and

conduction. This mechanism is not well understood and its importance in the microwave region is not well defined.

2.4 Applications

While the vast majority of the microwave frequency range is used for telecommunication applications, the two open frequencies are used in devices that are prevalent in the modern world. Almost every home in the developed world has at least one microwave oven. But microwaves also have many applications outside our domestic lives. Microwave heating has found numerous applications in the chemical world. Chemical applications of microwave heating are varied including organic synthesis,[87] analytical sample preparation,[88] nanoparticle synthesis[89] and even solid-state sample preparation.[90]

2.4.1 Organic Synthesis

The first reports of accelerated organic reactions due to microwave irradiation were published in 1986.[91,92] Despite the benefits that were apparent from this work, microwave heating was slow to gain wide acceptance and adoption in the field throughout the late 1980s and early 1990s. Several factors have been attributed to this slow uptake including a lack of controllability, a lack of reproducibility and a lack of understanding of the fundamentals behind microwave heating. There were also concerns about the flammability of organic solvents in a microwave field and no commercially available systems that had adequate temperature and pressure monitoring and control.

Eventually companies began to produce dedicated instruments for microwave-assisted organic synthesis and the literature saw a corresponding increase in the number of publications. A wide variety of reactions have been performed including cycloaddition reactions,[93] synthesis of radio isotopes,[94] fullerene chemistry,[95,96] polymer synthesis[97] and heterocyclic chemistry.[98,99] It has been found that microwave heating reduces reaction time, reduces side products, increases yields and increases reproducibility. These advantages can be attributed to either thermal or non-thermal effects.[100]

Most scientists agree that the primary reason for the observed advantages of microwave-assisted organic synthesis is a thermal effect. The thermal effect is due to the nature of heating by microwave irradiation. Solvents have been observed to heat very rapidly to temperatures well above their boiling points when irradiated. These rapid heating profiles are difficult, if not impossible, to recreate by standard thermal heating. Additionally, the increase in boiling point is a factor in the increased reaction rates. Looking at the Arrhenius law, $k=Aexp(-E_a/RT)$, a transformation that would require 68 days to reach 90 % completion at 27 °C will require only 1.61 seconds to reach 90 % completion at 227 °C, Table 1.[101]

Table 2.1. Relationship between temperature and time for a typical first-order reaction.*

Temperature (°C)	Rate (s^{-1})	Time
27	$1.55x10^{-7}$	68 days
77	$4.76x10^{-5}$	13.4 h
127	$3.49x10^{-3}$	11.4 min
177	$9.86x10^{-2}$	23.4 s
227	1.43	1.61 s

*Data from reference 101; $A=4x10^{10}$ $mol^{-1}s^{-1}$, $E_a=100$ $kJmol^{-1}$

The overheating observed in microwave-assisted organic synthesis is due to the inverted heat flow during microwave irradiation. In a conventionally heated reaction, heat is transferred from a heating mantle, oil bath or other apparatus to the outside of the reaction vessel. The heat must then pass into the solvent from the outside to the inside. In contrast, the whole solvent will heat at the same time when irradiated by microwaves and the heat will flow to the surroundings. This is important because nucleation of bubbles during the boiling process typically occurs on the vessel walls. In conventional heating, the vessel wall and nearby solution are at the highest temperature while the bulk solution is at a lower temperature. The opposite is true in a microwave reaction, where the vessel surface is cooler than the bulk solution. This allows the solution to appear over heated.

The existence of a non-thermal effect has been posited by some authors.[102,103,104,105,106] These effects should be identified as accelerations in the reaction that cannot be explained by thermal effects due to the unique nature of microwave heating.

Non-thermal effects are typically ascribed to the interaction of the electric field with specific molecules in the reaction mixture. The interaction of the electric field and molecules with a dipole could orient the molecule and change A or the E_a in the Arrhenius equation.[102,103,104] There is much debate about the existence of a true non-thermal effect that is beyond the scope of this work. [102,103,104,105,106]

2.4.2 Nanomaterial Synthesis

Nanomaterials are constructs that have at least one dimension on the order of nanometers. Reactions to form nanomaterials usually involve at least one reduction step that is carried out in a solvent. The use of a solvent for the reaction leads to many similarities between these syntheses and microwave-assisted organic synthesis. The heating is rapid and relatively uniform due to the thermal effects discussed previously. The same over heating that is observed in microwave-assisted organic synthesis reactions is observed in nanoparticle reactions.[107] This results in uniform nucleation and growth conditions for nanoparticles. This is an ideal situation because one of the goals of nanoparticle synthesis is to have control of the size and a narrow size dispersion. Uniform nucleation and growth are the best way to achieve these goals and are inherent to this heating method.

There is also evidence that hot spots form in some nanoparticle reactions when some solids form or are present in these reactions. This is especially the case in reactions involving coordinating surfactants that have a large dielectric loss constant. When these molecules attach to the surface of a nanoparticle they can couple with the microwave field and heat, resulting in the formation of a hot spot. Increased temperatures at these hot

spots will result in the enhancement in the reduction rates of the metal ions reducing the reaction time.[107]

There are numerous examples of nanomaterials that have been synthesized using microwave irradiation. Some of the first materials that were synthesized were metal nanoparticles, such as Au, Pt, Ir, Ag, Pd, Rh, Ru and Ni.[108-127] Since those reactions, work with nanoparticles has been expanded to include binary and ternary compounds. Some of the binary compounds that have been synthesized include PtRu, TiO_2, CdS, CdSe, $MoSe_2$, PbS and HgS.[128-134] This work then led into research with ternary compounds such as the diamond-like semiconductor $CuInSe_2$.[135] Though there is large amount of work that has been performed using this synthetic method, there is still room for growth. For example, doping of nanoparticles with magnetic ions could be attempted, which could result in a viable way to obtain materials for spin-based electronic applications.

2.4.3 Analytical Sample Preparation

Elemental analysis of most samples requires their dissolution. Once dissolved, the solution containing the sample is then introduced into an analytical instrument. Though great strides had been made in instrument technology, sample preparation techniques remained relative unchanged until the widespread adoption of microwave techniques. Until microwave digestions became the standard, open-vessel digestion and closed-vessel digestion using a Carius tube were the most common techniques for sample preparation. The introduction of microwave irradiation to analytical sample preparation occurred in 1975 with open vessel digestions that used microwave irradiation to heat acid that dissolved the samples.[136,137] Digestion times were reduced from 2 hours to 15 minutes.

Then in the 1980s, researchers working with nuclear waste samples began using closed vessels in the microwave.[138] As the technology was adopted the technique began to be refined including the introduction of temperature and pressure monitors so that the temperatures and pressures could be measured not only to determine ideal digestion conditions, but also to make sure that experiments were conducted safely.[139,140]

The first laboratory-grade multimode microwave was introduced in 1985.[140] This was followed, in 1986, by a laboratory microwave system that only irradiated the bottom of the vessel, so that the top would remain cool and allow for condensation.[141] In 1989, a commercial microwave unit with pressure feedback control was developed, followed closely by a unit with temperature feedback control in 1992.[140] This allowed for more accurate control of sample digestion procedures. Vessel design was also evolving concurrent with the developments in microwave cavities. These developments have allowed researchers to develop and publish methods that have now become industry standards rather than aberrations.

2.4.4 Solid State Microwave Synthesis

Solid-state microwave synthesis provides an interesting alternative to more traditional materials synthesis techniques. Like microwave-assisted organic synthesis and nanoparticle synthesis, reactions carried out using solid-state microwave synthesis have reaction times that are much shorter than comparable high-temperature methods. There are several other materials synthesis techniques that also have short reaction times, but each has its own unique disadvantages. One such method is chemical vapor deposition,

which does not require long reaction times, but can have difficulty producing homogeneous samples.

Solid-state microwave synthesis is promising because the reaction times using this technique are short, like chemical vapor deposition, and homogeneous samples can be prepared, like high-temperature solid-state synthesis. Previous research with the solid state microwave synthetic method has included the synthesis of compounds from a variety of classes of materials. For example, several chalcogenides, including CrS, CrSe, Cr_2Te_3, MnS and SnS_2 were synthesized from mixtures of the metal powder and the chalcogen, in the appropriate ratio, sealed in silica tubes under vacuum and irradiated with microwaves.[142] These reactions were found to heat to between 800 and 1000 °C rapidly, though it is not reported how the temperature is measured, and go to completion in less than 10 minutes. It was also noted that there was a lower limit to the amount of metal powder that was required to drive the reaction, especially for reactions involving sulfur due its low loss tangent.[142] Other work that has been performed with chalcogenides includes the synthesis of single crystals of ZnSe using a modified Bridgman technique.[143] The Bridgman method is typically used to obtain large single crystals of a sample. For this method the sample is slowly lowered through a temperature gradient, which controls melting and recrystallization in the tube. To perform this type of experiment in a microwave, the cavity of the microwave would need to be heavily modified or built specifically for this type of work. For this experiment, zinc pieces with dimensions of approximately 1 mm and a finely ground tellurium powder were placed into a quartz ampoule which was evacuated and sealed. Though zinc is a metal that is known to heat as a result of microwave irradiation,[144] this report also mentions that SiC rods were used as

heating elements. The use of SiC rods allows for stricter control of the temperature gradient, a necessity of the Bridgman method, in the microwave. In addition, using larger pieces of zinc could have turned the zinc from a microwave absorbing material into a microwave reflector.

In addition to binary compounds, there have also been reports of ternary, chalcopyrite compounds being synthesized using microwave irradiation.[145,146] The focus of these reports are copper-containing I-III-VI_2 semiconductors, with III=Al, Ga, In, and VI=S, Se, Te, though it is mentioned that silver analogs were also synthesized. Like the reactions to synthesize binary compounds, these reactions also involve metal powders and chalcogens being sealed in evacuated tubes and then irradiated. In addition to binary chalcogenide and chalcopyrite compounds, the zintl phase compounds Na_3SnTe_3, $NaSbTe_2$ and K_3SbTe_3 were synthesized using microwave irradiation.[147] Once again powdered starting materials are sealed in quartz tubes and then irradiated. There is a slight modification to the synthetic procedure for these compounds in that the reaction tubes were carbon coated to prevent the alkali metal from reacting with the quartz tube. Though carbon absorbs microwaves and heats rapidly, this is not discussed in the report. It would be interesting to determine the effect that the presence of carbon has on the reaction.

In addition to chalcogenides, metal vanadates have been synthesized using solid-state microwave synthesis. In a report that included the synthesis of chalcogenides, such as Ag_2S and ZnS, $Bi_4V_2O_{11}$ and PbV_2O_6 were prepared by the irradiation of metal oxides.[148] While the chalcogenides were synthesized in sealed ampoules, the oxides used to synthesize the vanadates were simply placed into clean silica crucibles. The crucibles

were placed on a firebrick and irradiated for 10-15 minutes. The compounds were then annealed for 2 hours in a muffle furnace. Substituted bismuth vanadate ionic conductors were also prepared using solid-state microwave synthesis from metal oxide starting materials.[149] The oxide starting materials were thoroughly mixed and then pressed into pellets before being placed into silica crucibles and irradiated for 15 minutes. Vanadates are not the only complex oxygen-containing compounds that have been prepared using microwave irradiation. Garnets, ferrites and spinels have also been prepared by microwave irradiation. [150] $Y_3Fe_5O_{12}$, $BaFe_{12}O_{19}$ and $NaAl_2O_4$ were each prepared in under 10 minutes from binary oxide starting materials.[150]

Oxide precursors have also been used for reactions to prepare nitrides, such as GaN, VN, and TiN.[151,152] The nitrides were synthesized using three different reactions. The first set of reactions exposed metal powders to microwaves while flowing nitrogen gas over the metal. The second and third reaction sets started with metal oxides. For the second set of reactions, the metal oxides were mixed with amorphous carbon and irradiated with a flowing nitrogen gas stream to achieve a carbothermal readuction reaction. In this reaction, nitrogen replaces the oxygen and carbon reacts with the displaced oxygen to form CO gas according to the following equation.

$$MO_2 + 2C + \tfrac{1}{2}N_2(g) \rightarrow MN + 2CO(g)$$

The third set of reactions was similar to the second set as they both used metal oxides mixed with carbon. However, instead of nitrogen, the third set of reactions used ammonia. It is also important to note that amorphous carbon was used instead of graphitic carbon because amorphous carbon was found to heat to higher temperatures more rapidly.[153] Nitrides are typically difficult compounds to synthesize and this provides

a relatively quick and easy route to obtain these materials. Solid-state microwave synthesis has also been used to prepare other compounds that can prove challenging to synthesize, such as MgB_2.[154] For this reaction, powdered boron and magnesium were pressed into a pellet and then placed into an alumina boat. The boat was then placed into a crucible filled with SiC. Argon was passed through the crucible to limit oxidation. Magnesium is extremely volatile and susceptible to oxidation at high temperatures, however using this synthetic procedure evaporation and oxidation of the magnesium were significantly reduced.

Reactions have also been performed by reacting metal powders with gases, such as chlorine and bromine. Metal chlorides, bromides and nitrides were prepared using several set-ups including a fluidized bed apparatus and a suspended sample apparatus.[155] The fluidized bed apparatus is constructed entirely of silica. The metal powder sits between two frits while gas is passed through the vessel from beneath the sample. This allows the flow rate to be controlled to achieve a fluidized-bed condition. The suspended apparatus is similar to placing a porcelain boat in a Schlenk tube, only in this case a special apparatus was constructed to keep the sample suspended in the middle of the apparatus. Compounds synthesized using one or both of these set-ups include $CrCl_3$, WCl_6, $InCl_3$, $TeCl_4$, TiN, Cr_2N, $TiBr_4$ and CuBr.

There have also been reports that solid-state microwave synthesis has the capability to produce samples that are highly dense[156] and samples that have enhanced properties compared to samples prepared by conventional methods.[157,158] Several systems were studied, including the Fe-Cu-C and Fe-Ni-C systems, and found to have higher densities than samples prepared via conventional methods.[157] In addition metal samples,

such as cobalt, were sintered in a microwave and also found to exhibit higher densities than samples that were conventionally sintered due to a finer grain size. Additionally, the shape of the porosity is different in samples sintered in a microwave as opposed to using conventional preparations. [157] Microwaves also have been observed to result in products that have unique morphologies and microstructures.[156,159] For example, vanadyl hydrogen phosphate hemihydrates ($VOHPO_4 \cdot 0.5H_2O$) were prepared by a conventional method, by sonochemical reaction and by microwave irradiation. The samples prepared by microwave irradiation were shown to have a higher BET surface area than either of the other samples.[159] This indicates that the surface morphology is different for the samples prepared in the microwave.

Though there have been examples of numerous types of materials prepared via solid-state microwave synthesis as described above, the total number of compounds remains relatively small for a technique that offers so many advantages such as short reaction times. One reason for this could be a lack of understanding of this synthetic method. In order to better understand the solid-state microwave synthetic method, several recent experiments have been performed using *in-situ* X-ray and neutron diffraction.[160,161] These experiments use special set-ups that allow sample to be irradiated with microwaves during a diffraction experiment. In the X-ray diffraction experiment, the $\beta-\alpha$ phase transition in AgI was studied.[160] Under conventional heating the β-α phase change occurs at 412 K. The temperature of the phase change was found to decrease significantly, to 380 K, under microwave irradiation. This was explained by multi-phonon interactions with the microwave field. For the neutron powder diffraction experiment, aspirin and $BaTiO_3$ were examined.[161] The anisotropic displacement parameters for the atoms in

aspirin were found to be much larger when the microwaves were applied compared to when they were turned off. It was not determined if this was a thermal or a non-thermal effect. The results for $BiTiO_3$ was not as simple to rationalize. The compound was heated using both conventional means and microwave irradiation. The lattice parameters for corresponding temperatures were found to be larger in the microwave heated samples while the anisotropic displacement parameters were smaller. Both of these values should be temperature dependent, but the discrepancies between the conventional and microwave heated samples cannot be simply explained. It is clear that further work is required, both to understand this synthetic method and to determine which compounds can be prepared using this microwave irradiation procedure.

For most of the reports of solid-state microwave synthesis, the research has been conducted using custom-built systems, due to the lack of commercially available microwaves designed for the needs of solid-state microwave synthesis. Most commercially designed systems are engineered for analytical sample preparation and organic synthesis. The conditions for these applications are quite different than those required for solid-state synthesis. For example, temperature monitoring is frequently performed by a fiber optic thermocouple. This is not feasible for solid-state reactions for two reasons, the extremely high temperatures achieved during solid-state microwave reactions and the problem of bringing the thermocouple into intimate contact with the reaction vessel. Additionally, commercial microwaves are now frequently controlled by software that uses a feedback system that is intimately linked with temperature monitoring equipment. This means that there are not just hardware, but software, barriers to using commercial systems for solid-state microwave synthesis. These barriers have

lead determined researchers to create their own custom-built systems, but can be too great for new researchers to overcome. This is yet another problem in the widespread adoption of this synthetic method.

2.5 Understanding Solid-State Microwave Synthesis

One reason for the lack of use of solid-state microwave synthesis could be the poor understanding of this method coupled with the complexity of these reactions. The solid-state community, in general, has not been trained to utilize microwave irradiation for synthetic applications. Most researchers, however, are very familiar with traditional heating methods. The current situation resembles that of microwave-assisted organic synthesis during the late 1980s. There are scattered accounts of successful syntheses, but not a wide-spread adoption by the community as a whole. This could be due to several factors including a lack of training, microwave companies focusing on other areas of chemistry (organic synthesis, combinatorial chemistry and analytical sample preparations) and the general complexity of this method. The first problem, a lack of training, stems from the lack of courses that teach this synthetic method and a lack of exposure of researchers to this method. This can be overcome by increased exposure of the solid-state community to this method through presentations at conferences and publications. The second problem, commercial microwave companies focusing on other areas of chemistry, means that there is no commercially available equipment that is specially designed for the needs of solid-state microwave synthesis. Researchers would need to build their own equipment or modify existing microwaves. This can prove to be a barrier that few are willing to overcome. The final problem of complexity is readily

apparent when reaction conditions vary greatly between closely related materials.[162] An additional problem is that the literature is often lacking significant synthetic details. This "omission" is likely not intentional, but results because the author did not realize which seemingly trivial aspects of their set-up were actually integral synthetic parameters. Due to the complex interactions that occur between the microwaves and the samples, reactions appear to be highly sensitive to subtle changes. Consequently the omission of synthetic parameters can result in the discouragement of a researcher who is attempting to learn about this synthetic method but failing to reproduce a literature example.

The ideal situation would be to gain a better understanding of the fundamental interactions that are occurring in these reactions, so that all reaction variables can be identified and future researchers will be able to describe, in detail, how to reproduce their experiments. As previously explained, there are several groups currently attempting to gain a better understanding of this synthetic method by performing *in-situ* experiments with several materials.[160,161] We have also been conducting experiments that are attempting to identify synthetic variables while synthesizing compounds for the first time using microwave irradiation.[162,163,164]

2.6 Conclusions

Solid-state microwave synthesis is a promising alternative to other more traditional synthetic methods. One of the primary advantages of this method is the short timescales for these reactions, especially when compared to more traditional synthetic methods, such as high-temperature solid-state synthesis. The short reaction times also mean that less energy is required to perform these reactions. With energy costs

escalating, a method that uses significantly less energy could be quite beneficial. Additionally, there are no solvents used for SSMS resulting in little or no waste produced. These two advantages make solid-state microwave synthesis a relatively "green" alternative synthetic method.[165,166]

Solid state microwave synthesis is also a promising research area because it has been used to prepare a variety of different materials. Despite this promise, there is still a lack of understanding about this method. It is not understood as well as many other synthetic methods, such as high-temperature solid-state synthesis. This is possibly due to the complexity of this method, but it is also due to a lack of attention that has been given to this method. The lack of attention and understanding coupled with the promise that this method has shown make this synthetic method due to experience the kind of renaissance that analytical sample preparation saw during middle years of the 1980's.

2.7 References

74 J.C. Maxwell *Philos.T. Roy. Soc.* **1865**, *155*, 459-512.

75 H.R. Hertz *Annalen der Physik* **1887**, *267*, 421-448.

76 H.R. Hertz *Annalen der Physik* **1887**, *267*, 983-1000.

77 H.R. Hertz *Annalen der Physik* **1888**, *270*, 155-170.

78 H.R. Hertz *Annalen der Physik* **1888**, *270*, 551-569.

79 *Telegraph and Telephone Journal XVII* **1931**, *179*.

[80] D.M.P. Mingos, D.R. Baghurst *Microwave Enhanced Chemistry: Fundamentals, Sample Preparation and Applications*, H.M. Kingston, S.J. Haswell eds. The American Chemical Society: Washington, D.C., 1997, 3.

[81] P. Debye. *Polar Molecules* Chemical Catalog: New York, 1929.

[82] H. Frohlich *Theory of Dielectrics 2nd Edition* Oxford University Press: London, 1958.

[83] V. Daniel *Dielectric Relaxation* Academic Press: Orlando, 1967.

[84] K.S. Coke, R.H. Cole *J. Chem. Phys.* **1941**, *9*, 341.

[85] N. Hill, W.E. Vaughan, A.H. Price, M. Davies *Dielectric Properties and Molecular Behavior* von Nostrand: New York, 1969.

[86] J.B. Hasted *Aqueous Dielectrics* Chapman and Hall: London, 1973.

[87] C.O. Kappe *Angew. Chem. Int. Ed.* **2004**, *43*, 6250.

[88] L. Chen, D. Song, Y. Tian, L. Ding, A. Yu, H. Zhang *TrAC Trend. Anal. Chem.* **2008**, *27*, 151.

[89] M. Tsuji, M. Hashimoto, Y. Nishizawa, M. Kubowkawa, T. Tsuji *Chem. Eur. J.* **2005**, *11*, 440.

[90] D.M.P. Mingos, D.R. Baghurst *Microwave Enhanced Chemistry: Fundamentals, Sample Preparation and Applications*, H.M. Kingston, S.J. Haswell eds. The American Chemical Society: Washington, D.C., 1997, 523.

[91] R. Gedye, F. Smith, K. Westway, H. Ali, L. Baldisera, L. Laberge, J. Rousell *Tetrahedron Lett.* **1986**, *27*, 279.

[92] R.J. Giguere, T.L. Bray, S.M. Duncan, G. Majetich *Tetrahedron Lett.* **1986**, *27*, 4945.

[93] S.A. Stone-Elander, N. Elander, J.-O. Thorell, G. Solas, J. Svennebrink *J. Label. Compd. Radiopharm.* **1994**, *34*, 949.

[94] J.-O. Thorell, S. Stone-Elander, N. Elander *J. Label. Compd. Radiopharm.* **1992**, *31*, 207.

[95] D. Hesk, J.R. Jones, W.J.S. Lockley, D.J. Wilkinson *J. Label. Compd. Radiopharm.* **1990**, *28*, 1309.

[96] J.L. Whalley, M.F. Oldfield, N.P. Botting *Tetrahedron* **2000**, *56*, 455.

[97] I.C. Cotterill, A.Y. Usyatinsky, J.M. Arnold, D.S. Clark, J.S. Dordick, P.C. Michels, Y.L. Khmeinitsky *Tetrahedron Lett.* **1998**, *39*, 1117.

[98] D. Scharn, H. Wenschuh, U. Reineke, J. Schneider-Mergener, L. Germeroth *J. Comb. Chem.* **2000**, *2*, 361.

[99] C.O. Kappe, D. Kumar, R.S. Varma *Synthesis* **1999**, *10*, 1799.

[100] A. de la Hoz, Á. Díaz-Ortiz, A. Moreno *Chem. Soc. Rev.* **2005**, *34*, 164.

[101] D.R. Baghurst, D.M.P. Mingos *Chem. Soc. Rev.* **1991**, *20*, 1.

[102] L. Perreux, A. Loupy *Tetrahedron* **2001**, *57*, 9199.

[103] F. Langa, P. de la Cruz, A. de la Hoz, A. Díaz-Ortiz, E. Díez-Barra *Contemp. Org. Synth.* **1997**, *4*, 373.

[104] K.C. Westaway, R. Gedye *J. Microwave Power* **1995**, *30*, 219.

[105] C.R. Strauss *Angew. Chem.* **2002**, *114*, 3741.

[106] N. Kuhnert *Angew. Chem.* **2002**, *114*, 1943.

[107] M. Tsuji, M. Hashimoto, Y. Nishizawa, M. Kubokawa, T. Tsuji *Chem. Eur. J.* **2005**, *11*, 440.

[108] T. Yamamoto, H. Yin, Y. Wada, T. Kitamura, T. Sakata, H. Mori, S. Yanagida *Bull. Chem. Soc. Jpn.* **2004**, *77*, 757.

[109] M. Tsuji, M. Hashimoto, Y. Nishizawa, T. Tsuji *Hoshasen Kagaku (Radiation Chem.)* **2004**, *77*, 8.

[110] M. Tsuji, M. Hashimoto, Y. Nishizawa, T. Tsuji *Mater. Lett.* **2004**, *58*, 2326.

[111] Y.J. Zhu, X.L. Hu *Mater. Lett.* **2004**, *58*, 1517.

[112] F. Liu, Y. Chang, F. Ko, T. Chu *Mater. Lett.* **2004**, *58*, 373.

[113] W.X. Chem, J. Zhao, J.Y. Lee, Z.L. Liu *Chem. Lett.* **2004**, *33*, 474.

[114] M. Tsuji, Y. Nishizawa, M. Hashimoto, T. Tsuji *Chem. Lett.* **2004**, *33*, 370.

[115] T. Yamamoto, Y. Wada, T. Sakata, H. Mori, M. Goto, S. Hibino, S. Yanagida *Chem. Lett.* **2004**, *33*, 158.

[116] R. Harpeness, A. Gedanken, A.M. Weiss, M.A. Slifkin *J. Mater. Chem.* **2003**, *13*, 2603.

[117] Y.J. Zhu, X.L. Hu *Chem. Lett.* **2003**, *32*, 1140.

[118] M. Tsuji, M. Hashimoto, Y. Nishizawa, T. Tsuji *Chem. Lett.* **2003**, *32*, 1114.

[119] F.K. Liu, C.J. Ker, Y.C. Chang, F.K. Ko, T.C. Chu, B.T. Dai *Jpn. J. Appl. Phys. Part 1* **2003**, *42*, 4152.

[120] R. He, X. Qian, J. Yin, Z. Zhu *Chem. Phys. Lett.* **2003**, *369*, 454.

[121] R. He, X. Qian, J. Yin, Z. Zhu *J. Mater. Chem.* **2002**, *12*, 3783.

[122] S. Komarneni, D. Li, B. Newalkar, H. Katsuki, A.S. Bhalla *Langmuir*, **2002**, *18*, 5959.

[123] I. Pastoriza-Santos, L. Liz-Marźan *Langmuir* **2002**, *18*, 2888.

[124] M. Tsuji, M. Hashimoto, T. Tsuji *Chem. Lett.* **2002**, *31*, 1232.

[125] Z.L. Jiang, Z.W. Feng, X.C. Shen *Chin. Chem. Lett.* **2001**, *12*, 551.

[126] W. Tu, H. Liu *J. Mater. Chem.* **2000**, *10*, 2207.

[127] Y. Wada, H. Kuramoto, T. Sakata, H. Mori, T. Sumida, T. Kitamura, S. Yanagida *Chem. Lett.* **1999**, *28*, 607.

[128] O. Palchik, R. Kerner, A. Gedanken, A.M. Weiss, M.A. Slifkin, V. Palchik *J. Mater. Chem.* **2001**, *11*, 874.

[129] Y. Wada, H. Kuramoto, J. Anand, T. Kitamura, T. Sakata, H. Mori, S. Yanagida *J. Mater. Chem.* **2001**, *11*, 1936.

[130] T. Yamamoto, Y. Wada, H. Yin, T. Sakata, H. Mori, S. Yanagida *Chem. Lett.* **2002**, *31*, 964.

[131] T. Ding, J. Zhang, S. Long, J. Zhu *Microelectron. Eng.* **2003**, *66*, 46.

[132] R Harpeness, A. Gedanken, A.M. Weiss, M.A. Slifkin *J. Mater. Chem.* **2003**, *13*, 2603.

[133] Z.L. Liu, X.Y. Ling, J.Y. Lee, X.D. Su L.M. Gam *J. Mater. Chem.* **2003**, *13*, 3049.

[134] Z.L. Liu, J.Y. Lee, W.X. Chen, M. Han, L.M. Gan *Langmuir* **2004**, *20*, 181.

[135] H. Grisaru, O. Palchik, A. Gedanken, V. Palchik, M.A. Slifkin, A.M. Weiss *Inorg. Chem.* **2003**, *42*, 7148.

[136] A. Abu-Samra, J.S. Morris, S.R. Koirtyohann *Anal. Chem.* **1975**, *47*, 1475-1477.

[137] A. Abu-Samra, J.S. Morris, S.R. Koirtyohann *Trace Subst. Environ. Health* **1975**, *9*, 297.

[138] H.M. Kingston, D.J. Cronin, M.S. Epstein *Nucl. Chem. Waste Manage.* **1984**, *5*, 3.

[139] H.M. Kingston, L.B. Jassie *Anal. Chem.* **1986**, *58*, 2534.

[140] H.M. Kingston, L.B. Jassie *Introduction to Microwave Sample Preparation: Theory and Practice* L.B. Jassie, H.M. Kingston eds., American Chemical Society: Washington, D.C., 1988, 93.

[141] P.J. Walker, S. Chalk, H.M. Kingston *Microwave Enhanced Chemistry: Fundamentals, Sample Preparation and Applications*, H.M. Kingston, S.J. Haswell eds. The American Chemical Society: Washington, D.C., 1997, 55.

[142] A.G. Whittaker, D.M.P. Mingos *J. Chem. Soc. Dalton Trans.* **1992**, *18*, 2751.

[143] S. Bhunia, D.N. Bose *J. Cryst. Growth* **1998**, *186*, 535.

[144] K.J. Rao, B. Vaidhyanathan, M. Ganguli, P.A. Ramakrishnan *Chem. Mater.* **1999**, 882.

[145] C.C. Landry, A.R. Barron *Science* **1993**, *260*, 1653.

[146] C.C. Landry, J. Lockwood, A.R. Barron *Chem. Mater.* **1995**, *7*, 699.

[147] G.-T. Zhou, V.G. Pol, O. Palchik, R. Kerner, E. Sominski, Y. Koltypin, A. Gedanken *J. Solid State Chem.* **2004**, *177*, 361.

[148] B. Vaidhyanathan, M. Ganguli, K.J. Rao *Mater. Res. Bull.* **1995**, *30*, 1173.

[149] B. Vaidhyanathan, K. Balaji, K.J. Rao *Chem. Mater.* **1998**, *10*, 3400.

[150] R.D. Peelamedu, R. Roy, D. Agrawal *Mater. Res. Bull.* **2001**, *36*, 2723.

[151] R.D. Peelamedu, M. Fleming, D.K. Agrawal, R. Roy *J. Am. Ceram. Soc.* **2002**, *85*, 117.

[152] B. Vaidhyanathan, K.J. Rao *Chem. Mater.* **1997**, *9*, 1196.

[153] J.W. Walkiewicz, G. Kazonich, S.L. McGill *Miner. Metall. Processing* **1988**, *5*, 39.

[154] C. Dong, J. Guo, G.C. Fu, L.H. Yang, H. Chen *Supercond. Sci. Technol.* **2004**, *17*, L55.

[155] A.G. Whittaker, D.M.P. Mingos *J. Chem. Soc. Dalton Trans.* **1993**, *16*, 2541.

[156] A.G. Whittaker *Chem. Mater.* **2005**, *17*, 3426.

[157] R. Roy, D. Agrawal, J. Chang, S. Gedevanishvili *Nature* **1999**, *399*, 668.

[158] R. Roy, D. Agrawal, J. Chang, S. Gedevanishvili *Nature* **1999**, *401*, 304.

[159] U.R. Pillai, E. Sahle-Demessie, R.S. Varma *Appl. Catal. A* **2003**, *252*, 1.

[160] G.R. Robb, A. Harrison, A.G. Whittaker *Phys. Chem. Comm.* **2002**, *5*, 135.

[161] A. Harrison, R. Ibberson, G. Robb, G. Whittaker, C. Wilson, D. Youngson *Faraday Discuss.* **2002**, *122*, 363.

[162] C. Mastrovito, J.W. Lekse, J.A. Aitken *J. Solid State Chem.* **2007**, *180*, 3262.

[163] J.W. Lekse, A.M. Pischera, J.A. Aitken *Mater. Res. Bull.* **2007**, *42*, 395.

[164] J.W. Lekse, T.J. Stagger, J.A. Aitken *Chem. Mater.* **2007**, *19*, 3601.

[165] C. Villa, E. Mariani, A. Loupy, C. Grippo, G.C. Grossi, A. Bargagna *Green Chem.* **2003**, *5*, 623.

[166] M. Ješelnik, R.S. Varma, S. Polanc, M. Kočevar *Green Chem.* **2002**, *4*, 35.

3 Understanding the Solid-State Microwave Synthetic Method Using $AgInSe_2$, as a Case Study

3.1 Introduction

The use of microwaves in analytical sample preparation,[167] materials processing[168] and organic synthesis[169,170] is becoming increasingly common; however, the utilization of microwaves in solid-state inorganic synthesis has been limited.[171] This is due, in part, to a lack of understanding about the interactions of microwaves with solids in dry (solventless) media and the effect that reaction variables have on these interactions. If researchers had the knowledge necessary to rationally design and predict solid-state microwave reactions, instead of using the method as a "black box" technique, the potential of this approach could be maximized. For this reason, we have begun investigating the synthetic variables and reaction mechanisms involved in solid-state microwave synthesis using the diamond-like semiconductor[172,173] $AgInSe_2$[174] as a case study.

Our motivation to develop solid-state microwave synthesis stems from the fact that microwave irradiation can offer several advantages over conventional heating techniques, such as traditional, high-temperature solid-state synthesis. Microwave reactions reach high temperatures rapidly and do not require a long time to go to completion. Reactions, which normally require hours or days via conventional heating, can be carried out in the microwave within a matter of minutes. Shorter reaction

procedures are advantageous, not only because they save time and are more economical, but also because they may allow for the synthesis of kinetically stable or meta-stable compounds, which may be difficult to synthesize via other methods. Another advantage is that, unlike other alternative methods to traditional, high-temperature solid-state preparations, such as solvothermal synthesis, no solvent waste is generated in these reactions. These advantages allow solid-state microwave synthesis to be considered a relatively green technique.[175,176] Additionally, microwave heating can offer the ability to prepare highly dense samples,[177] frequently resulting in materials with substantially enhanced physical properties, compared to those prepared by convential techniques.[178] Often times, microwave heating can result in different morphologies and microstructures in the resulting products.[177,179] Furthermore, microwaves can allow reactions to occur at lower temperatures.[180]

The exact processes that occur during solid-state microwave synthesis are uncertain and most of the literature on this subject is speculative.[181] Recent studies have been attempting to probe the interactions of solid matter with microwaves using *in-situ* diffraction experiments.[182,183] Currently, it is well accepted that materials can be generally categorized into three groups with respect to how they interact with microwaves. The first group is microwave reflectors, usually bulk metals or alloys, which are used in the construction of microwave ovens. The second group, microwave transmitters, are transparent to microwaves. Most chemical reaction containers used in the microwave are made out of microwave transparent materials, for example fused-silica and fluoropolymers. The last category of materials is microwave absorbers, which heat rapidly under the influence of microwave irradiation. Many inorganic materials are

known to behave this way when exposed to microwave radiation, for example: powdered metals, metal oxides and metal halides.[181,184]

Solid-state microwave irradiation has been used to prepare a variety of different materials such as carbides, oxides, silicides, phosphates and borides.[180,181,185] Metal vanadates and chalcogenides have also been prepared with high purity.[186-189] In addition, traditionally difficult to synthesize materials, such as nitrides, have been prepared by irradiation of the metals under nitrogen gas.[190,191] More recently, intermetallic compounds have also been prepared using microwave irradiation.[192,193] Although the types of materials that have been prepared by solid-state microwave synthesis are varied, the total number of compounds produced via this method is still relatively small.

Our research has shown that the solid-state microwave synthetic method is not straightforward. Additionally, reaction variables in this method have not been adequately identified and discussed in the literature. For these reasons, we chose to explore three reaction variables for the solid-state microwave synthesis of $AgInSe_2$: sample volume, irradiation time and grinding time of reactants. Also, irradiation of the constituent elements as well as binary mixtures is described. All products were characterized using powder X-ray diffraction (PXRD), differential thermal analysis (DTA) and diffuse reflectance spectroscopy in the UV/Vis/Near IR region. The knowledge gained from these investigations could be used to tailor the microwave syntheses of other solid-state materials.

3.2 Experimental

3.2.1 Reagents

Chemicals in this work were used as obtained: (i) silver powder, -325 mesh, 99.99%, Cerac; (ii) selenium powder, 200 mesh, 99.99%, Strem; (iii) indium powder, -325 mesh, 99.99%, Strem; (iv) copper powder, -100 mesh, 99.999%, Strem (v) sulfur, sublimed powder, 99.5%, Fisher. All elements were stored and handled in a glovebox under argon.

3.2.2 Powder X-Ray Diffraction

PXRD patterns were collected using a Rigaku Geigerflex Model D2013 diffractometer operating in Bragg-Brentano geometry using Cu K_α radiation.

3.2.3 Diffuse Reflectance Spectroscopy

Diffuse reflectance spectra were obtained using a Cary 5000 UV-Vis-NIR spectrometer. Samples were placed into a Harrick Praying Mantis diffuse reflectance accessory that uses elliptical focusing mirrors. $BaSO_4$ was used as a 100% reflectance standard. The reflectance data were converted to absorption units.[194]

3.2.4 Differential Thermal Analysis

DTA was performed using a Shimadzu DTA-50 thermoanalyzer. The reference, Al_2O_3, and sample were contained in fused-silica and carbon-coated, fused-silica ampoules, respectively, and sealed under vacuum. Two heating/cooling cycles were carried out to determine if the thermal events were reversible.

3.2.5 Synthesis

3.2.5.1 General Synthetic Methods

$AgInSe_2$ was synthesized in a CEM MDS 2100, 1000 W research-grade microwave. Varying amounts, 1-6 mmoles, of a stoichiometric elemental mixture were weighed and then ground together for varying amounts of time, 10-30 minutes. The reagent mixture was placed into a 9 mm O.D. fused-silica tube, which was sealed under a vacuum of approximately 10^{-3} torr using a natural gas/oxygen torch. The sealed tube was placed into a fused-silica holder that maintained the sample in a vertical orientation inside the microwave. All samples were subjected to irradiation intervals at 100% power. After microwave irradiation, the sample was removed from the tube, inspected and ground.

3.2.5.2 Synthesis of Phase-Pure $AgInSe_2$

Phase-pure $AgInSe_2$ was synthesized in a CEM MDS 2100 1000W research-grade microwave. 3 mmole silver, 3 mmole indium and 6 mmole sulphur were weighed and then ground together for 20 minutes in an agate mortar. This mixture was placed into a 9 mm O.D. fused-silica tube, which was sealed under a vacuum of approximately 10^{-3} torr using a natural gas/oxygen torch. The sealed tube was placed vertically into a fused-silica

holder and irradiated for 3, 1-minute intervals at 100 % power. After irradiation, the sample was removed from the tube and ground for 20 minutes. The sample was then placed into a 9 mm O.D. fused-silica tube and sealed under vacuum. The sample was again irradiated for 3, 1-minute intervals at 100 % power. Following the second irradiation, the sample was removed from the tube, inspected and ground.

3.2.5.3 High-Temperature Synthesis of $AgInSe_2$

$AgInSe_2$ was also synthesized in a programmable furnace. The sample was placed into a fused-silica tube identical to those used for the microwave reactions. The tube was then sealed under vacuum using a torch, as in the microwave reactions. The sample was heated from room temperature to 850 °C in 8 hours and maintained at 850 °C for 72 hours, before being cooled to room temperature in 8 hours. After cooling, the sample was removed from the tube, inspected and ground.

3.3 Results and Discussion

Syntheses of $AgInSe_2$ were attempted in a research-grade microwave. Within seconds of beginning the microwave irradiation, a bright, whitish-blue plasma forms in the reaction tube, Figure 3.1. When removed from the tube, most of the sample ingot consists of sintered powder. PXRD of each sample was performed. For most samples, the majority of the diffraction peaks in the resulting pattern were indexed to $AgInSe_2$; however, a few peaks were usually present that did not index to $AgInSe_2$, indicating the presence of an alternate phase. Based upon the position and intensity of these diffraction peaks, the alternate phase was identified as $AgIn_5Se_8$.[195,196] Several series of reactions indicated that a few synthetic variables had a profound effect on the phase purity[197] of the

product. These variables, which were investigated thoroughly to determine a method to prepare phase-pure $AgInSe_2$, included sample volume, irradiation time and grinding time of the reactants.

Figure 3.1. A digital photo of the reaction to make $AgInSe_2$ taken through the microwave door. The fused-silica reaction tube is situated in a vertical fused-silica holder, which is barely visible in the photo. The holder is placed on top of a quartz brick, which is positioned on the center of the microwave cavity floor. As microwave radiation is applied to the sample, a bright, whitish-blue plasma is observed in the fused-silica reaction tube directly above the reaction mixture.

3.3.1 Microwave Synthesis Variables

In order to determine the effect of sample volume on the phase purity of the product, reaction mixtures to prepare 0.5, 1, 2, 3, 4 and 6 mmoles of product were investigated, Figure 3.2. Changes in the sample volume, on this scale, would not usually have an effect on the outcome of a traditional, high-temperature solid-state reaction; but, due to the unique nature of microwave reactions, these small volume changes have a substantial effect. All samples reacted to yield $AgInSe_2$ as the major phase and varying amounts of the minor, alternate phase, $AgIn_5Se_8$.[195,196] It was found that the phase purity increased with increasing sample size until the sample became larger than 4 mmoles. The optimal sample volume was determined to be 3-4 mmoles; because, both of these sample volumes appeared to yield equally phase-pure materials, as determined by PXRD.

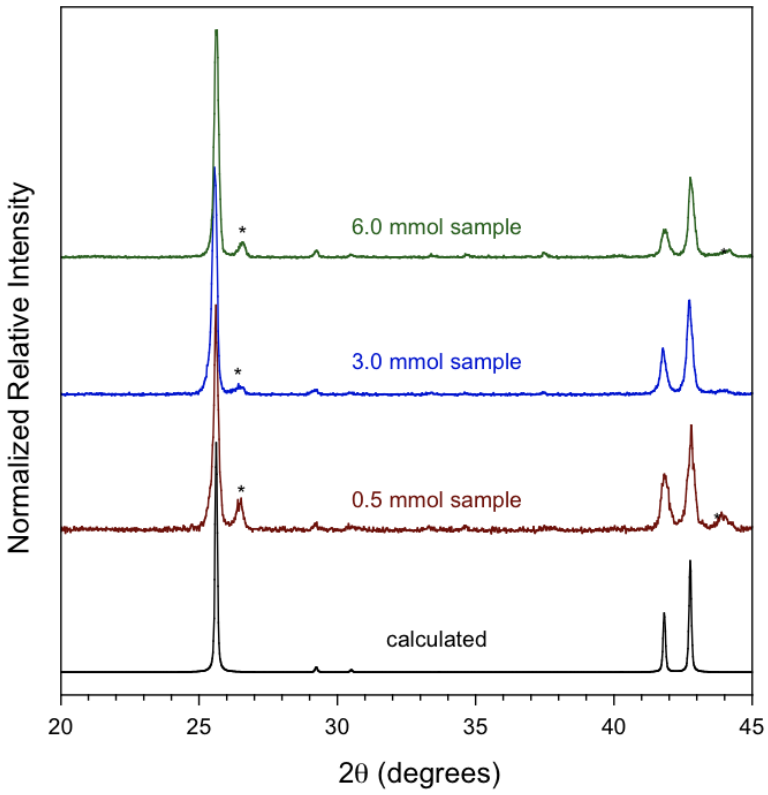

Figure 3.2. Powder X-ray diffraction patterns obtained for select microwave reactions of different sample volumes intended to make $AgInSe_2$, compared to the calculated pattern for $AgInSe_2$.[174] All three samples were ground for 20 min followed by irradiation for 3, 1-minute intervals. The asterisks mark diffraction peaks due to the presence of $AgIn_5Se_8$.[195,196]

There are three principles which one should consider to help explain the observations for sample-volume experiments. The first is that diffusion between solids is typically slow and often a limiting factor in solid-state reactions. Microwave irradiation can increase the diffusion rate,[198] leading to shorter reaction times; however, diffusion will still play a role in these reactions. The second factor is a relationship that exists in

microwave solution chemistry, which states that the power absorbed by the sample is directly proportional to the amount of sample present.[167] Though solid-state microwave synthesis does not involve solutions, the relationship between sample volume and power absorbed could be extended to solid-state reactions. Increased power absorption should correspond to higher temperatures, which drive the reaction to completion. The main difference between solid-state and solution reactions is the third factor; microwave penetration depth, the distance in the direction of penetration at which the incident microwave power is reduced to half of its original amount. Microwaves can only penetrate a sample to a certain depth; because, the sample absorbs energy from the electromagnetic waves as they travel through the material, until eventually the energy of the waves is reduced to zero. In solid-state reactions the microwave penetration depth is significantly smaller than in most solutions. As the sample volume of the solid-state reaction increases, this effect becomes increasingly important. Eventually, the sample can be so large that the center of the reaction mixture may never experience any microwave energy. In the case of $AgInSe_2$, there exists an ideal sample size, between 3 and 4 mmoles, that can be rationalized by a combination of the above factors. As the sample volume increases, the increased power absorbed drives the reaction until there is too much material. At this point, diffusion and penetration depth begin to limit the reaction. The combined effects of diffusion and penetration depth result in the phase purity of $AgInSe_2$ decreasing, instead of continuing to increase.

In addition to sample volume, the effects due to irradiation time were investigated. Samples that were irradiated for 1, 3, 6 and 9, one-minute intervals were studied, Figure 3.3. The phase purity was found to increase with increasing irradiation

time, up to 3, one-minute irradiations. After 3 minutes, the phase purity decreases with increasing irradiation time. The results of these experiments indicate that there is an optimal irradiation time of approximately 3, one-minute intervals for this compound. We also determined that irradiation procedure is yet another variable that needs to be considered. For instance, a comparison of 3, one-minute intervals and 1, three-minute interval showed a marked difference in the phase purity of the product, Figure 3.4. Trends in phase purity as a fuction of irradiation time and procedure are difficult to understand, as they involve reaction kinetics and thermodynamics. Usually, the effects of reaction time are also difficult to understand in conventional heating techniques.

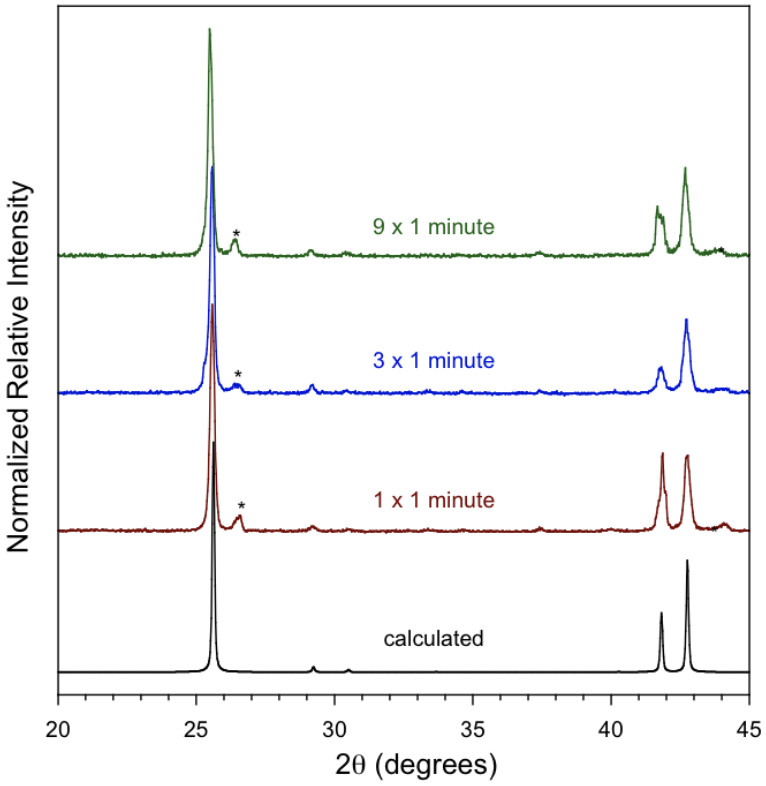

Figure 3.3. Powder X-ray diffraction patterns obtained for select microwave reactions irradiated for different time periods compared to the calculated pattern for $AgInSe_2$.[174] All three samples were ground for 20 min and were calculated to yield 4 mmol of product. The asterisks mark diffraction peaks due to the presence of $AgIn_5Se_8$.[195,196]

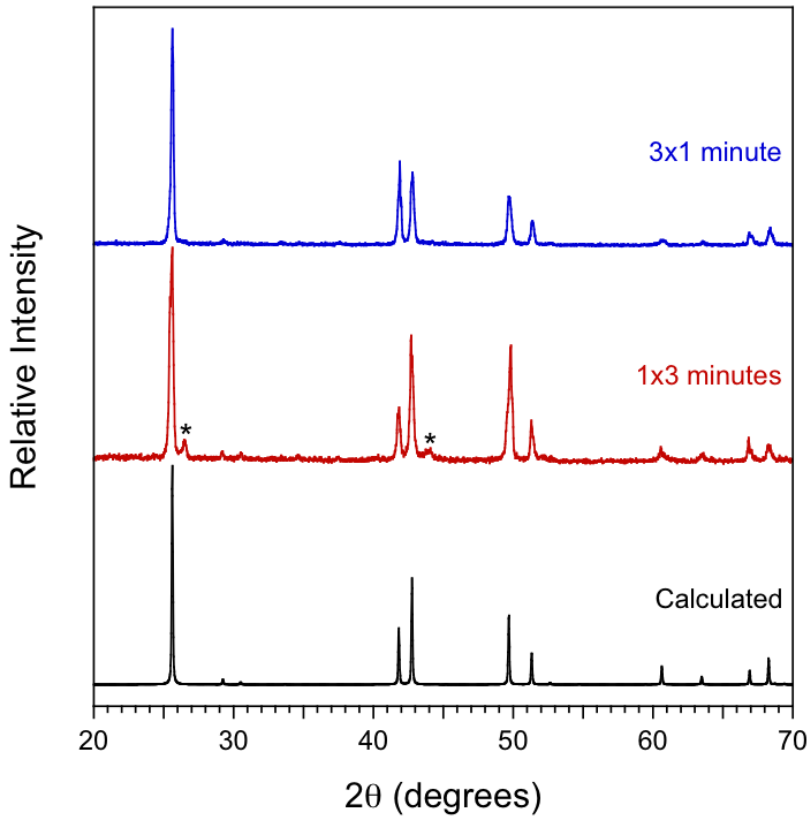

Figure 3.4. Powder X-ray diffraction patterns obtained for select microwave reactions with different irradiation procedures, 1, 3-minute interval and 3, 1-minute intervals, compared to the calculated pattern for $AgInSe_2$.[174] All three samples were ground for 20 min and were calculated to yield 4.5 mmol of product. The asterisks mark diffraction peaks due to the presence of $AgIn_5Se_8$.[195,196]

We initially set out to explore reactant grinding times from 10 to 60 minutes using 2 mmole samples, irradiated for 3, one-minute intervals; however, we discovered that the starting material reacted during grinding after approximately 35 minutes. Additionally, a sample that was ground for 30 minutes reacted on the vacuum line while the tube was being sealed. This was later avoided by cooling the sample using liquid N_2 during the

sealing process, resulting in no observable prereaction. PXRD patterns of the reaction products indicated that there was an optimal grinding time of 20 minutes, Figure 3.5. Samples which were ground for shorter or longer periods of time contained a significantly greater amount of the alternate phase. One would expect that increased grinding time would result in a more homogeneous reagent mixture and, subsequently, a more phase-pure product; however, this is not supported by the data. The fact that the sample ground for 30 minutes yielded a less phase-pure product than that ground for 20 minutes could possibly be due to a visibly unnoticable pre-reaction that could have occurred during the grinding of the reagents or the sealing of the tube.

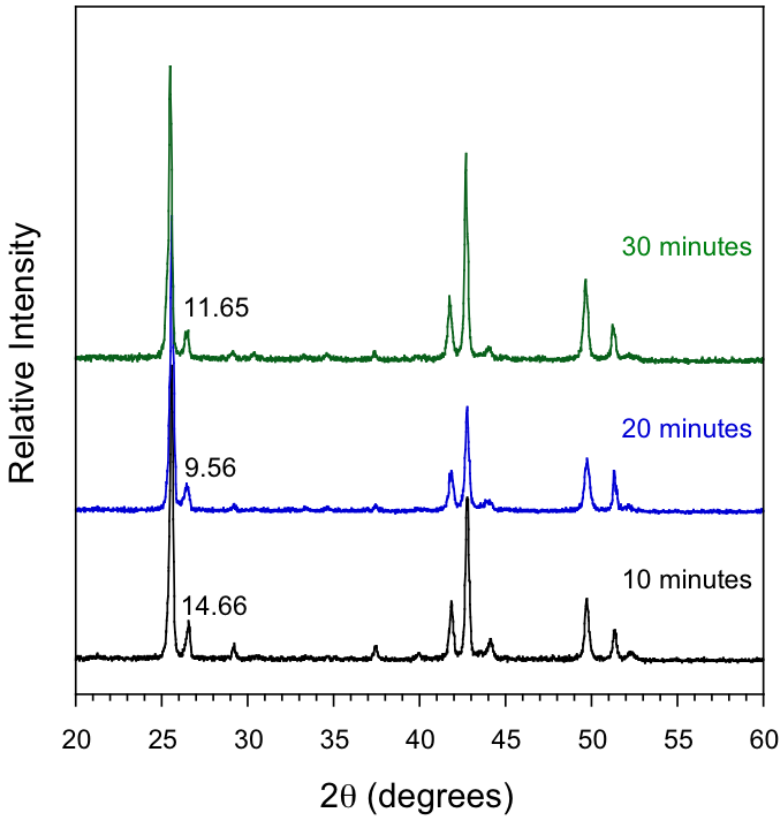

Figure 3.5. Powder X-ray diffraction patterns obtained for select microwave reactions ground for different amounts of time compared to the calculated pattern for $AgInSe_2$.[174] All three samples were ground for 20 min and were calculated to yield 2 mmol of product. The relative values of the impurity phase in each sample are found above the primary diffraction peak of $AgIn_5Se_8$.[195,196]

In an attempt to prepare phase-pure $AgInSe_2$, products of microwave reactions that contained a small amount of $AgIn_5Se_8$,[195,196] the alternate phase, were reground for 20 minutes and re-irradiated using the 3, one-minute irradiation procedure. As a result, the phase purity of all of the reground and re-irradiated samples increased, in some cases resulting in phase-pure $AgInSe_2$. Regrinding and re-irradiating is the only method, thus

far, that yielded phase-pure $AgInSe_2$, Figure 3.6. In an ideal situation, the experiment would begin with perfectly mixed starting material so that regrinding and re-irradiating would not be necessary.

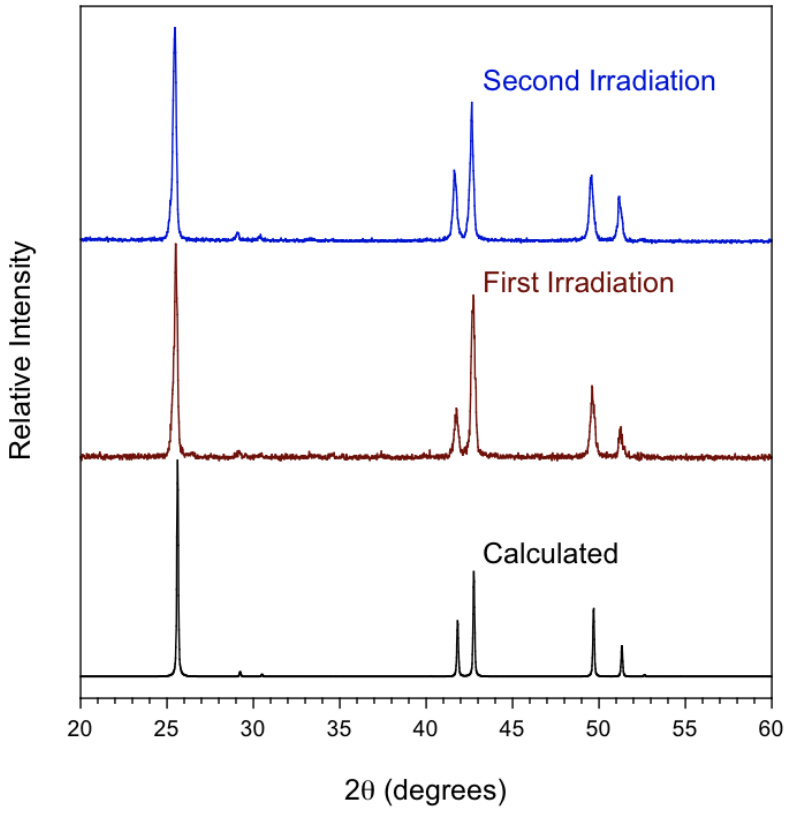

Figure 3.6. Powder X-ray diffraction patterns obtained for one sample that was irradiated twice compared to the calculated pattern for $AgInSe_2$.[174] The sample was reground prior to the second irradiation. Phase-pure samples of $AgInSe_2$ could only be obtained by performing multiple irradiations on the same sample.

For comparison purposes a sample of $AgInSe_2$ was prepared in a furnace via traditional, high-temperature solid-state synthesis. The PXRD pattern of the sample prepared in the furnace was almost identical to the PXRD patterns from the microwave

prepared samples, Figure 3.7. The full width at half maximum (FWHM) of the diffraction peaks observed for the furnace and microwave prepared samples is not significantly different. This implies that samples prepared using microwave irradiation are as crystalline as the sample prepared by conventional heating in a furnace. Despite requiring regrinding and re-irradiating to obtain phase-pure samples, solid-state microwave synthesis requires decreased reaction times (6 min vs. 5280 min) and is therefore more energy efficient and a greener method compared to traditional, high-temperature synthesis.[175,176]

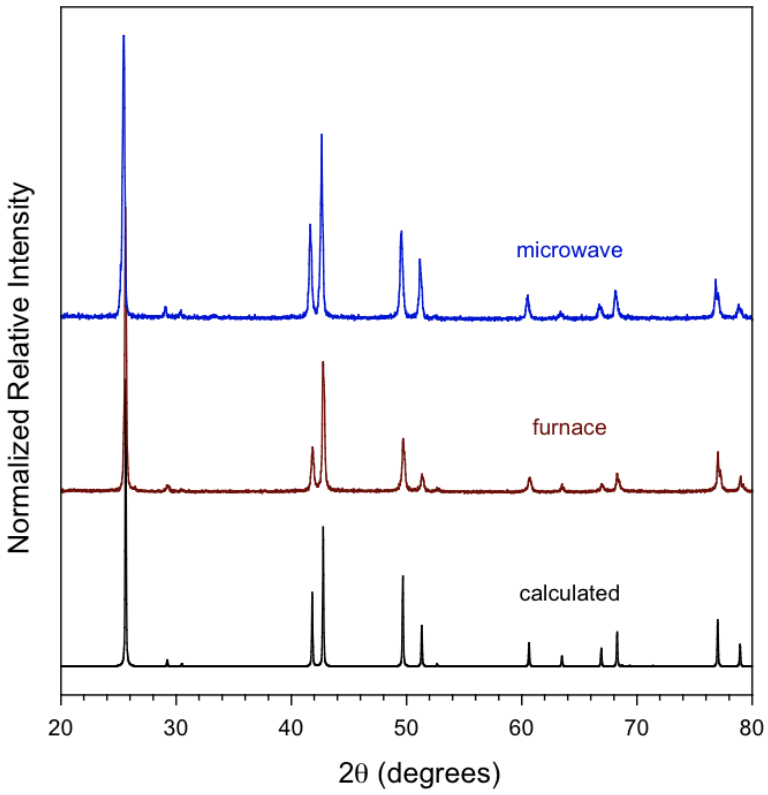

Figure 3.7. Powder X-ray diffraction patterns of $AgInSe_2$ prepared in the microwave (top), compared to $AgInSe_2$ prepared in a furnace (middle) and the calculated pattern (bottom).[174] One should observe that there is very little difference in the powder diffraction patterns of the microwave and furnace prepared samples and that these both match the calculated pattern.

3.3.2 Additional Charcterization

In addition to PXRD, diffuse reflectance UV/Vis/NIR measurements were carried out on samples of $AgInSe_2$, Figure 3.8. All bandgap measurements agree with the known value of 1.2 eV,[199] even though most products contain a minor amount of $AgIn_5Se_8$.[195,196]

The bandgap of $AgIn_5Se_8$, the alternate phase, is similar to $AgInSe_2$, the principal component in the samples.[200]

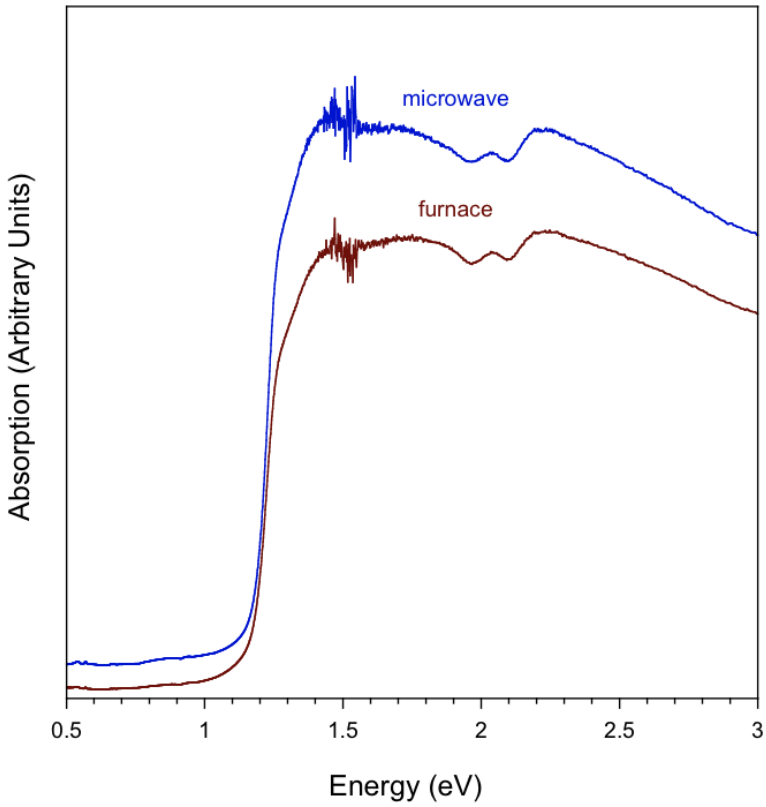

Figure 3.8. Optical diffuse reflectance spectra converted to absorption for $AgInSe_2$ prepared in the microwave and in the furnace. The energy gap, E_g, estimated from both spectra is 1.2 eV.

DTA indicated that the melting point of the samples prepared in the microwave was ~780 °C, which agrees with the reported value of 773 °C[201] and the value determined for the $AgInSe_2$ sample that was prepared traditionally, at 850 °C in a furnace.

3.3.3 Microwave Synthesis Mechanism

During the solid-state microwave reaction to form $AgInSe_2$, a plasma is observed in the tube. In an attempt to gain insight into the reaction of silver, indium and selenium

and the composition of the plasma observed during the reaction, the elements, as well as binary mixtures of the elements were irradiated.

A plasma was found to form during the irradiations of silver and indium. The plasma formed during the irradiation of silver was light blue in color, while that which formed during the irradiation of indium was a light purple, but changed to blue as the irradiation continued, Figure 3.7. When irradiated, the indium became so hot that the liquid metal melted the fused-silica tube, which has a melting point of ~1200 °C. Unlike silver and indium, the selenium did not form a plasma or heat during irradiation. Therefore, the plasma observed during the reaction to prepare $AgInSe_2$ is most likely due to the presence of the metals.

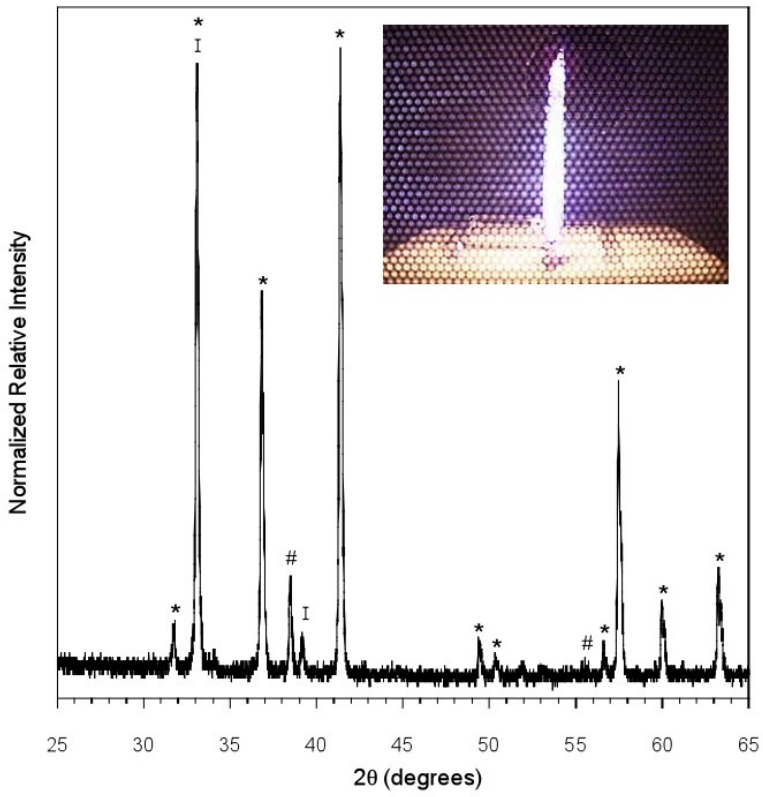

Figure 3.9. Powder X-ray diffraction pattern of the microwave reaction of Ag and In metal. $AgIn_2$ (*) was determined to be the major phase, while Ag_9In_4 (#) and In metal (I) were identified as additional components of the reaction product. The inset shows the pinkish-purple plasma observed during the microwave irradiation of powdered indium metal.

In addition to individual elements, irradiation of binary mixtures of silver, indium and selenium were carried out. Reactions were performed on a 2 mmole scale, using metal particles of the same mesh size as those used in the synthesis of $AgInSe_2$. The reaction of silver and indium in the same ratio (1:1) found in the reactions to synthesize $AgInSe_2$, yielded, $AgIn_2$,[202] Ag_9In_4,[203] and indium metal, Figure 3.9. Microwave irradiation of Ag and Se in a 1:2 ratio produced Ag_2Se[204] and elemental Se. When the ratio was adjusted to 2:1, the result was phase-pure Ag_2Se, Figure 3.10, as expected based on previous reports.[205] The reaction of indium and selenium in a 1:2 ratio, respectively, resulted in a mixture of several indium selenide phases and possibly elemental selenium. No elemental indium was present in this reaction product.

The results of this work differ from the results of similar experiments performed previously on the $CuInS_2$ system.[187,206] Since $CuInS_2$ and $AgInSe_2$ are both chalcogenides with the chalcopyrite structure, we expected them to have similar syntheses.[201] Due to this discrepancy, we attempted to reproduce the binary experiments with copper, indium and sulfur. The PXRD pattern of the product of a reaction of copper and indium in a 1:1 ratio consisted of diffraction peaks that could be indexed to copper metal, indium metal and the intermetallic compound $Cu_{11}In_9$,[207] contrary to previous reports that the two metals

segregated and did not form a compound.[187,206] A 1:2 mixture of Cu and S resulted in CuS[208] and S, just as previously observed, Figure 3.11.[187,206] The 1:2 mixture of In and S resulted in mostly In_2S_3,[209] InS[210] and S. It was previously reported that the mixture of In and S did not react and that the tube only warmed slightly as a result of microwave irradiation.[187,206]

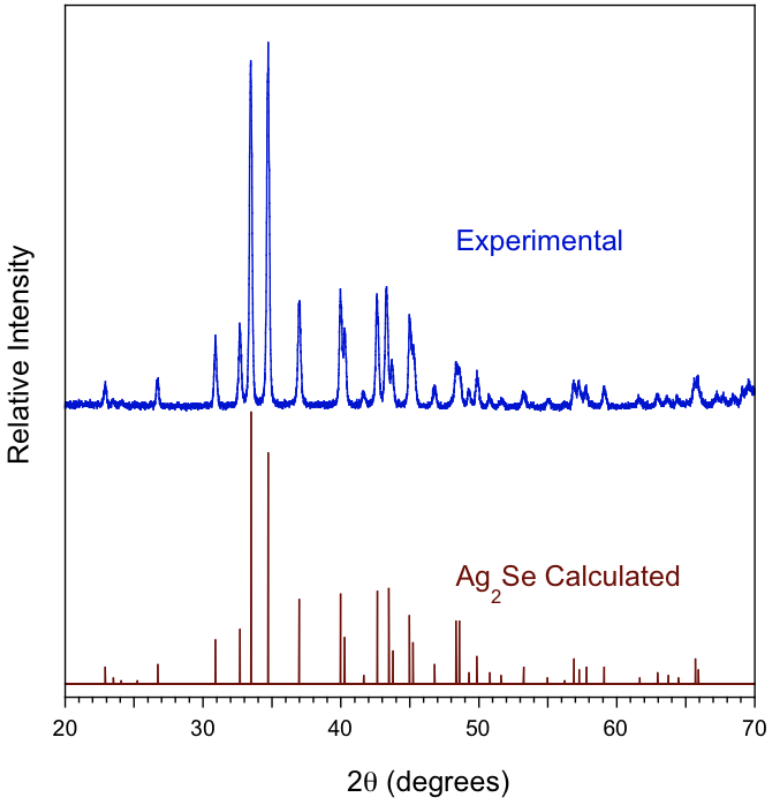

Figure 3.10. Powder X-ray diffraction pattern of the product of the 2:1 microwave reaction of Ag and Se. Initial reactions were performed using the ratio found in the irradiations to prepare $AgInSe_2$, 1:2. When the ratio of Ag to Se was adjusted from 1:2 to 2:1, the product was phase-pure Ag_2Se.

The differences between the previously reported results and those discussed here could be due to variations of the synthetic variables. These discrepancies exemplify the importance of the identification and control of synthetic variables to solid-state microwave synthesis. In this case, the dissimilar results could be explained by differing microwave power, microwave type, or a combination of these factors. All samples in this work were prepared in a 1000 W, research-grade microwave, while the previous experiments were performed in a 400 W, domestic microwave oven.[187,206] The 400 W microwave may not have heated the reactions to the same temperatures as those attained in the 1000 W microwave. The temperatures reached in these reactions should play a critical role in solid-state microwave synthesis. Additionally, domestic microwave ovens do not have as uniform a microwave field as those found in research-grade microwaves. Research-grade microwaves have a mode stirrer, which redirects microwaves as they enter the main cavity of the microwave. This results is the most homogenous field possible in a mutimode microwave. Any object placed into an electromagnetic field can distort the field. This means that the field could be distorted near the sample changing the uniformity of the field. The uniformity of the microwave field could also have an effect on the reaction outcome and the reproducibilty of the results. In an attempt to determine the extent of reproducibility of these reactions, the temperatures of these reactions will be monitored in future experiments. This will be accomplished using a modified microwave and optical pyrometry.

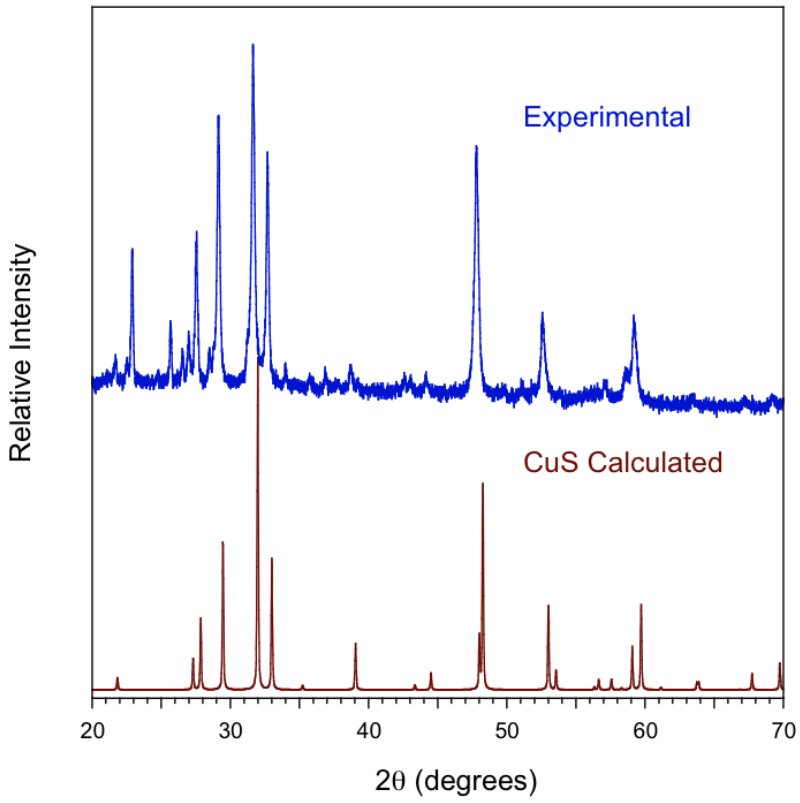

Figure 3.11. Powder X-ray diffraction pattern of the product of the microwave reaction of Cu and S. The primary product of this reaction was CuS, with a small impurity. This result agrees with that reported by Landry, *et. al.*[206]

Silver, indium and copper all heat within seconds of exposure to microwaves. Although sulfur and selenium do not heat when irradiated by themselves, they have low melting points and are relatively volatile, allowing them to get involved in these reactions relatively quickly. Additionally, every binary reaction occurs rapidly. Therefore, if the reactions to prepare $AgInSe_2$ and $CuInS_2$ are indeed step-wise, it is not possible to determine the steps with the current data and experimental set-up.

3.4 Conclusions

We have shown that sample volume, irradiation time, irradiation procedure and reactant grinding time have a profound effect on the phase purity of the products obtained from solid-state microwave reactions. Sample volume should be proportional to the power absorbed, as in microwave solution chemistry; therefore, samples that are too small may not fully react, while samples that are too large may exceed the microwave penetration depth. An increase in the reactant grinding time increases the phase purity of the product, unless prereaction occurs prior to microwave irradiation. Identification and discussion of reaction variables in solid-state microwave synthesis is crucial, in order to ensure experimental reproducibility and encourage other researchers to make use of this synthetic approach. Better understanding of this technique and increasing the possibility of reproducible results are vital steps forward in the adaptation and implementation of microwave synthesis to prepare solid-state materials.

3.5 References

[167] P.J. Walter, S. Chalk, and H.M. Kingston, in *Microwave-Enhanced Chemistry: Fundamentals, Sample Preparation, and Applications* H. M. Kingston and S.J. Haswell, eds., The American Chemical Society; Washington, DC, 1997, ch. 2, pp. 55.

[168] D.K. Agrawal, *Curr. Opin. Solid St. M.* **1998**, *3*, 480.

[169] C.O. Kappe, *Angew. Chem. Int. Ed.* **2004**, *43*, 6250.

[170] P. Lidström, J. Tierney, B. Wathey, and J. Westman, *Tetrahedron* **2001**, *57*, 9225.

[171] A.G. Whittaker and D.M.P. Mingos, *J. Microwave Power E.E.* **1994**, *29*, 195.

[172] N.A. Goryunova *The Chemistry of Diamond-like Semiconductors* J. C. Anderson, ed., The MIT Press; Cambridge, MA, 1965.

[173] E. Parthé *Crystal Chemistry of Tetrahedral Structures* Gordon and Breach Science Publishers, New York, NY, 1964.

[174] P. Benoit, P. Charpin, R. Lesueur, and C. Djeda-Mariadassou, *Jpn. J. Appl. Phys.* **1980**, *19*, 85.

[175] M. Ješelnik, R.S. Varma, S. Polanc, and M. Kočevar, *Green Chem.* **2002**, *4*, 35.

[176] C. Villa, E. Mariani, A. Loupy, C. Grippo, G.C. Grossi, and A. Bargagna, *Green Chem.* **2003**, *4*, 35.

[177] A.G. Whittaker, *Chem. Mater.* **2005**, *17*, 3426.

[178] (a) R. Roy, D. Agrawal, J. Cheng, and S. Gedevanishvili, *Nature* **1999**, *399*, 668. (b) R.Roy, D. Agrawal, J. Cheng, and S. Gedevanishvili, *Nature* **1999**, *401*, 304.

[179] U.R. Pillai, E. Sahle-Demessie, and R.S. Varma, *Appl. Catalysis A* **2003**, *252*, 1.

[180] M.P. Mingos, and D.R. Baghurst, in *Microwave-Enhanced Chemistry: Fundamentals, Sample Preparation, and Applications*, H.M. Kingston, S.J. Haswell, eds., The American Chemical Society; Washington, DC, 1997, ch. 10, pp. 523.

[181] K.J. Rao, B. Vaidhyanathan, M. Ganguli, and P.A. Ramakrishnan, *Chem. Mater.* **1999**, *11*, 882.

[182] G.R. Robb, A. Harrison, and A.G. Whittaker, *Phys. Chem. Comm.* **2002**, *5*, 135.

[183] A. Harrison, R. Ibberson, G. Robb, G. Whittaker, C. Wilson, and D. Youngson. *Faraday Discuss.* **2002**, *122*, 363.

[184] A.G. Whittaker, and D.M.P. Mingos, *J. Chem. Soc. Dalton Trans.* **1992**, 2751.

[185] D.R. Baghurst, A.M. Chippindale, and D.M.P. Mingos, *Nature* **1988**, *332*, 311.

[186] B. Vaidhyanathan, M. Ganguli, and K.J. Rao, *Mater. Res. Bul.* **1995**, *30*, 1173.

[187] C.C. Landry, and A.R. Barron, *Science* **1993**, *260*, 1653.

[188] G.-T. Zhou, V.G. Pol, O. Palchik, R. Kerner, E. Sominski, Y. Koltypin, and A. Gedanken, *J. Solid State Chem.* **2004**, *177*, 361.

[189] G.-T. Zhou, V.G. Pol, O. Palchik, R. Kerner, E. Sominski, Y. Koltypin, and A. Gedanken, *J. Solid State Chem.* **2004**, *177*, 361.

[190] B. Vaidhyanathen, and K.J. Rao, *Chem. Mater.* **1997**, *9*, 1196.

[191] J.D. Houmes, and H.C. zur Loye, *J. Solid State Chem.* **1997**, *130*, 266.

[192] G.-T. Zhou, O. Palchik, V.G. Pol, E. Sominski, Y. Koltypin, and A. Gedanken, *J. Mater. Chem.* **2003**, *13*, 2607.

[193] M. Vondrova, T. Klimczuk, V.L. Miller, B.W. Kirby, N. Yao, R.J. Cava, and A.B. Bocarsly, *Chem. Mater.* **2005**, *17*, 4755.

[194] P. Kubelka, and F. Munk, *Zeitschrift fur Technishen Physik*, tr. Stephen H. Westin, **1932**, *12*, 112.

[195] P. Benoit, P. Charpin, and C. Djega-Mariadassou, *Mater. Res. Bull.* **1983**, *18*, 1047.

[196] AgIn5Se8 is an ordered defect structure of AgInSe2. L. S. Palatnik and E. I. Rogacheva, *Neorg. Mater.* **1995**, *2*, 478.

[197] The material is considered to be phase-pure if the product of the reaction contains only a single component/phase.

[198] S.A. Freeman, J.H. Booske and R.F. Cooper, *Phys. Rev. Lett.* **1995**, *74*, 2042.

[199] J.L. Shay, B. Tell, H.M. Kasper, and L.M. Schiavone, *Phys. Rev. B* **1973**, *7*, 4485.

[200] P. Benoit, C. Djega-Mariadassou, R. Lesueur and J. H. Albany, *Phys. Lett.* **1979**, *73A*, 55.

[201] J.L. Shay, and J.H. Wernick, *Ternary Chalcopyrite Semiconductors: Growth, Electronic Properties and Applications*, Pergamon Press; Oxford, 1975, ch. 2, 3.

[202] E.E. Havinga, H. Damsma, and P. Hokkeling, *J.Less-Common Met.* **1972**, *27*, 169.

[203] J.K. Brandon, R. Brezard, W.B. Pearson, and D.J.N. Tozer, *Acta Crystallogr. B* **1977**, *B33*, 527.

[204] G.A. Wiegers, *Am. Mineral.* **1971**, *56*, 1882.

[205] S.S. Manoharan, S.J. Prasanna, D.E. Kiwitz, and C.M. Schneider, *Phys. Rev.* **2001**, *B63*, 212405.

[206] C.C. Landry, J. Lockwood, and A.R. Barron, *Chem. Mater.* **1995**, *7*, 699.

[207] T.P. Rajasekharan, and K. Schubert, *Z. Metallkd.* **1981**, *72*, 275.

[208] Y. Takeuchi, Y. Kudoh, and G. Sato, *Z. Kristallogr.* **1985**, *173*, 119.

[209] *Natl. Bur. Stand. (U.S.) Monogr. 25*, **1974**, *11*, 30.

[210] U. Schwarz, H. Hillebrecht, and K. Syassen, *Z. Kristallogr.* **1995**, *210*, 494.

4 Microwave Metallurgy: Synthesis of Intermetallic Compounds via Microwave Irradiation

4.1 Introduction

For years, we have been told not to put metals in the microwave. A close examination of the literature, however, reveals that *powdered* metals can be used to synthesize a wide variety of compounds in a microwave. Carbides, borides, halides, nitrides and chalcogenides have all been prepared via solid-state microwave synthesis from precursors that included powdered metals, metal oxides or metal halides.[211-216] A logical extension of this work would be to synthesize intermetallic compounds via the solid-state microwave synthetic method. However, the current understanding of the interactions of solids with microwaves has limited the use of this method for the preparation of intermetallics.[211a]

Intermetallic compounds are useful for applications including hydrogen storage,[217] electronics[218] and catalysis[219] and exhibit intriguing properties such as superconductivity[212,213,220] and ferromagnetism.[221] However, these compounds are normally difficult and time-consuming to synthesize due to the large energy barrier for the diffusion of solids. Traditionally, intermetallic compounds have been prepared by high-temperature solid-state synthesis, using a furnace, and/or arc melting. Solid-state microwave synthesis offers a quicker and greener option, due primarily to the short reaction times.[222] Recently, several intermetallic compounds such as Li_3Bi and Li_3Sb, have been prepared in a microwave in only a few minutes.[223] In related work, Bocarsly and coworkers reported the solid-state transformation of a cyanogel to an alloy with the aid of

microwave radiation.[224] Here we report on the general synthesis of a variety of intermetallic compounds using the solid-state microwave synthetic method.

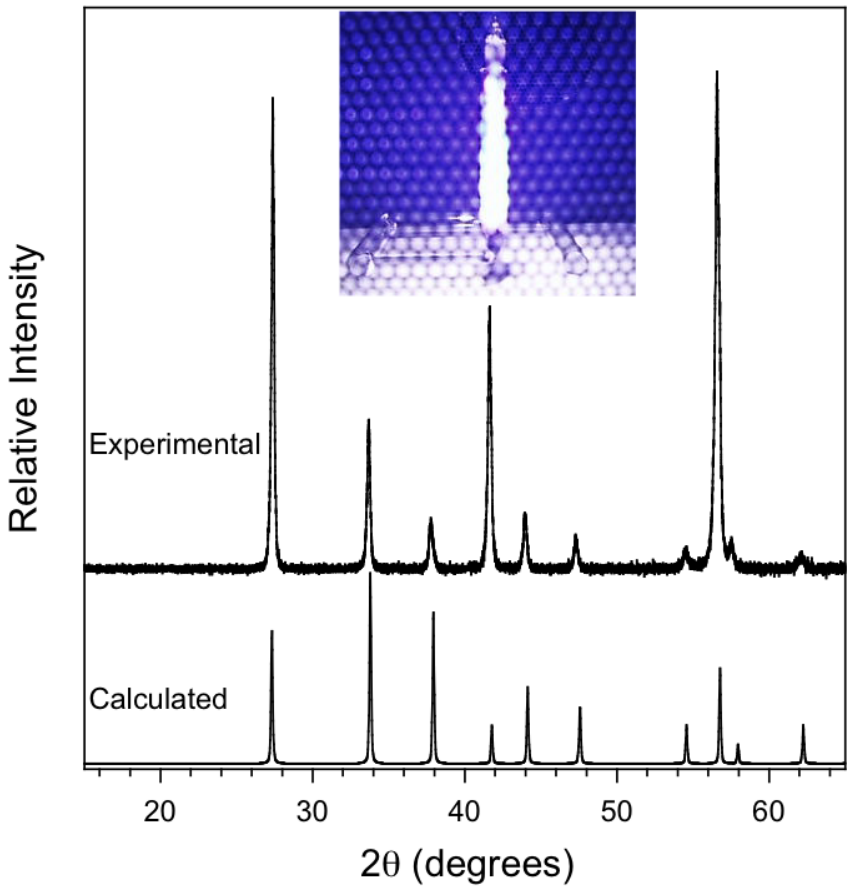

Figure 4.1.Powder X-ray diffraction pattern of a sample of phase-pure Bi_2Pd prepared by solid-state microwave synthesis compared to Bi_2Pd (JCPDS 00-013-0160). Experimental intensities vary from the reference pattern due to the inability to effectively grind the soft ingot that was obtained after reaction. The inset shows a digital photo of the reaction to make Bi_2Pd taken through the microwave door. The reaction tube is situated in a vertical fused-silica holder, which is barely visible in the photo. The holder is placed on top of a quartz brick, which is positioned in the center of the microwave cavity floor.

The intermetallic compounds that have been prepared in this work by solid-state microwave synthesis have a variety of uses. Ag_3In is used as a solder in the electronics industry due to its increased corrosion resistance compared to pure silver. It can be prepared electrochemically as a coating in a relatively short time;[218] but, bulk preparation of Ag_3In, for property measurements, requires 48 hours using a furnace.[225] Solid-state microwave synthesis reduces this preparation time to only 2 minutes. Recently, Bi_2Pd has been investigated for catalytic purposes, specifically, the oxidation of glucose to gluconic acid.[226] Bi_2Pd supported on SiO_2 for catalytic research has been prepared in about 12 hours,[226] and bulk Bi_2Pd has been synthesized via arc melting.[227] Solid-state microwave synthesis offers a relatively simple alternative to synthesize Bi_2Pd in as little as 4 minutes, Figure 4.1.

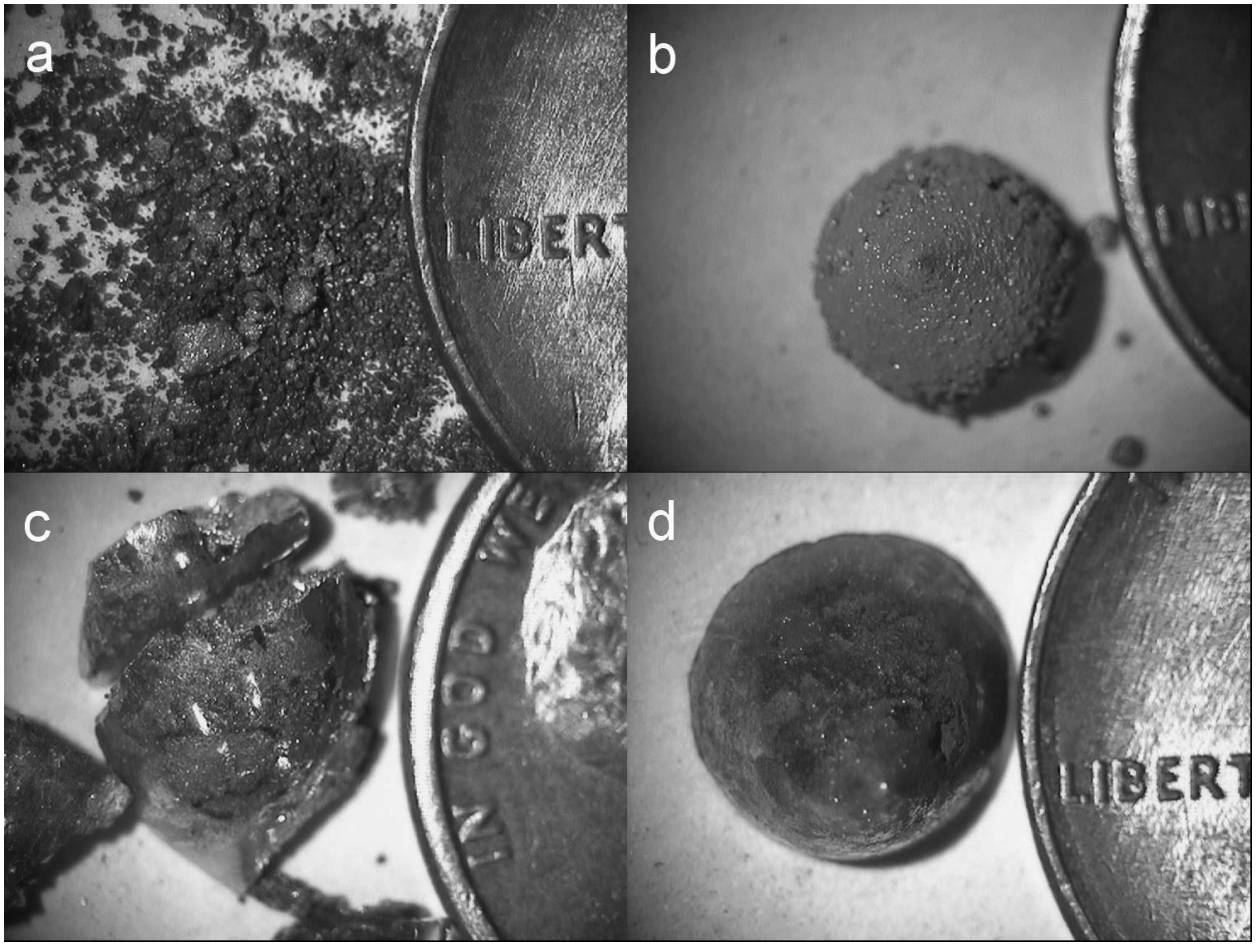

Figure 4.2. Images obtained with a digital microscope show a variety of morphologies that can result from solid-state microwave synthesis: (a) Bi_3Ni, a sintered powder; (b) $AuIn_2$, a sintered ingot; (c) Bi_3In_5, a cracked ingot; and (d) Bi_2Pd, a solid ingot. A penny was used as a scale in the images.

One important aspect of these reactions is their expeditious nature; products are always prepared in much less time than a traditional, high-temperature solid-state reaction. Within seconds of applying microwave radiation to the sample, a brilliant plasma, Figure 4.1, is formed above the metal powders and the reactants begin to heat. In as little as a couple of seconds, materials can reach high temperatures in the range of 500-1100 °C, or greater. The products can

exhibit a number of different morphologies ranging from sintered powders to solid ingots, Figure 4.2.

4.2 Experimental

4.2.1 Reagents

Silver metal powder, -325 mesh, 99.99%, Cerac; indium metal powder, 99.99%, Strem; bismuth metal powder, -200 mesh, 99.999%, Cerac; palladium metal powder, -60 mesh, 99.95%, Strem; nickel metal powder, -325 mesh, 99%, Sargent and Welch; and gold metal powder, -325 mesh, 99.95%, Cerac were used as obtained.

4.2.2 Ag_3In

Stoichiometric amounts of the elemental starting materials to make 1 mmol of product were weighed out and placed into a 9 mm o.d. fused-silica tube. Samples were not ground to prevent smearing of the soft metals. The tube was then sealed under a vacuum of approximately 10^{-3} mbar and shaken vigorously to mix the silver and indium. The sealed tube was placed into a vertical sample holder in a CEM MDS 2100 microwave that was set to irradiate the sample for 2, one-minute intervals at 100 % power. The sample was removed from the microwave and shaken in between intervals. Following irradiation, the tube was opened under ambient conditions and the sample was collected and analyzed.

4.2.3 $AuIn_2$

Stoichiometric amounts of the elemental starting materials to make 3 mmol of product were weighed out and placed into a 9 mm o.d. fused-silica tube. Samples were not ground to prevent smearing of the soft metals. The tube was then sealed under a vacuum of approximately 10^{-3} mbar and shaken vigorously to mix the gold and indium. The sealed tube was placed into a vertical sample holder in a CEM MDS 2100 microwave that was set to irradiate the sample for 10 minutes at 100 % power. Following irradiation, the tube was opened under ambient conditions and the sample was collected, analyzed and ground. After grinding the sample was placed into a 9 mm o.d. fused-silica tube and sealed under a vacuum of 10^{-3} mbar. The tube was again placed into a vertical sample holder in a CEM MDS 2100 microwave and irradiated for 10 minutes at 100 % power. Following the second irradiation the sample was removed from the tube under ambient conditions and analyzed.

4.2.4 Bi_2Pd

Stoichiometric amounts of the elemental starting materials to make 1 mmol of product were weighed out and placed into a 9 mm o.d. fused-silica tube. Samples were not ground to prevent smearing of the soft metals. The tube was then sealed under a vacuum of approximately 10^{-3} mbar and shaken vigorously to mix the bismuth and palladium. The sealed tube was placed into a vertical sample holder in a CEM MDS 2100 microwave that was set to irradiate the sample for 10 minutes at 100 % power. Reactions were stopped after approximately 4 minutes to prevent implosion of the tube. Following irradiation, the tube was opened under ambient conditions and the sample was collected and analyzed.

4.2.5 Bi_3Ni

Stoichiometric amounts of the elemental starting materials to make varying amounts of product were weighed out and placed into a 9 mm o.d. fused-silica tube. Samples were not ground to prevent smearing of the metals. The tube was then sealed under a vacuum of approximately 10^{-3} mbar and shaken vigorously to mix the bismuth and nickel. The sealed tube was placed into a CEM MDS 2100 microwave that was set to irradiate the sample for 10 minutes at 100 % power. Both vertical and horizontal sample holders were used for samples of Bi_3Ni to determine the effect of sample geometry on the phase-purity of the product. Following irradiation, the tube was opened under ambient conditions and the sample was collected and analyzed.

4.2.6 Bi_3In_5

Stoichiometric amounts of the elemental starting materials to make 1 mmol of product were weighed out and placed into a 9 mm o.d. fused-silica tube. Samples were not ground to prevent smearing of the soft metals. The tube was then sealed under a vacuum of approximately 10^{-3} mbar and shaken vigorously to mix the bismuth and indium. The sealed tube was placed into a vertical sample holder in a CEM MDS 2100 microwave that was set to irradiate the sample for 10 minutes at 100 % power. Following irradiation, the tube was opened under ambient conditions and the sample was collected and analyzed.

4.3 Results and Discussion

Our work with the above compounds, in addition to those described in Table 4.1, demonstrates that solid-state microwave synthesis of alloys and intermetallics is not an isolated phenomenon for a few selected substances. We believe that given any reaction between two or more powdered metals to form an alloy or intermetallic, if at least one metal can be an absorber of the microwave radiation, the reaction should proceed. Using this synthetic method, we have prepared a variety of intermetallic compounds, Table 4.1. The list includes compounds containing main group and transition metals. It was observed that all group 11 elements formed intermetallic compounds with indium upon microwave irradiation, contrary to previous reports, which state that irradiation of copper and indium resulted in phase segregation.[215]

One caveat of this method is that there are many important synthetic variables that can have a profound effect on the reaction outcome. Some of our previous work has documented this fact.[228] For some intermetallic compounds, we optimized their syntheses in order to find the proper conditions to prepare phase-pure products; in the process, the effect of irradiation time and sample quantity was studied. For other systems, only a few reactions were performed, until the desired product was the major phase; further synthesis optimization is still necessary, Table 4.1.

Table 4.1. Intermetallic compounds prepared by our laboratory using solid-state microwave synthesis

Target Compound	Elemental Ratio	Irradiation Time (min)	Product Phase(s)*
$Cu_{11}In_9$	1:1	3 x 1	Cu, $Cu_{11}In_9$, In
Ag_3In	3:1	2 x 1	Ag_3In
$AgIn_2$	1:2	2 x 1	$AgIn_2$, Ag_9In_4
Ag_9In_4	9:4	2 x 1	Ag_9In_4, $AgIn_2$
$AuIn_2$	1:2	2 x 10	$AuIn_2$
Bi_3In_5	3:5	1 x 10	Bi_3In_5, BiIn
Bi_3Ni	3:1	1 x 10	Bi_3Ni, Bi
Bi_2Pd	1:2	1 x 4	Bi_2Pd

*Product phases were identified using powder X-ray diffraction. The first product listed is the major phase of the reaction, followed by minor phases.

Keeping all other variables constant, irradiation time in the Ag-In system was found to have an important effect on the product, with pure Ag_3In[229] being obtained only when the sample was irradiated for 2 minutes, Figure 4.3. When the reaction time was either increased or decreased by one minute, the resulting samples contained little or no Ag_3In; instead, the products were mixtures of Ag_9In_4,[230] $AgIn_2$[231] and indium. Using a constant irradiation time of ten minutes, the effect of sample quantity was studied in the Au-In system. The phase purity, of samples intended to synthesize 1 to 3 mmols of $AuIn_2$, increased as the sample quantity was increased, the only impurities being a small amount of unreacted starting material.

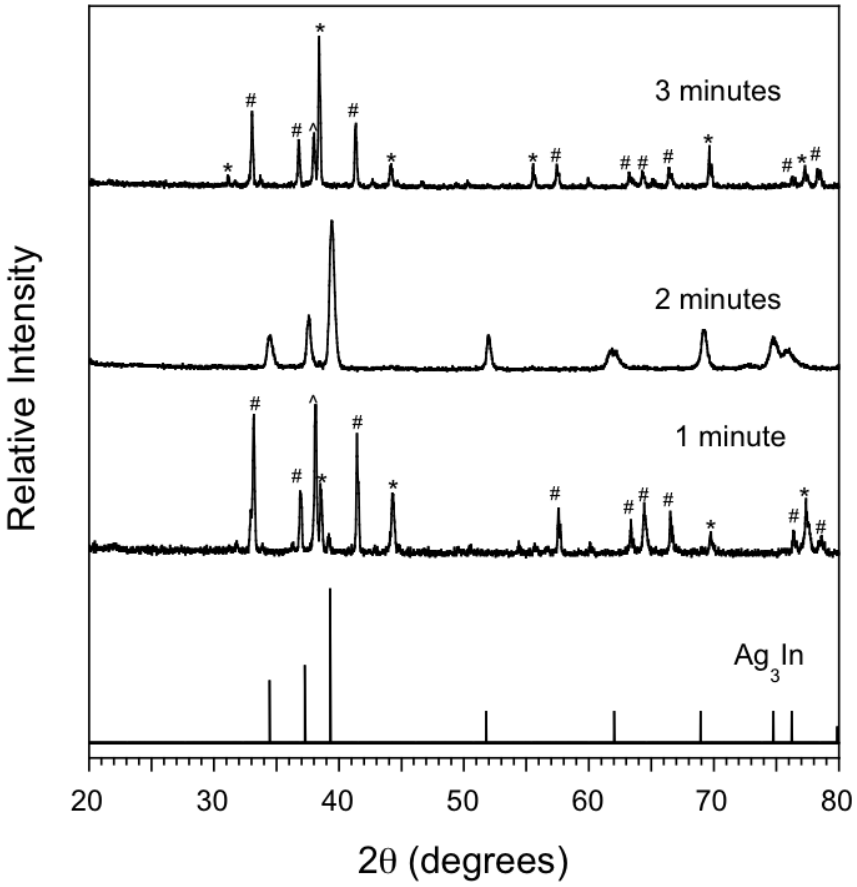

Figure 4.3. Powder X-ray diffraction patterns obtained for selected microwave reactions intended to produce 1 mmol of Ag_3In, irradiated for different time periods 3, 2, and 1 min, compared to Ag_3In (JCPDS 00-015-0163). Peaks due to $AgIn_2$ (JCPDS 00-025-0386), Ag_9In_4 (JCPDS 00-029-0678), and indium (JCPDS 01-071-0128) are indicated with *, # and ^, respectively.

For some unsuccessful reactions to prepare intermetallics via solid-state microwave synthesis, the product contained no competing phases. Instead, the unwanted diffraction peaks were attributed to unreacted starting material. In these cases, there are several possible reasons for incomplete reaction; the first is that the sample did not have enough time for the reaction to

go to completion. It is also possible that the sample did not couple strongly with the microwave field and does not absorb the energy necessary to completely react. Another possibility is that the starting mixture is not homogenous because the starting materials could not be ground. However, in some cases where the starting materials are very soft and cannot be ground, gold and indium for example, the corresponding *product*, $AuIn_2$, is brittle enough to grind. In these situations the product was analyzed using powder diffraction and if found to contain unreacted starting material it was irradiated for a second 10 minute interval. For $AuIn_2$, the result of a second irradiation is phase-pure $AuIn_2$, Figure 4.4. The second grinding step and subsequent irradiation are most likely necessary because the staring materials cannot be properly mixed due to the metals being soft. Grinding after the first irradiation homogenizes the sample so that the subsequent irradiation produces a phase-pure product.

In other cases where it was determined that the reaction product contained unreacted starting material, the product mixture could not be replaced in the microwave and irradiated for additional time because it could not be ground effectively. If the product could not be ground the "particle size" would be rather large, making the sample a microwave reflecting instead of microwave absorbing. In an attempt to take the reactions to completion before a change in absorptivity rendered this impossible, longer irradiation times were tested.

In some reactions, such as Bi-Pd, one must be careful when increasing irradiation time. These reactions can reach temperatures in excess of 1100 °C in as little as two minutes. In these cases, we have difficulty conducting the experiment in fused-silicia ampoules because, the tube *implodes*, as the fused-silica softens at elevated temperatures. To date, there have been no *explosions* during the synthesis of intermetallic compounds in our microwave. However, one should always exercise caution. These experiments were all conducted in a reinforced, research-

grade microwave; domestic microwaves are not recommended for the heating of metals.[232] Even with a research-grade microwave, there are still safety issues that should be addressed.[233]

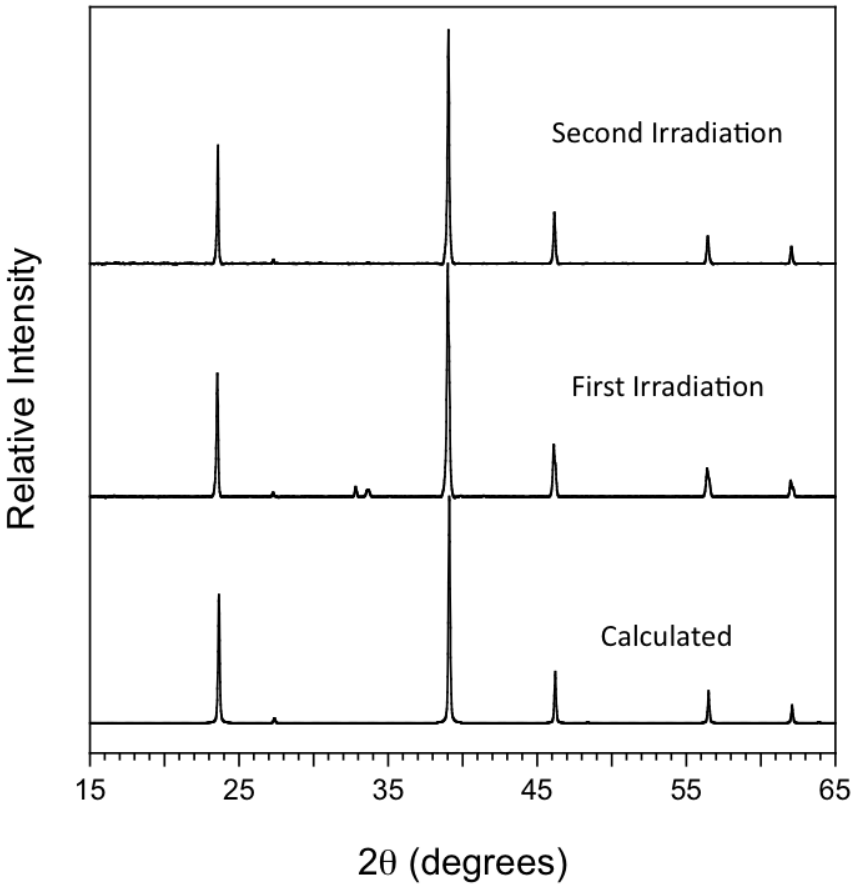

Figure 4.4. Powder X-ray diffraction patterns showing the improved phase purity of a sample of $AuIn_2$ that was irradiated, then ground and irradiated a second time. The patterns are compared to $AuIn_2$ (JCPDS 03-065-2993).

In some cases, longer irradiation times were still not enough to result in a phase-pure product and the samples could not be irradiated a second time. One such compound is Bi_3In_5. A reaction mixture to synthesize one mmol was prepared and irradiated for ten minutes, but was

found to contain a small amount of BiIn, Figure 4.5. The product was soft and could not easily be ground, which precluded attempting to perform a second irradiation. Additional experiments were not attempted, but there is still room for exploration in this system.

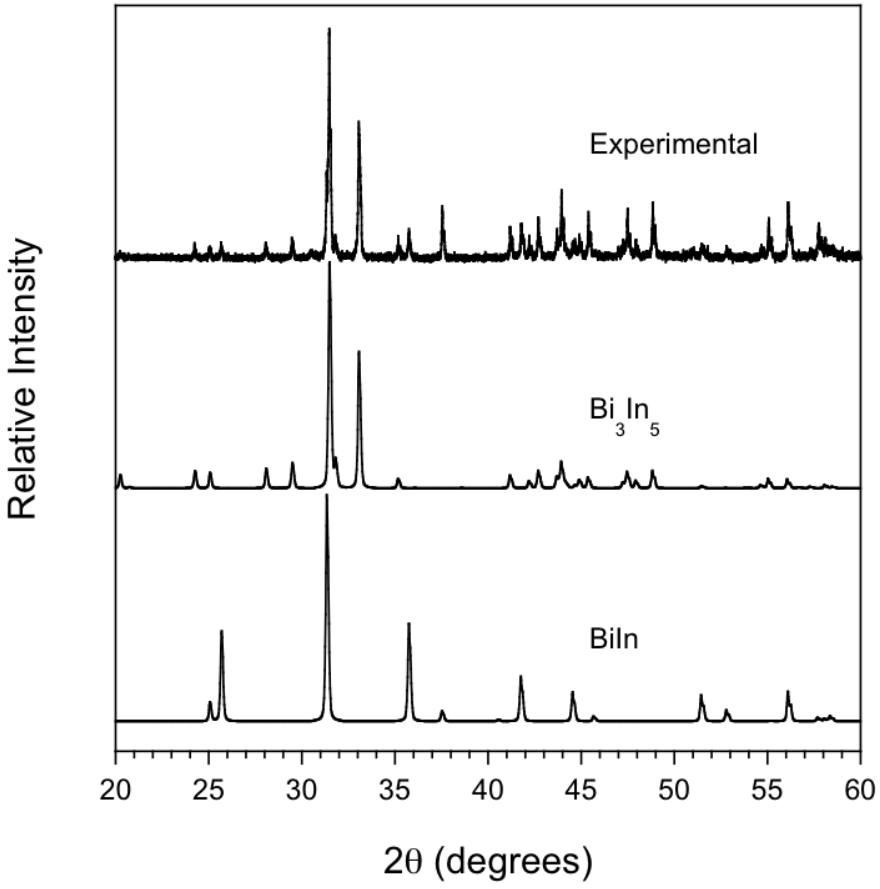

Figure 4.5. Powder X-ray diffraction patterns obtained for selected microwave reactions intended to produce 1 mmol of Bi_3In_5, compared to Bi_3In_5 (JCPDS 01-071-0225) and BiIn (JCPDS 01-085-0343).

Experiments were also conducted to prepare Bi_3Ni. The effects of sample volume and sample geometry on the phase-purity of the product were examined using 1, 2 and 3 mmol samples. Sample geometry is intimately linked to the orientation of powdered samples in the

microwave, due to the powdered samples being free to flow and take the shape of their container.[234] If the sample is placed into the microwave vertically, the powdered sample collects into a compact space at the bottom of the tube. Conversely, if the sample is placed into the microwave horizontally, the sample can spread out to cover the length of the tube, resulting in a longer, thinner sample than in the vertical orientation. The samples of various volumes were first irradiated in a vertical orientation. The products consisted of a large amount of unreacted bismuth and the intermetallic Bi_3Ni. Unreacted nickel could not be observed by powder X-ray diffraction due to the nickel being amorphous. The reaction to prepare 3 mmol Bi_3Ni was the sample that appeared to be the most phase-pure of the vertical reactions. Samples of various volumes were then irradiated in a horizontal orientation to determine if this could improve the phase-purity of the products. Instead it was determined that horizontal irradiation resulted in products with decreased phase purity compared to samples irradiated horizontally, Figure 4.6. Grinding of the samples and a second irradiation were not tested, but could potentially result in samples with increased phase-purity.

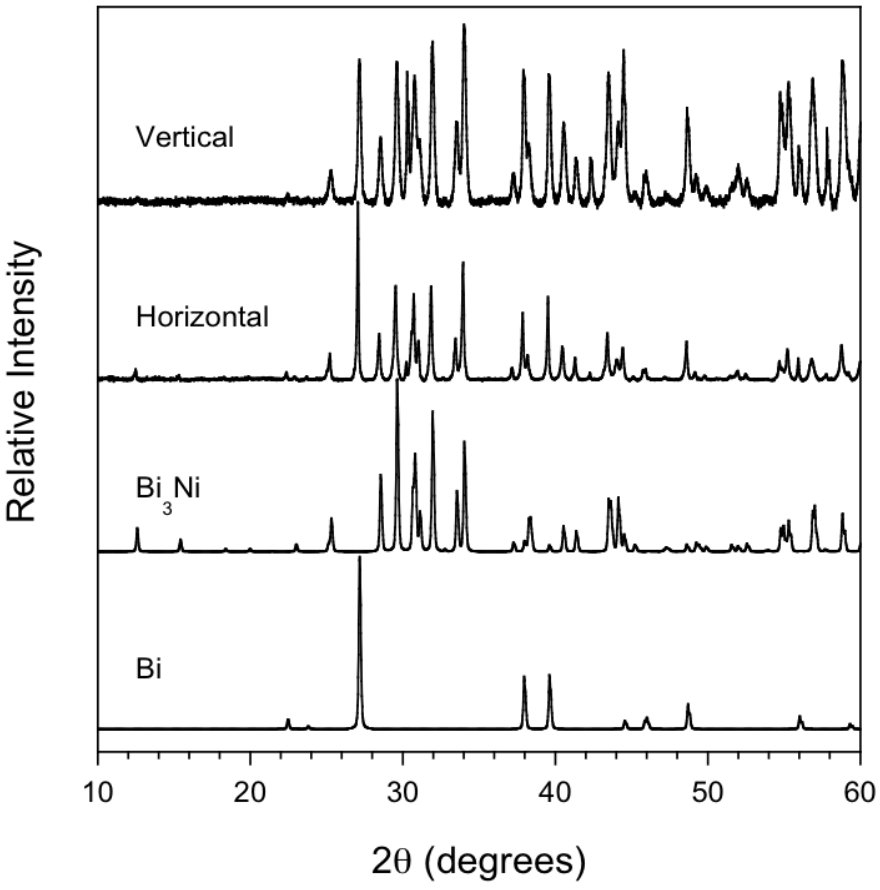

Figure 4.6. Powder X-ray diffraction patterns of two samples to prepare 3 mmol of Bi_3Ni. One sample was irradiated in a vertical sample holder while the other was irradiated in a horizontal sample holder. Both were irradiated for one, ten-minute interval. The patterns are compared to Bi_3Ni (JCPDS 03-065-0088) and Bi (JCPDS 00-044-1246).

4.4 Conclusions

In conclusion, solid-state microwave synthesis has proven to be a viable method for the preparation of a wide variety of intermetallic compounds. Three compounds Bi_2Pd, $AuIn_2$ and Ag_3In have been prepared phase-pure by optimizing the synthetic variables of this technique.

Additional experimentation with synthetic variables, such as sample geometry, is required to optimize the synthesis of additional intermetallic compounds. This method contributes to a relatively new palette of several other nontraditional techniques, such as metal fluxes,[235] mixed-metal eutectic fluxes[236] and solution methods,[237,238] which provide convenient avenues towards the synthesis of intermetallics. Reaction times for solid-state microwave synthesis are greatly reduced compared to other synthetic methods. Though this method is not without its caveats, we believe it has real potential in this area because many of these intermetallic compounds are of technological interest and a quicker, greener synthetic method[222] could be advantageous to their development.

4.5 References

[211] (a) Rao, K. J.; Vaidhyanathan, B.; Ganguli, M.; Ramakrishnan, P. A. *Chem. Mater.* **1999**, *11,* 882. (b) Vaidhyanathan, B.; Ganguli, M.; Rao, K. J. *Mater. Res. Bull.* **1995**, *30,* 1173. (c) Vaidhyanathan, B.; Rao, K. J. *Chem. Mater.* **1997**, *9,* 1196.

[212] Ahlers, R.; Ruschewitz, U. *Z. Anorg. Allg. Chem.* **2005**, *631*, 1241.

[213] Agostino, A.; Volpe, P.; Castiglioni, M.; Truccato, M. *Mater. Res. Innov.* **2004**, *8*, 75.

[214] Baghurst, D. R.; Mingos, M. P. *Microwave-Enhanced Chemistry: Fundamentals, Sample Preparation, and* Applications, 1st ed.; Kingston, H. M., Haswell, S. J., Eds.; The American Chemical Society: Washington, D.C., **1997**; Chapter 10, pp 523.

[215] (a) Landry, C. C.; Barron, A. R. *Science* **1993**, *260,* 1653. (b) Landry, C. C.; Lockwood, J.; Barron, A. R. *Chem. Mater.* **1995**, *7,* 699.

[216] Houmes, J. D.; zur Loye, H.-C. *J. Solid State Chem.* **1997**, *130*, 266.

[217] (a) Kirchheim, R.; Mutschele, T.; Keiniger, W.; Gleiter, H.; Birringer, R.; Koble, T. D. *Mater. Sci. Eng.* **1988**, *99,* 457-462. (b) Kamakoti, P.; Sholl, D. S. J. *J. Membr. Sci.* **2003**, *225,* 145.

[218] (a) Dobrovolska, Ts.; Veleva, L.; Krastev, I.; Zielonka, A. *J. Electrochem. Soc.* **2005**, *152*, C137. (b) Dobrovolska, Ts.; Krastev, I.; Zielonka, A. *J. Appl. Electrochem.* **2005**, *35*, 1245.

[219] (a) Roucoux, A.; Schulz, J.; Patin, H. *Chem. Rev.* **2002**, *102,* 3757. (b) Zhang, C. J.; Baxter, R. J.; Hu, P.; Alavi, A.; Lee, M.-H. *J. Chem. Phys.* **2001**, *115,* 5272. (c) Mathauser, A. T.; Teplyakov, A. V. *Catal. Lett.* **2001**, *73,* 207.

[220] (a) Cava, R. J.; Takagi, H.; Zandbergen, H. W.; Krajewski, J. J.; Peck, W. F.; Siegrist, T.; Batlogg, B.; Vandover, R. B.; Felder, R. J.; Mitzuhashi, K.; Lee, J. O.; Eisaki, H.; Uchida, S. *Nature* **1994**, *367,* 252. (b) Gavaler, J. R.; Janocko, M. A.; Bradinski, A. I.; Rowland, G. W. *IEEE Trans. Magn.* **1975**, *2,* 192. (c) Nagamatsu, J.; Makagawa, N.; Muranaka, T.; Zenitani, Y.; Akimitsu, J. *Nature* **2001**, *410,* 63

[221] (a) Sun, S.; Murray, C. B.; Weller, D.; Folks, L.; Moser, A. *Science* **2000**, *287,* 1989. (b) Goll, D.; Kronmuller, H. *Naturewissenschaften* **2000**, *87*, 423. (c) Paduani, C. J. *J. Appl. Phys.* **2001**, *90*, 6251.

[222] Marjan, J.; Varma, R. S.; Polanc, S.; Kočevar, M. *Green Chem.* **2002**, *4*, 35.

[223] (a) Zhou, G.-T.; Palchik, O.; Pol, V. G.; Sominshi, E.; Koltypin, Y.; Gedanken, A. *J. Mater. Chem.* **2003**, *13*, 2607. (b) Zhou, G.-T.; Palchik, O.; Nowik, I.; Herber, R.; Koltypin, Y.; Gedanken, A. *J. Solid State Chem.* **2004**, *177*, 3014.

[224] Vondrova, M.; Majsztrik, P. W.; Gould, S.; Bocarsly, A. B. *Chem. Mater.* **2005**, *17*, 4755.

[225] (a) Satow, T.; Uemura, O.; Yamakawa, S. *T. Jpn. I. Met.* **1974**, *15*, 253-255. (b) Lee, C. C.; So, W. W. *Thin Sol. Films* **2000**, *366*, 196.

[226] (a)Wenkin, M.; Renard, C; Ruiz, P.; Delmon, B.; Devillers, M. *Stud. Surf. Sci. Catal.* **1997**, *108*, 391. (b) Karski, S.; Witonska, I. *J. Mol. Catal. A-Chem.* **2003**, *191*, 87.

[227] Oberndorff, P. J. T. L.; van Vinken, M. G. A.; Kodentsov, A. A.; van Loo, F. J. J. *J. Phase Equilbr.* 2001, *22*, 265.

[228] Lekse, J. W.; Pischera, A. M.; Aitken, J. A. *Mater. Res. Bull.* **2007**, *42*, 395.

[229] Campbell, A. N.; Reynolds, W. F. *Can. J. Chem.* **1962**, *40*, 37.

[230] Brandon, J. K.; Brezard, R.; Pearson, W. B.; Tozer, D. J. N. *Acta Crystallogr. B* **1977**, *33*, 527.

[231] Havinga, E. E.; Damsma, H.; Hokkeling, P. *J. Less-Common Met.* **1972**, 27, 169.

[232] We also chose to use a research-grade microwave to ensure reproducibility, because research-grade microwaves have a more uniform microwave field compared to domestic microwaves.

[233] It is highly recommended that eye protection be worn while performing microwave syntheses. Additionally, these reactions reach temperatures that can burn through many gloves that are made for "high-temperature" applications.

[234] C. Mastrovito, J.W. Lekse, J.A. Aitken *J. Solid State Chem.* **2007**, *180*, 3262.

[235] Kanatzidis, M. G.; Pottgen, R.; Jeitschko, W. *Angew. Chem. Int. Edit.* **2005**, *44*, 6996.

[236] Stojanovic, M.; Latturner, S. E. *J. Solid State Chem.* **2007**, *180*, 907.

[237] Cable, R. E.; Schaak, R. E. *Chem. Mater.* **2005**, *17*, 6835.

[238] Schaak, R. E.; Sra, A. K.; Leonard, B. M.; Cable, R. E.; Bauer, J. C.; Han, Y. F.; Means, J.; Teizer, W.; Vasquez, Y.; Funck, E. S. *J. Am. Chem. Soc.* **2005**, *127*, 3506.

5 Synthesis, Physicochemical Characterization and Crystallographic Twinning of Li_2ZnSnS_4

5.1 Introduction

Diamond-like semiconductors (DLS) are normal valence compounds, which are homeotypes of the crystal structure of diamond.[239-243] These compounds are technologically useful and have been investigated for a variety of applications including photovoltaics,[244] nonlinear optics,[245,246] thermoelectrics[247] and spintronics.[248] In order to be considered a diamond-like semiconductor, a compound must obey a number of criteria. First, the average number of valence electrons must equal four and the number of valence electrons per anion must equal eight. Additionally, all atoms must possess tetrahedral environments and obey Pauling's electrostatic valency rule, which states that the valence of each anion must be satisfied by the valence of the cations in its immediate coordination sphere. The number of compounds that satisfy these criteria is finite, but not insubstantial. To date, a large volume of research has been conducted on binary and ternary DLS; however, related quaternary DLS[241,242,243] have not attracted as much interest. Quaternary DLS should possess similar properties and the possibility of physical property tuning should increase as the degree of cationic substitution increases. The progression of diamond-like homeotypes from binary to quaternary using three known compounds, ZnS,[249,250] $AgInS_2$[251] and Cu_2CdGeS_4[241] can be found in Figure 5.1.

Quaternary DLS possess a number of structural features that can result in interesting physical properties. Pauling's electrostatic valency principle predicts that each

sulfide anion can only be bound to one divalent cation, two univalent cations and one tetravalent cation. This should be important when using these systems as host materials for dilute magnetic semiconductors, as the divalent cations are significantly further apart than those found in the binary DLS materials and can be separated by low-electron-density, univalent cations, such as lithium.

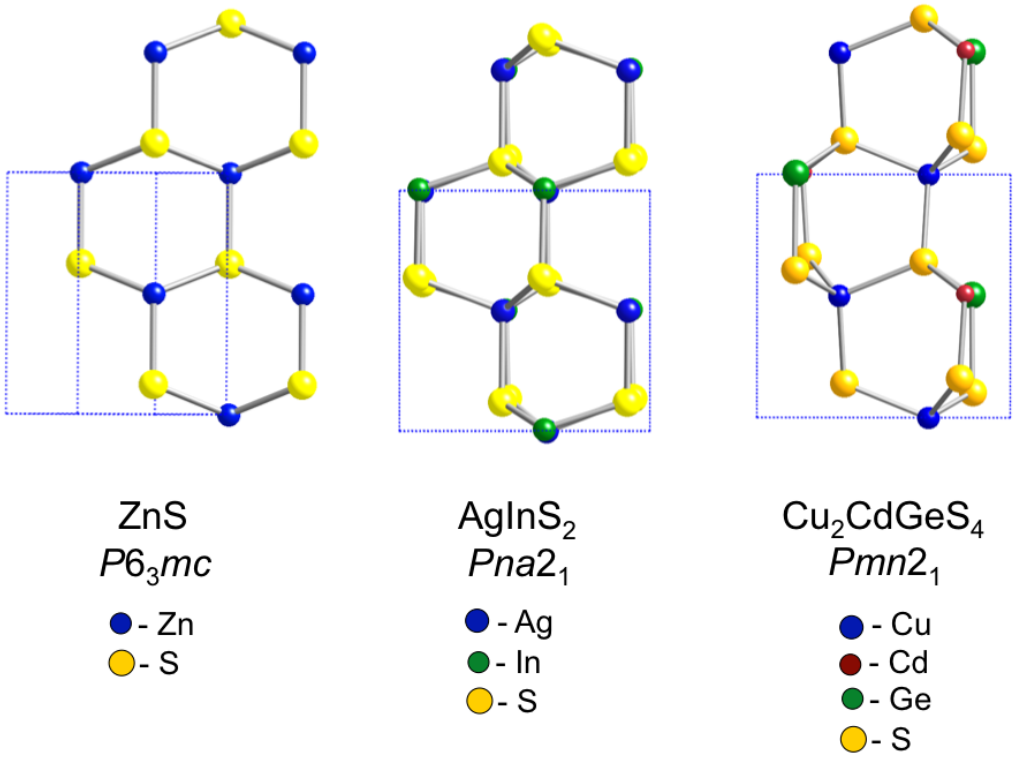

Figure 5.1. The structural progression from binary to quaternary diamond-like semiconductors with hexagonal close packing (hcp) is illustrated by three compounds. A similar progression can be derived from cubic diamond (ccp).

In this work, the synthesis and characterization of the quaternary DLS, Li_2ZnSnS_4, will be described. This will include a detailed discussion of how a structure that was initially thought to possess crystallographic disorder was determined to be a

pseudo-merohedral twin, using a combination of chemical and crystallographic principles.

5.2 Experimental

5.2.1 Reagents

Chemicals in this work were used as obtained: 1) lithium sulfide (Li_2S) powder, -200 mesh, 99.9%, Cerac; 2) zinc powder, -140 +325 mesh, 99.9%, Cerac; 3) tin powder, -100 mesh, 99.999%, Strem; and 4) sulfur powder, sublimed, 99.5%, Fisher.

5.2.2 Synthetic Procedure

5. 2.2.1 Li_2ZnSnS_4 Powder

1 mmol of Li_2ZnSnS_4 was prepared by weighing and grinding Li_2S (1.2 mmol), Zn (1 mmol), Sn (1 mmol), and S (3 mmol) using an agate mortar and pestle in an argon-filled glovebox. The ground mixture was placed into a graphite crucible inside a 12 mm o.d. fused-silica tube. The tube was sealed under a vacuum of approximately 10^{-3} mbar, heated to 700 °C in 12 h and then held at 700 °C for 96 h. The sample was then slowly cooled to room temperature in 12 h. The graphite crucible is necessary to prevent lithium from reacting with the fused-silica. The tube was opened under ambient conditions and the contents were examined using a light microscope. A yellow-green, microcrystalline powder was obtained and used for property measurements.

5.2.2.2 Li_2ZnSnS_4 Crystals

Stoichiometric amounts of Li_2S, Zn, Sn and S to prepare 1 mmol of Li_2ZnSnS_4 were weighed and ground in an argon-filled glovebox. The ground mixture was placed into a graphite crucible inside a 12 mm o.d. fused-silica tube. The tube was sealed under a vacuum of approximately 10^{-3} mbar, heated to 825 °C in 9 h and then held at 825 °C for 72 h. The sample was cooled slowly to 500 °C in 32.5 h and then rapidly to room temperature in 3 h. The tube was opened under ambient conditions and the contents were examined using a light microscope. Yellow-green, trapezoidal plate, X-ray-quality single crystals of the product were obtained and used for structure determination.

5.2.3 Physical Property Measurements

5.2.3.1 Scanning Electron Microscopy and Energy Dispersive Spectroscopy (EDS)

A CamScan Series 4 scanning electron microscope was used to image samples and a Princeton Gamma Tech detector was used for EDS. The working distance was 35 mm and the accelerating voltage was set to 22.5 kV. Samples were mounted onto double-sided carbon tape, which was adhered to an aluminum specimen holder. EDS data were collected for 60 s. The presence of zinc, tin and sulfur in each of the yellow-green crystals was confirmed, though the presence of lithium cannot be determined by this technique. Elemental mapping confirmed that each element was dispersed evenly throughout the crystals.

5.2.3.2 Differential Thermal Analysis (DTA)

DTA was performed using a Shimadzu DTA-50 thermal analyzer calibrated with a three-point calibration curve using indium, zinc and gold. The reference, Al_2O_3, and sample, of comparable masses, were contained in fused-silica ampoules (carbon coated for the sample) and sealed under a vacuum of ~10^{-3} mbar. The temperature was programmed to increase at a rate of 10 °C/min from 25 °C to 1000 °C. The temperature then decreased to 100 °C at 10 °C/min. To distinguish reversible events from irreversible ones, a second cycle was performed in the same manner.

5.2.3.3 Diffuse Reflectance UV/Vis/NIR Spectroscopy

Optical diffuse reflectance spectra were obtained using a Cary 5000 UV/Vis/NIR spectrometer. Samples were ground and loaded into a Harrick Praying Mantis diffuse reflectance accessory that uses elliptical mirrors. $BaSO_4$ was used as a 100 % reflectance standard. Scans were performed from 2500 nm to 200 nm. Wavelength data were converted to electron volts and the percent reflectance data were converted to absorbance units using the Kubelka-Munk equation.[252]

5.2.3.4 Second Harmonic Generation (SHG) Measurements

SHG of a powdered sample of Li_2ZnSnS_4 was measured using a modified Kurtz NLO system[253] with a Nd:YAG laser, as described elsewhere.[254] The response of Li_2ZnSnS_4 was compared to that of α-quartz, a typical standard for this technique.

5.2.3.5 Powder X-Ray Diffraction

Powder diffraction patterns were collected using a Panalytical X'Pert Pro MPD powder X-ray diffractometer. Data were collected from 5 to 80 °2θ with a sampling interval of 0.083556 °. The scan rate used was 0.010577 °/s. Samples were spun during data collection. The instrument was set to an accelerating voltage of 45 kV and a filament current of 40 mA. Copper K_α radiation with a wavelength of 1.541871 Å was used for measurements. Samples were prepared for analysis by spreading powder onto a piece of double-sided tape adhered to a glass slide placed into the aluminum sample holder.

5.2.3.6 Single Crystal X-Ray Data Collection and Reduction

Single crystal X-ray diffraction data were collected on a Bruker SMART Apex 2 CCD diffractometer at room temperature. Data were collected for 20 s per frame using Mo K_α radiation with a wavelength of 0.71073 Å and a graphite monochrometer. During data collection the instrument was set to 50 kV and 30 mA. The Bruker SAINT[255] program was used for data integration. After integration, there were a total of 4751 reflections collected with 1493 unique. An empirical absorption correction was performed using the SADABS[255] program.

5.2.3.7 Solving and Refining the Crystal Structure

The data were analyzed using the SHELXTL-PC package.[256] Based on the suspected Laue symmetry and systematic absences, two space groups seemed possible: noncentrosymmetric $Pmn2_1$ (No.31) and centrosymmetric *Pmmn* (No. 51). The intensity statistic, |E*E-1| = 0.846, favored neither option. Li_2ZnSnS_4 was predicted to be a

homeotype of the hexagonal mineral wurtzite (ZnS), therefore the noncentrosymmetric orthorhombic space group $Pmn2_1$ was selected. The structure was initially determined in this space group with the tin and zinc sites discovered by Patterson methods. Other atoms were located by difference-Fourier methods and chemical reasoning. The resulting structure model produced an *R*-index of 3.21 %. While the model appeared fine statistically, the structure had serious anomalies. In the difference-Fourier map, a spherical 3 e negative feature occupied one potential lithium site, while the second lithium site possessed an odd static disorder between lithium and zinc ions. This disorder problem was particularly alarming, for it represented a random scrambling of lithium and zinc ions at that site throughout the crystal structure. While this type of disorder has been observed in other compounds,[257,258] in this case it represents a major violation of Pauling's electrostatic valency principle, since in this model the disorder could result in a sulfur anion with one lithium ion, two zinc ions and one tin ion in its immediate coordination sphere. For these reasons, the noncentrosymmetric option was abandoned and the centrosymmetric option was evaluated.

The structure was redetermined in space group *Pmmn* resulting in a model that converged with an *R*-index of 4.38 %. Both lithium ions were located and refined; but the Li/Zn disorder remained. In this case, the sulfur tetrahedra showed static disorder, which was considered highly unlikely. After much thought, the centrosymmetric model was also abandoned.

Finally, it was determined that the data were actually from a pseudo-merohedrally twinned crystal, which mimicked disorder. In a pseudo-merohedral twin, the twin operator belongs to a higher crystal system than the structure.[259] In this case, the metric

symmetry possessed an additional 2-fold axis, which allowed a monoclinic structure to mimic orthorhombic symmetry. Therefore, the crystal consists of multiple ordered domains related by 2-fold axes. The orientation of the two ordered domains can be found in Figure 5.2. The appearance of the 50/50 Li/Zn disorder in the orthorhombic models shows that the crystal is a perfect twin.

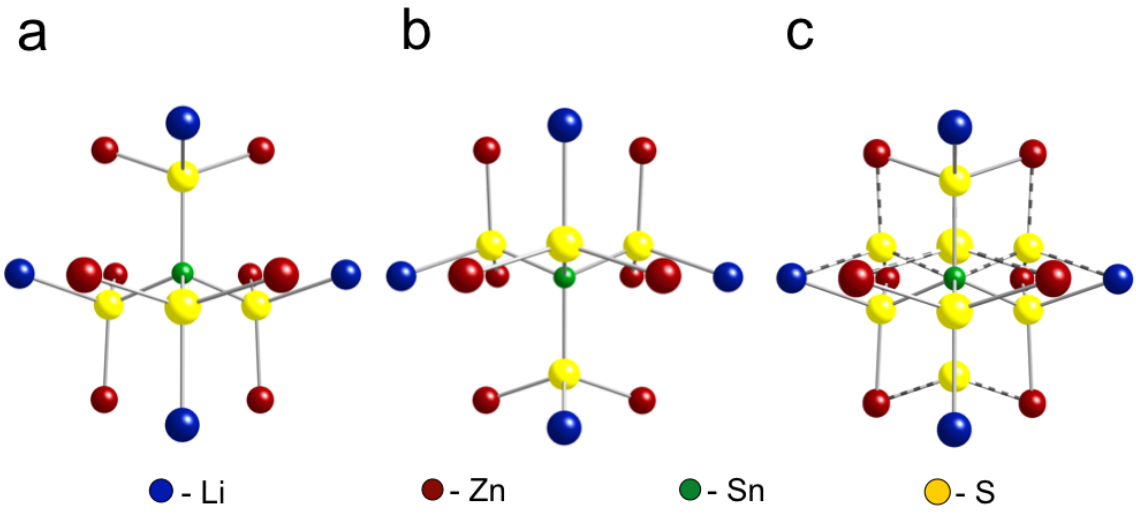

Figure 5.2. The orientation of the twin components is shown separately (a) and (b) and then combined in (c).

The crystal structure was re-evaluated in space group *Pn* (no. 7, a subgroup of the predicted $Pmn2_1$). The twin law, 1 0 0 0 -1 0 0 0 -1, was added to the instruction file. The lithium ions were refined isotropically. No anomalous features were present in the

structure model, Figure 5.3. The scattering factors for the lithium and zinc ions were used instead of those for the neutral atoms. The final model refined with $R1 = 1.68$ % and $wR^2 = 3.68$ % (all data). The largest positive and negative features remaining on the difference Fourier map were 0.56 eÅ^{-3} and -0.35 eÅ^{-3}, respectively. Crystallographic data and experimental details of the data collection are listed in Table 5.1, final atomic coordinates and equivalent displacement parameters are in Table 5.2 and selected bond distances and angles are given in Table 5.3.

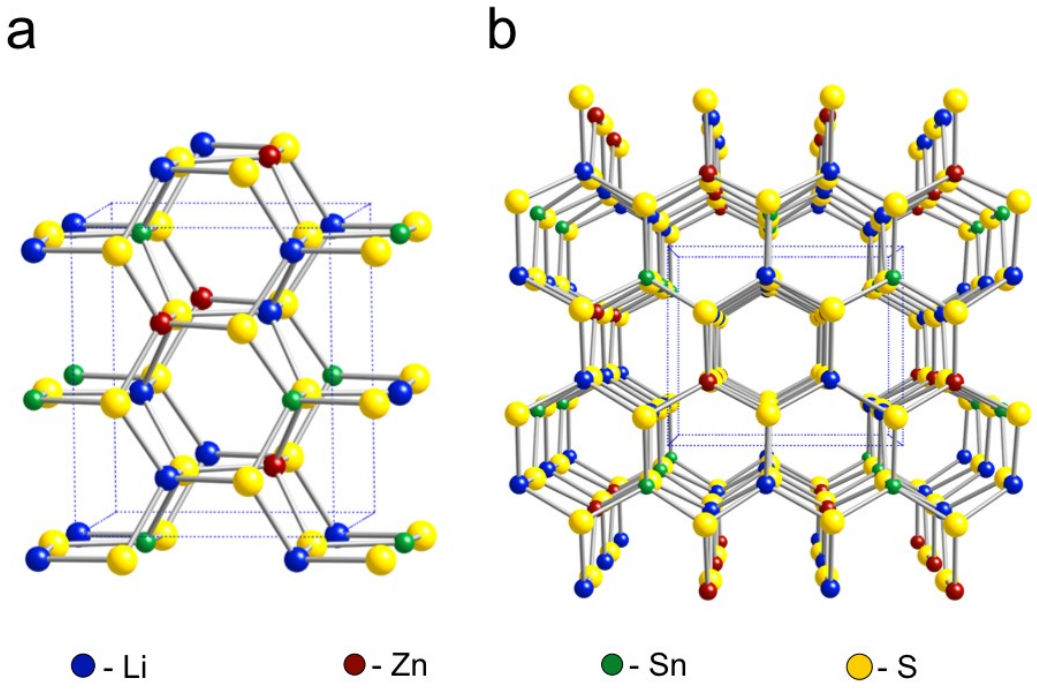

Figure 5.3. (a) The crystal structure of Li_2ZnSnS_4 viewed slightly skewed from the *a*-axis, in order to better visualize the cation arrangement in the structure and (b) the expanded view directly down the *a*-axis.

Table 5.1 Crystallographic data and experimental details for Li_2ZnSnS_4

Empirical Formula	Li_2ZnSnS_4
Formula Weight	326.20
Temperature	293(2) K
Wavelength	0.71073 Å
Space Group	*Pn*
Unit Cell Dimensions	a = 6.3728(13) Å α = 90 °
	b = 6.7286(13) Å β = 90.00(3) °
	c = 7.9621(16) Å γ = 90.00 °
Volume	341.42 (12) $Å^3$
Z, Calculated Density	2, 3.173 Mg/m^3
Absorption Coefficient	4.859 mm^{-1}
F(000)	292
Reflections Collected / Unique	4751 / 1493
Data / Restraints / Parameters	1493 / 2 / 64
Completeness to theta = 27.06	100.0 %
Goodness of Fit	1.058
Final R indices [I>2sigma (I)]	R1 = 0.0161, wR2 = 0.0363
R indices (all data)	R1 = 0.0168, wR2 = 0.0368

Table 5.2 Atomic coordinates and equivalent isotropic displacement parameters ($Å^2$ x 10^3) for Li_2ZnSnS_4.

	x	y	z	U(eq)*
Li(1)	0.6070(80)	0.1640(11)	0.5800(30)	7(3)
Li(2)	0.1280(80)	0.3390(30)	0.8200(50)	61(9)
Zn(1)	0.1111(4)	0.3263(1)	0.3174(3)	15(1)
Sn(1)	0.6113(3)	0.1726(1)	0.0658(2)	13(1)
S(1)	0.9883(9)	0.1815(3)	0.0711(13)	16(1)
S(2)	0.9890(9)	0.1618(3)	0.5644(12)	14(1)
S(3)	0.4925(15)	0.3393(5)	0.8260(11)	16(1)
S(4)	0.4785(14)	0.3303(5)	0.3181(11)	13(1)

*** U(eq) is defined as one third of the trace of the orthogonalized U_{ij} tensor.**

Table 5.3 Selected bond distances (Å) and angles (°) found in Li_2ZnSnS_4.

Li(1)-S(1)	2.43(6)	S(1)-Li(1)-S(2)	108.1(12)
Li(1)-S(2)	2.431(18)	S(1)-Li(1)-S(3)	110.14(13)
Li(1)-S(3)	2.39(2)	S(1)-Li(1)-S(4)	106.4(14)
Li(1)-S(4)	2.52(2)	S(2)-Li(1)-S(3)	114.3(13)
		S(2)-Li(1)-S(4)	106.3(12)
		S(3)-Li(1)-S(4)	110.9(12)
Li(2)-S(1)	2.46(5)	S(1)-Li(2)-S(2)	110.1(18)
Li(2)-S(2)	2.45(4)	S(1)-Li(2)-S(3)	113.0(2)
Li(2)-S(3)	2.36(7)	S(1)-Li(2)-S(4)	108.0(2)
Li(2)-S(4)	2.45(3)	S(2)-Li(2)-S(3)	109.0(2)
		S(2)-Li(2)-S(4)	105.2(18)
		S(3)-Li(2)-S(4)	111.4(16)
Zn(1)-S(1)	2.400(9)	S(1)-Zn(1)-S(2)	113.1(2)
Zn(1)-S(2)	2.320(9)	S(1)-Zn(1)-S(3)	107.6(3)
Zn(1)-S(3)	2.351(4)	S(1)-Zn(1)-S(4)	108.9(3)
Zn(1)-S(4)	2.335(9)	S(2)-Zn(1)-S(3)	108.8(3)
		S(2)-Zn(1)-S(4)	109.8(3)
		S(3)-Zn(1)-S(4)	108.6(3)
Sn(1)-S(1)	2.395(2)	S(1)-Sn(1)-S(2)	110.15(14)
Sn(1)-S(2)	2.406(6)	S(1)-Sn(1)-S(3)	111.0(2)
Sn(1)-S(3)	2.349(9)	S(1)-Sn(1)-S(4)	106.7(2)
Sn(1)-S(4)	2.415(9)	S(2)-Sn(1)-S(3)	109.2(4)
		S(2)-Sn(1)-S(4)	109.0(4)
		S(3)-Sn(1)-S(4)	110.66(14)

5.3 Results and Discussion

The synthesis of quaternary DLS materials is relatively straightforward; however, obtaining a *phase-pure* product can often be problematic. This is due to the possibility of phase segregation resulting in stable binary products such as wurtzite (ZnS)[249,250] and herzenbergite (SnS).[260,261] Initial high-temperature syntheses at 825, 775 and 760 °C of Li_2ZnSnS_4 did not result in a phase-pure product. Secondary phases of ZnS[262] and SnS[263] were detected by powder X-ray diffraction with a few very small peaks that could not be attributed to any known phase. Lowering the reaction temperature to 700°C resulted in a more phase-pure sample, with smaller amounts of the ZnS and SnS components. Additionally, the phase purity could be increased slightly by carrying out the reaction with a slight excess of Li_2S, see Figure 5.4. This is not unexpected, as the Li_2S is highly volatile and small amounts can escape from the graphite crucible and deposit on the cold end of the fused-silica tube.

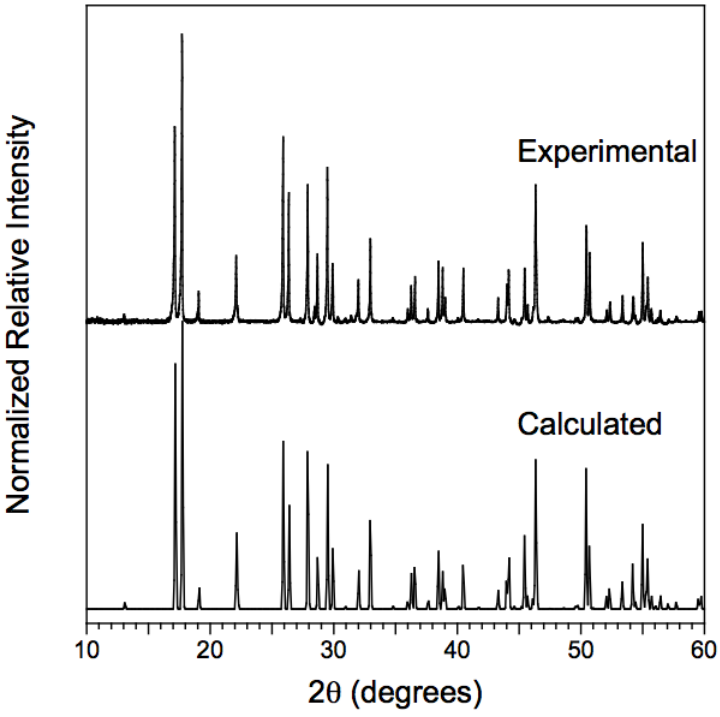

Figure 5.4. A comparison of the diffractogram of an experimentally obtained sample of Li_2ZnSnS_4 compared to that calculated from the X-ray structure solution.

Thermal analysis of the product shows an endothermic event occurring at 919 °C, which we believe to be the melting point of Li_2ZnSnS_4, see Figure 5.5. Upon cooling there is a corresponding exothermic event at 904 °C which can be attributed to the recrystallization of the material. The small SnS impurity, which was indicated by powder X-ray diffraction, may be showing up as the shoulder on these events, since SnS has a melting point of 880 °C.[264] Events due to ZnS are not present because it melts at 1700 °C,[264] out of the range of this experiment. We suppose that Li_2ZnSnS_4 partially decomposes after melting, yielding increased amounts of the binary impurity phases;

however, powder diffraction of the DTA residue was complicated by side reactions with the sample tube, despite careful carbon coating to prevent such reactions. Therefore, the several exothermic events upon cooling have not been assigned, as they are likely due to side reactions with the fused-silica ampoule. Examination of the ampoule after analysis showed glass attack as the ampoule became discolored and brittle and the sample appeared oxidized, with some white color present.

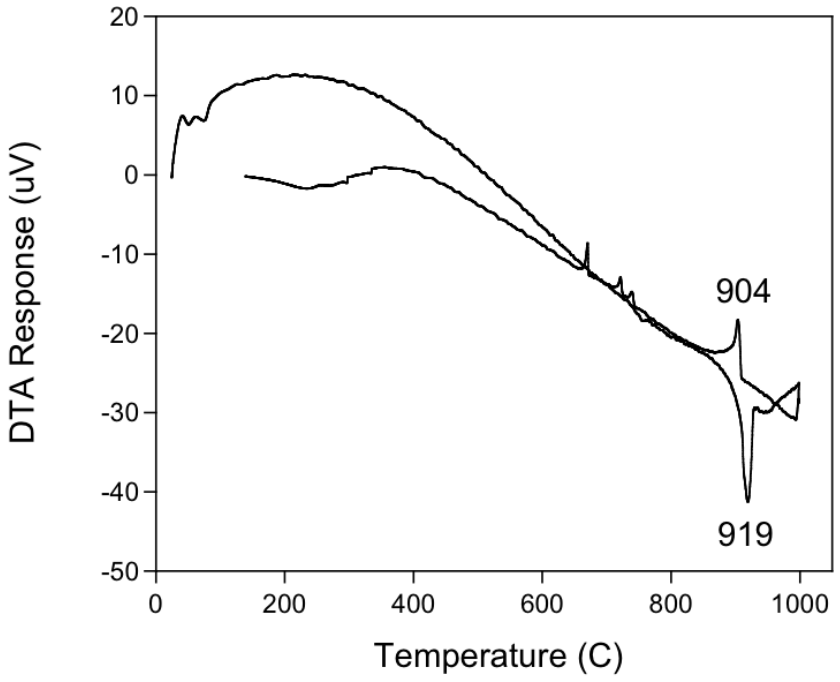

Figure 5.5. Differential thermal analysis of a sample obtained for Li_2ZnSnS_4.

Diffuse reflectance UV/Vis/NIR spectroscopy was performed on the most phase-pure sample. The spectrum can be found in Figure 5.6. The bandgap of Li_2ZnSnS_4 was estimated to be 2.87 eV from these data. In agreement with the powder X-ray diffraction results, the optical absorption spectrum suggests the presence of small

impurities. The shoulder on the higher energy side of the band edge should be due to ZnS, which has a bandgap of 3.8-3.9 eV.[265] SnS has a lower bandgap, approximately 1.1 eV,[266] and is likely responsible for the tail on the band edge at lower energies.

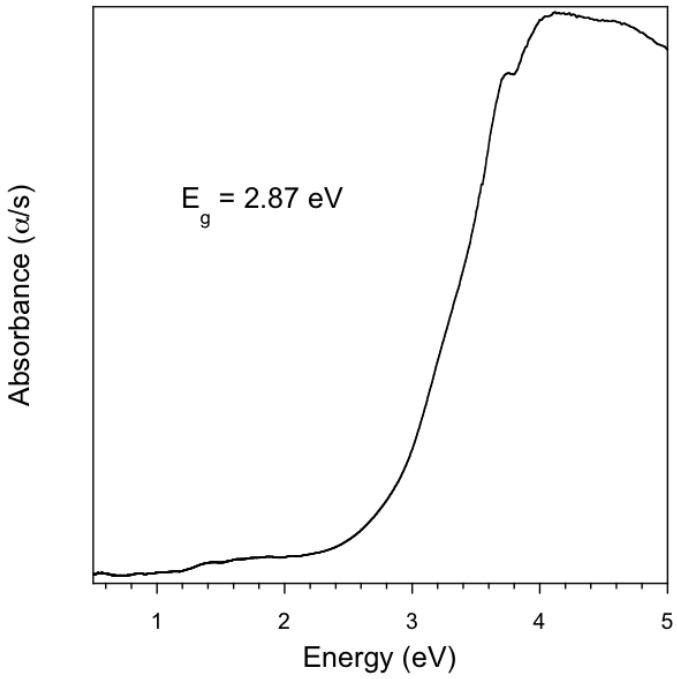

Figure 5.6. Diffuse reflectance UV/Vis/NIR spectrum of Li_2ZnSnS_4.

Second harmonic generation, a frequency doubling effect, requires the absence of an inversion center in a compound. DLS compounds are inherently noncentrosymmetric, which makes them ideal candidates for SHG. Interestingly, even though Li_2ZnSnS_4 is noncentrosymmetric, it did not exhibit any SHG response. One possible reason why SHG was not observed could be that the signal is very weak and/or suppressed by the presence of impurities. Additionally, we believe that this may be due to the nature of the perfect

twin, although we could not find any precedent for this phenomenon in the literature. Further studies on the suppression of the second harmonic response are in progress.[267]

Known quaternary DLS normally crystallize in one of three space groups: *I*-42*m*,[268] *Pmn*2$_1$,[241] or *Pna*2$_1$, with stannite and wurtz-stannite structure types. The *I*-42*m* structure can be derived from that of cubic diamond while *Pmn*2$_1$ and *Pna*2$_1$ are superstructures of hexagonal diamond. The name "wurtz-stannite" was originally applied to the predicted, disordered wurtzite structures,[269] although no mineral was found to posses this structure until the discovery of orickite ($CuFeS_2$ doped with <0.05 % K^+, Na^+).[270] Li_2ZnSnS_4 crystallizes in the monoclinic space group *Pn*, which is a subgroup of *Pmn*2$_1$.

The loss of symmetry, resulting in the crystallization in *Pn*, cannot be attributed to deviations from perfect tetrahedral geometry; however, it can be explained by a variation in the ordering of the cations. To determine if there was a difference in the cation ordering, the structure of Li_2ZnSnS_4 was compared to that of Cu_2CdGeS_4,[241] with space group *Pmn*2$_1$. A difference exists in the cation ordering down each crystallographic axis. As an example, the difference in cation ordering down the b-axis is apparent in Figure 5.7. Cu_2CdGeS_4 has two rows of cations. The first row consists of alternating Cd and Ge atoms, while the second row contains exclusively copper atoms. The lithium atoms in Li_2ZnSnS_4 are split between the rows, with one row containing Zn and Li and the other containing Sn and Li. Another possible space group for quaternary DLS is *Pna*2$_1$. This option is related to *Pmn*2$_1$ but a difference in the ordering of the cations leads to the doubling of one unit cell edge.

All ions in Li_2ZnSnS_4 possess tetrahedral environments, with each sulfide anion being surrounded by one zinc, one tin(IV) and two lithium cations as shown in Figure 5.3. The Sn-S bond distances range from 2.349(9) - 2.415(9) Å (average = 2.39(1) Å), with S-Sn-S angles from 106.7(2) - 111.1(2) °. These distances compare favorably with the Sn-S distance found in stannite (Cu_2FeSnS_4), which is 2.393(3) Å.[271] The Zn-S bond distances range from 2.320(9) - 2.400(9) Å (average = 2.35(2) Å), with angles ranging from 107.6(3) - 113.1(2) °. The Zn-S bonds in this compound are slightly larger than the 2.283 Å bond lengths found in the related quaternary compound Cu_2ZnGeS_4,[272] but are very similar to the bond distances of 2.340 Å in ZnS.[249] The distance between divalent cations in Li_2ZnSnS_4 is 5.609 Å, which is significantly longer than 3.803 Å, as found in wurtzite.[249] The LiS_4 tetrahedra are the least perfect in the structure. The Li-S bond distances range from 2.36(7) - 2.52(2) Å (average = 2.4(1) Å), with S-Li-S angles of 105.2(18) - 114.3(13) °. The bond distances for Li-S in this compound agree with a value of 2.4534(9) Å for the bond lengths in the quaternary compound Li_2PbGeS_4.[273]

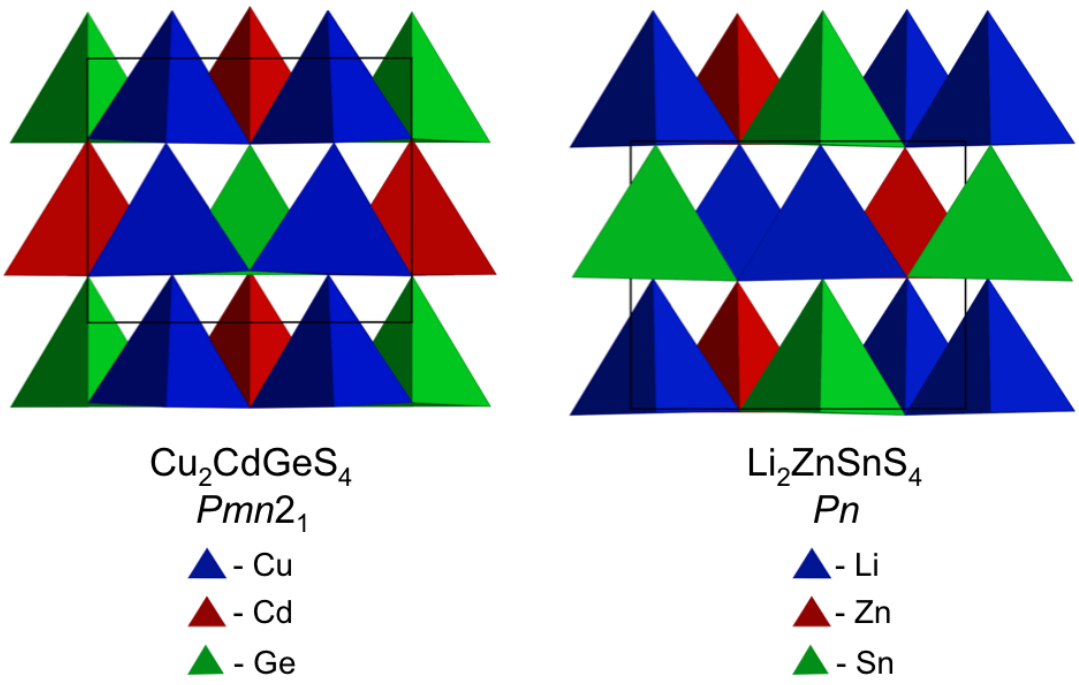

Figure 5.7. Polyhedral representation of (a) Cu_2CdGeS_4[241] and (b) Li_2ZnSnS_4 viewed down the b-axis to show the difference in the ordering of the cations.

5.4 Conclusions

The structure of the new diamond-like semiconductor Li_2ZnSnS_4 has been solved from a pseudo-merohedrally twinned crystal. This twin model may explain some of the anomalies found in the related compound Li_2CdSnS_4.[274] Future studies will investigate whether this twinning may be responsible for the lack of any SHG response exhibited by this compound. Future work will also include the use of this compound as a host structure for interesting electronic, magnetic and photovoltaic materials.

5.5 Reference

[239] N.A. Goryunova *The Chemistry of Diamond-like Semiconductors*, J.C. Anderson, ed., The M.I.T. Press; Cambridge, 1965.

[240] E. Parthé, *Crystal Chemistry of Tetrahedral Structures*, Gordon and Breach Science Publishers; New York, 1964.

[241] E. Parthé, K. Yvon, R.H. Deitch *Acta. Crystallogr.* **1969**, *B25*, 1164.

[242] D. M. Schleich, A. Wold *Mater. Res. Bull.* **1977**, *12*, 111.

[243] M. Quintero, A. Barreto, P. Grima, R. Tovar, E. Quintero, G. S. Porras, J. Ruiz, J. C. Woolley, G. Lamarche, A. M. Lamarche *Mater. Res. Bull.* **1999**, *34*, 2263.

[244] A. Goetzberger, C. Hebling, H. Schock *Mater. Sci. Eng.* **2003**, *40*, 1.

[245] M.C. Ohmer, R. Pandey *MRS Bull.* 1998, *23*, 16.

[246] G.C. Catella, D. Burlage *MRS Bull.* **1998**, *23*, 28.

[247] G.E. Davidyuk, O.V. Parasyuk, S.A. Semenyuk, Ya. E. Romanyuk *Inorg. Mater.* **2003**, *39*, 919.

[248] S.J. Pearton, C.R. Abernathy, D.P. Norton, A.F. Hebard, Y.D. Park, L.A. Boatner, J.D. Budai *Mater. Sci. Eng.* **2003**, *40*, 137.

[249] G. Aminoff *Z. Kristallogr. Krist.* **1923**, *58*, 203.

[250] H.T. Evans, Jr., E.T. McKnight *Am. Mineral.* **1959**, *44*, 1210

[251] H. Hahn, G. Frank, W. Klingler, A.D. Meyer, G. Stoerger *Z. Anorg. Allg. Chem.* **1953**, *271*, 153.

[252] P. Kubelka, F. Munk *Z. Tech. Phys.* **1931**, *12*, 593.

[253] S.K. Kurtz, T.T. Perry *J. Appl. Phys.* **1968**, *39*, 3798.

[254] K.M. Ok, N.S. Bhuvanesh, P.S. Halasyamani *Inorg. Chem.* **2001**, *40*, 1978.

[255] SAINT and SADABS are part of the Apex 2 software package v2.1-4 Program for Data Collection and Reduction on Bruker AXS CCD Area Detector Systems, Bruker Analytical X-ray Systems, Inc., Madison, WI, 2005.

[256] SHELXTL-PC release 6.14, Bruker AXS, Madison, WI 2007.

[257] B. Deng, G. H. Chan, F. Q. Huang, D. L. Gray, D. E. Ellis, R. P. Van Duyne, J. A. Ibers *J. Solid State Chem.* **2007**, *180*, 759.

[258] D. Schmitz, W. Bronger *Z. Anorg. Allgem. Chem.* **1987**, *553*, 248.

[259] R. Herbst-Irmer, in P. Müller, *Crystal Structure Refinement: A Crystallographer's Guide to SHELLXL*, Oxford University Press; New York, 2006.

[260] S. Del Bucchia, J.C. Jumas, M. Maurin *Acta Crystallogr.* **1981**, *B37*, 1903.

[261] L. Guen, W.S. Glaunsinger, A. Wold *Mater. Res. Bull.* **1979**, *14*, 463.

[262] E.A. Jumpertz *Z. Elektrochem.* **1955**, *59*, 419.

[263] S.B. Badachhape, A. Goswami *J. Phys. Soc. Jpn., Suppl.* **1962**, *17*, 251.

[264] D. R. Lide (Ed.), *Handbook of Chemistry and Physics*, CRC Press; New York, 2003.

[265] O. Madelung, M. Schulz (Eds.), *Numerical Data and Functional Relationships in Science and Technology. New Series. Group III: Crystal and Solid State Physics. Semiconductors. Supplements and Extensions to Volume III/17. Intrinsic Properties of Group IV Elements and III-V, II-VI and I-VII Compounds, vol. 22a*, Springer; Berlin, 1982.

[266] A.M. Elkorashy, *Chemtronics.* **1986**, *1*, 76.

[267] J.W. Lekse, M.A. Moreau, K.L. McNerny, J. Yeon, P.S. Halasyamani, J.A. Aitken *Inorg. Chem.* **2009**, *48*, 7516.

[268] L.O. Brockway *Z. Kristallogr. Krist.* **1934**, *89*, 434.

[269] W. Schäfer, R. Nitsche *Mater. Res. Bull.* **1974**, *9*, 645.

[270] R.C. Erd, G.K. Czamanske *Am. Mineral.* **1983**, *68*, 245.

[271] J. Llanos, M. Tapia, C. Mujica, J. Oro-Sole, P. Gomez-Romero *Bol. Soc. Chil. Quim.* **2000**, *45*, 605.

[272] A.F. Moodie and H.J. Whitfield *Acta Crystallogr B.* **1986**, *B42*, 236.

[273] J.A. Aitken, P. Larson, S.D. Mahanti, M.G. Kanatzidis *Chem. of Mater.* **2001**, *13*, 4714.

[274] M.S. Devi, K. Vidyasagar *J. Chem. Soc., Dalton Trans.* **2002**, 2092.

6 Second Harmonic Generation and Crystal Structure of the Diamond-Like Semiconductors, Li_2CdGeS_4 and Li_2CdSnS_4

6.1 Introduction

Beginning with the first observation of nonlinear optical (NLO) behavior in quartz crystals in 1961,[275] researchers have been finding uses for second-harmonic generating (SHG) materials in optical communications, laser medicine and molecular spectroscopy, among others. There are several notable materials, such as $KTiOPO_4$ (KTP),[276] $LiNbO_3$,[277,278,279] LiB_3O_5 (LBO)[280] that have found uses in either the ultraviolet or the visible region. While several chalcopyrites are commonly used in the infrared region, such as $AgGaS_2$,[281,282,283]$CuGaS_2$[284] and $AgGaSe_2$.[285] These materials posses higher SHG coefficients than the above mentioned oxides due to the presence of highly polarizable M-S or M-Se bonds, yet are somewhat limited in their applications due to lower laser damage thresholds, which are correlated to their relatively small band gaps[284] Consequently, new materials with exceptional SHG properties and higher laser damage thresholds are required for applications in the infrared.

Toward this goal, we have prepared two compounds, Li_2CdGeS_4 and Li_2CdSnS_4. These materials have polarizable M-S bonds resulting in high NLO coefficients; yet also have wider band gaps that may result in higher laser damage thresholds. Like the chalcopyrites, Li_2CdGeS_4 and Li_2CdSnS_4 are diamond-like semiconductors (DLS),[286287288289-290] which means that the structure of these compounds is derived from that of diamond, either the cubic or hexagonal form.[286,287] These compounds are built from tetrahedral building blocks that are orientated along

one crystallographic axis, rendering the structures inherently noncentrosymmetric, the first criterion for SHG.[291]

Much of the previous work with DLS has been focused on binary and ternary compounds, with less exploration in the area of quaternary materials.[288,289,290] Admittedly, there are difficulties involved in the synthesis of quaternary DLS that deter many researchers from exploiting the diversity that exists in these systems. The principle issue is the tendency of high-temperature, solid-state reactions to favor the formation of the most thermodynamically stable phases, which are quite frequently binary compounds. Despite this synthetic challenge, it is worth pursuing quaternary materials because of their increased compositional flexibility,[286,287] compared to binary and ternary phases. It is this flexibility that allows for the potential to tune the physical properties of the material for applications in nonlinear optics, as well as other areas where DLS have found utility such as light emitting diodes[292] and solar cells.[293]

The general formula used to represent the DLS reported here is I_2-II-IV-VI_4, where the Roman numeral corresponds to the number of valence electrons and the subscript denotes the number of that particular ion in the formula unit. While there are many known compounds with this formula where I=Ag or Cu,[290,294] there are few where I=Li.[295,296] The "replacement" of silver or copper with lithium widens the band gap in these materials, increasing their potential in SHG applications due to the possibility of increased laser damage thresholds. Additionally, the presence of lithium as the univalent cation allows for the use of a lithium polysulfide flux[297] as a reaction medium to promote crystal growth.

6.2 Experimental

6.2.1 Reagents

Most chemicals in this work were used as obtained: 1) lithium sulfide (Li_2S) powder, -200 mesh, 99.9%, Cerac; 2) zinc powder, -140 +325 mesh, 99.9%, Cerac; 3) tin powder, -100 mesh, 99.999%, Strem; and 4) sulfur powder, sublimed, 99.5%, Fisher. Germanium pieces, 99.999%, Strem, were ground to a powder prior to use.

6.2.2 Synthetic Procedure

6.2.2.1 Li_2CdGeS_4 powder

Stoichiometric amounts of Li_2S, Cd, Ge and S were weighed and ground for 20 minutes in an argon-filled glovebox. The ground mixture was placed into a graphite crucible, which was placed into a 12 mm o.d. fused-silica tube. The tube was sealed under a vacuum of approximately 10^{-3} mbar and placed into a furnace. The sample was heated from room temperature to 525 °C in 4.5 hours, held at 525 °C for 163.5 hours and quenched in an ice-water bath. The tube was opened under ambient conditions and the contents examined using a light microscope.

6.2.2.2 Li_2CdGeS_4 crystals

Single crystals of Li_2CdGeS_4 were prepared using a polychalcogenide flux. Li_2S,Cd,Ge and S were weighed out in a 2:1:1:12 ratio. Li_2S and S, in proportions greater than stoichiometric amounts, were used to form the polychalcogenide flux. The reaction mixture was ground and placed into a graphite crucible. The crucible was then placed into a 12 mm o.d. fused-silica tube that was sealed under vacuum of approximately 10^{-3} mbar. The tube was heated from room temperature to 650 °C in 12 hours, held at 650 °C for 96 hours and slowly cooled to 400 °C over

40 hours. The furnace was then cooled to room temperature in 3 hours. The tube was opened under ambient conditions and the sample transferred to a beaker. The flux was then removed by several washings with methanol. A final rinse with ether was used to dry the sample. The sample was analyzed and a single crystal selected for diffraction using a light microscope.

6.2.2.3 Li_2CdSnS_4 crystals and powder

Both single crystal and polycrystalline samples of Li_2CdSnS_4 were synthesized using a polychalcogenide flux at 750 °C and 650 °C, respectively. Though this is the first report of Li_2CdGeS_4, Li_2CdSnS_4 has been previously reported.[295] A synthesis using conditions identical to those reported by Devi, et. al.[295] was also attempted; however, the product was primarily CdS with a small amount of quaternary phase present. In our work, it was determined that the flux ratio, Li_2S:S, is very important in determining the product of these reactions. Varying this ratio by ~0.02 produces pure CdS and none of the quaternary phase.

6.2.3 Physical Property Measurements

6.2.3.1 Scanning Electron Microscopy and Energy Dispersive Spectroscopy (EDS)

A CamScan Series 4 scanning electron microscope was used to image samples and a Princeton Gamma Tech detector was used for EDS. The working distance was 35 mm and the accelerating voltage was set to 22.5 kV. Samples were mounted onto double-sided carbon tape, which was adhered to an aluminum specimen holder. EDS data were collected for 60 s. The presence of cadmium, sulfur and either tin or germanium in each of the crystals was confirmed, though the presence of lithium cannot be determined by this technique. Elemental mapping confirmed that each element was dispersed evenly throughout the crystals.

6.2.3.2 Differential Thermal Analysis (DTA)

DTA was performed using a Shimadzu DTA-50 thermal analyzer calibrated with a three-point calibration curve using indium, zinc and gold. The reference, Al_2O_3, and sample, of comparable masses, were contained in fused-silica ampoules (carbon coated for the sample) and sealed under a vacuum of ~10^{-3} mbar. The temperature was programmed to increase at a rate of 10 °C/min from 25 °C to 1000 °C. The temperature then decreased to 100 °C at 10 °C/min. To distinguish reversible events from irreversible ones, a second cycle was performed in the same manner.

6.2.3.3 Diffuse Reflectance UV/Vis/NIR Spectroscopy

Optical diffuse reflectance spectra were obtained using a Cary 5000 UV/Vis/NIR spectrometer. Samples were ground and loaded into a Harrick Praying Mantis diffuse reflectance accessory that uses elliptical mirrors. $BaSO_4$ was used as a 100 % reflectance standard. Scans were performed from 2500 nm to 200 nm. Wavelength data were converted to electron volts and the percent reflectance data were converted to absorbance units using the Kubelka-Munk equation.[298]

6.2.3.4 Infrared Spectroscopy

Infrared spectroscopy was performed using a Thermo Nicolet Nexus 470 FT-IR spectrometer. An ATR attachment with a germanium window was used to collect data from 650

cm^{-1} to 4000 cm^{-1}. The data collection software OMNIC was used to collect 32 scans for each compound in and to convert absorption to transmission.

6.2.3.5 Second Harmonic Generation (SHG) Measurements

SHG of powdered samples of Li_2CdGeS_4 and Li_2CdSnS_4 were measured using a modified Kurtz NLO system[299] with a Nd:YAG laser, as described elsewhere.[300] The responses of Li_2CdGeS_4 and Li_2CdSnS_4 were compared to that of α-quartz, a typical standard for this technique.

6.2.3.6 Powder X-Ray Diffraction

Powder diffraction patterns were collected using a Panalytical X'Pert Pro MPD powder X-ray diffractometer. Data were collected from 5 to 80 °2θ with a sampling interval of 0.083556 °. The scan rate used was 0.010577 °/s. Samples were spun during data collection. The instrument was set to an accelerating voltage of 45 kV and a filament current of 40 mA. Copper K_α radiation with a wavelength of 1.541871 Å was used for measurements. Samples were prepared for analysis by spreading powder onto a piece of double-sided tape adhered to a glass slide placed into the aluminum sample holder.

6.2.3.7 Single Crystal X-Ray Data Collection and Reduction

Single crystals of each compound were mounted onto a glass fiber using Krazy® glue.Over a hemisphere of data were collected using 0.3 ° steps in omega and phi on a Bruker SMART Apex 2 diffractometer with a CCD detector at room temperature. Data were collected

for 35 s per frame using Mo K_α radiation with a wavelength of 0.71073 Å and a graphite monochrometer. During data collection the instrument was set to 50 kV and 30 mA. The Bruker SAINT[301] program was used for data integration. After integration of the data collected for Li_2CdGeS_4, there were a total of 5848 reflections collected with 1228 unique. For Li_2CdSnS_4, there were a total of 6530 reflections collected with 1345 unique after integration. An empirical absorption correction was performed using the SADABS[255] program. The structure solution and full-matrix least-squares refinement on F^2 were performed using SHELXTL-97.[302] Probable space groups based on systematic absences for both compounds included *P*mmn (centrosymmetric) and *P*mn2_1 (noncentrosymmetric). *P*mn2_1 was selected for both compounds as diamond-like semiconductors should be noncentrosymmetric based upon the four rules for DLS. Important crystallographic data and structure refinement details can be found in Table 6.1.

6.3 Results and Discussion

Li_2CdGeS_4 and Li_2CdSnS_4 are both predicted to be diamond-like based upon a set of rules used to identify DLS.[286,287] The first of four rules is that the average valence electron concentration must be four. The second rule is that the valence electron concentration per anion must be eight. The last two are Pauling's first and second rules.[303] In a DLS, the atoms should be tetrahedrally coordinated and therefore should follow Pauling's first rule and have cation to anion ratios that lead to tetrahedral coordination. DLS should also conform to Pauling's second rule, also known as the electrostatic valence sum rule. In order to satisfy this rule, the charge of the anion should be compensated for by the valence bonds from the cations in the immediate coordination sphere.

Single crystal X-ray diffraction was used to determine that both compounds are indeed diamond-like and possess the wurtz-stannite structure type. The term wurtz-stannite does not represent a particular compound. Instead it was first used in 1974 to describe the distorted wurzite structure adopted by several compounds with the general formula, Cu_2-II-IV-S_4.[304] Li_2CdGeS_4 and Li_2CdSnS_4 crystallize in the orthorhombic space group *P*mn2_1 (Table 6.1, Figure 6.1). In accordance with Pauling's second rule, each sulfur anion is tetrahedrally coordinated to one cadmium cation, one germanium/tin cation and two lithium cations forming a three-dimensional, honeycomb structure. However, if the lithium-sulfur bonds are considered to be more ionic than either the cadmium-sulfur or tin/germanium-sulfur bonds, the structure can be thought of as two-dimensional with Li^+ cations, separating $[Cd(Ge/Sn)S_4]^{2-}$ layers, which extend in the *ab* plane. All of the tetrahedra are fairly regular with the greatest distortion from ideal occurring in the LiS_4 polyhedra, with values for S-Li-S angles range from 106.3(5)° to 113.4(5)°. This is in contrast to the previously reported structure of Li_2CdSnS_4 in the centrosymmetric space group *P*mmn using a disorder model.[295] Powder X-ray diffraction was also used to determine the phase-purity of the obtained products and validate the crystal structures, Figures 6.2 and 6.3.

Table 6.1. Selected Crystallographic Data for Li_2CdGeS_4 and Li_2CdSnS_4

Compound	Li_2CdGeS_4	Li_2CdSnS_4
Crystal System	Orthorhombic	Orthorhombic
Space Group	$Pmn2_1$	$Pmn2_1$
Unit Cell Parameters	a=7.7374(1) Å b=6.8498(1) Å c=6.3688(1) Å	a=7.9555(3) Å b=6.9684(3) Å c=6.4886(3) Å
Z	2	2
Reflections Collected	5848	6530
Independent Reflections	1228 [R(int)=0.0289]	1345 [R(int)=0.0211]
Goodness of Fit	0.949	1.149
R indices (all data)	R1=0.0193 wR2=0.0273	R1=0.0186 wR2=0.0419
Largest Peak/Hole	0.608/-0.716 $eÅ^{-3}$	0.854/-0.847 $eÅ^{-3}$

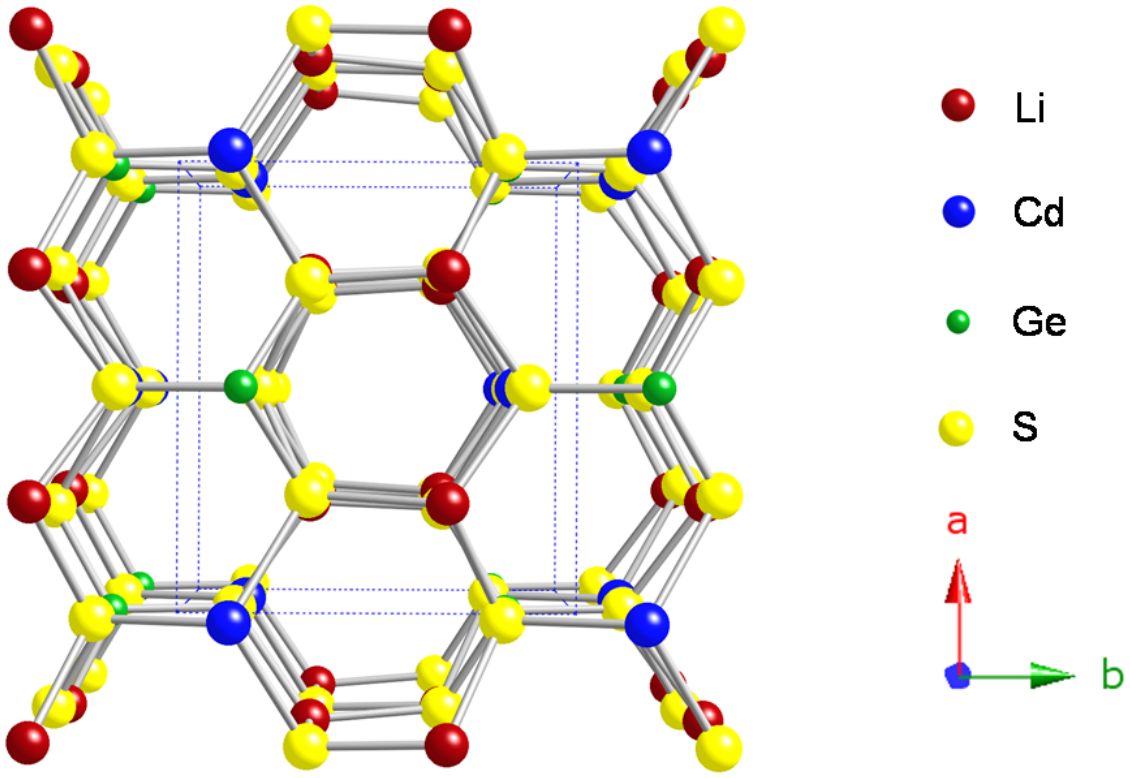

Figure 6.1. The structure of Li_2CdGeS_4 viewed down the *c*-axis.

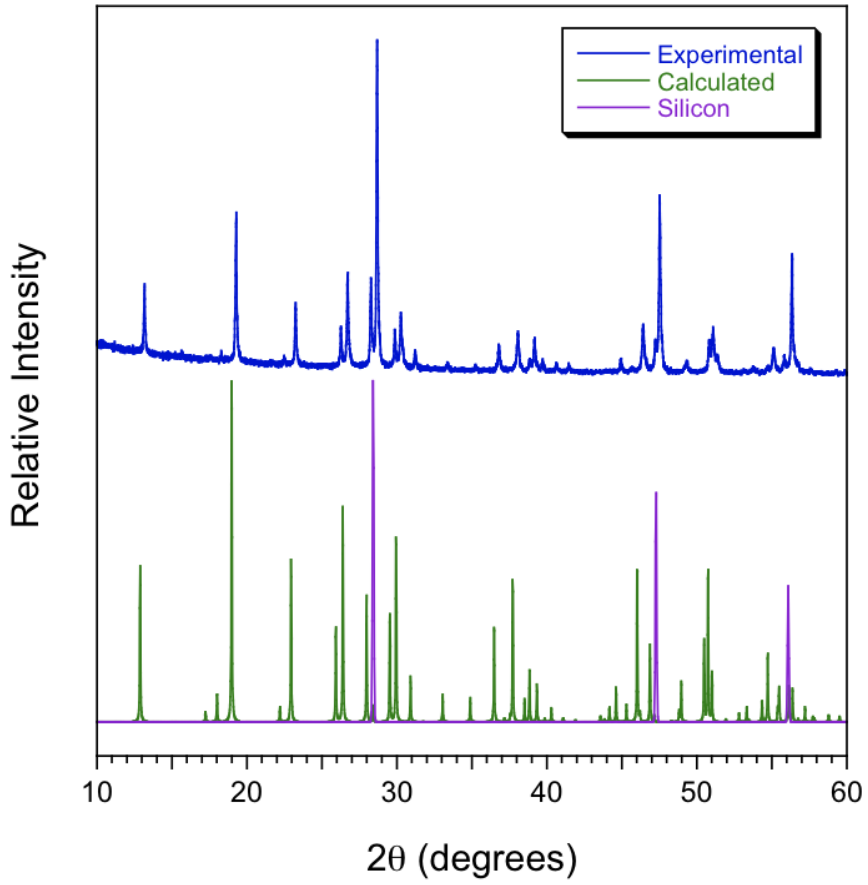

Figure 6.2. Powder X-ray diffraction of Li_2CdGeS_4. The sample was ground with a silicon standard and compared to the calculated pattern from single crystal data.

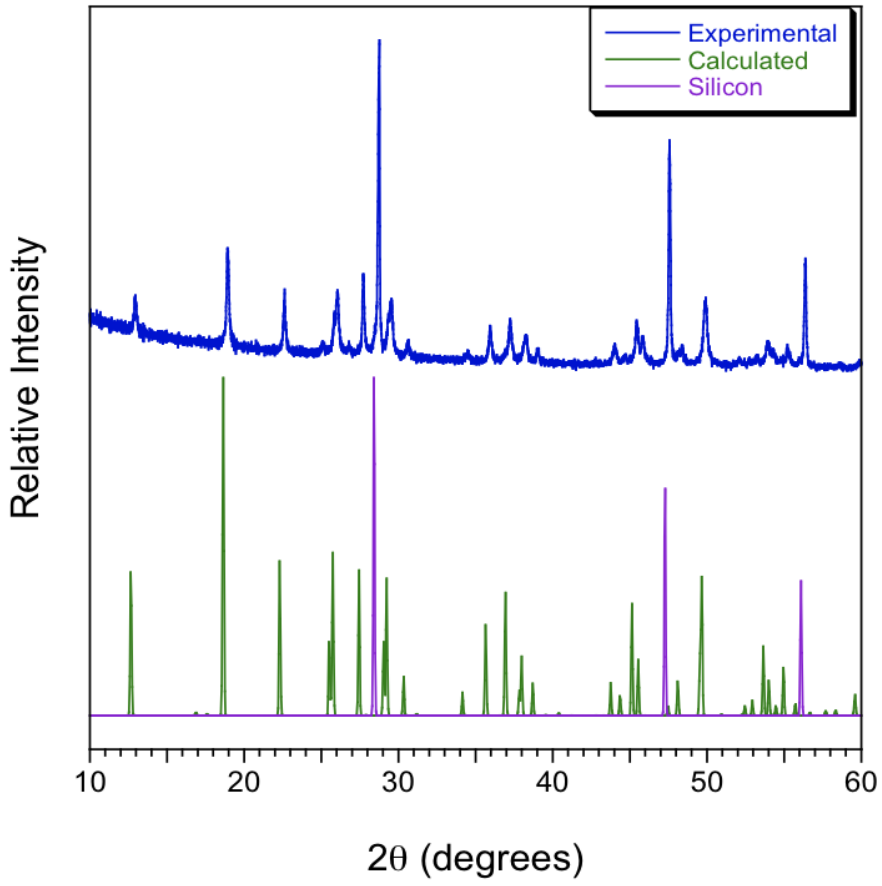

Figure 6.3. Powder X-ray diffraction of Li_2CdSnS_4. The sample was ground with a silicon standard and compared to the calculated pattern from single crystal data.

By virtue of being diamond-like, the compounds synthesized in this work are noncentrosymmetric (Figure 6.4), a prerequisite for SHG. A modified Kurtz NLO system was used to measure the SHG responses of both compounds.[305] Samples of Li_2CdGeS_4 displayed a type-I, phase-matchable, second harmonic response of approximately 70x α-quartz(ungraded) (Figure 6.5a). Li_2CdSnS_4 was also found to be SHG active, with a type-I, non-phase matchable response of 100x α-quartz(ungraded) (Figure 6.5b). However, this does not preclude the possibility that Li_2CdSnS_4 could display another type of phase-matchability, i.e. type II, that

cannot be measured on powder samples. Larger crystals than those obtained here are required to test for other types of phase-matchability. The presence of an SHG response by Li_2CdSnS_4 validates our structure solution in space group $Pmn2_1$.

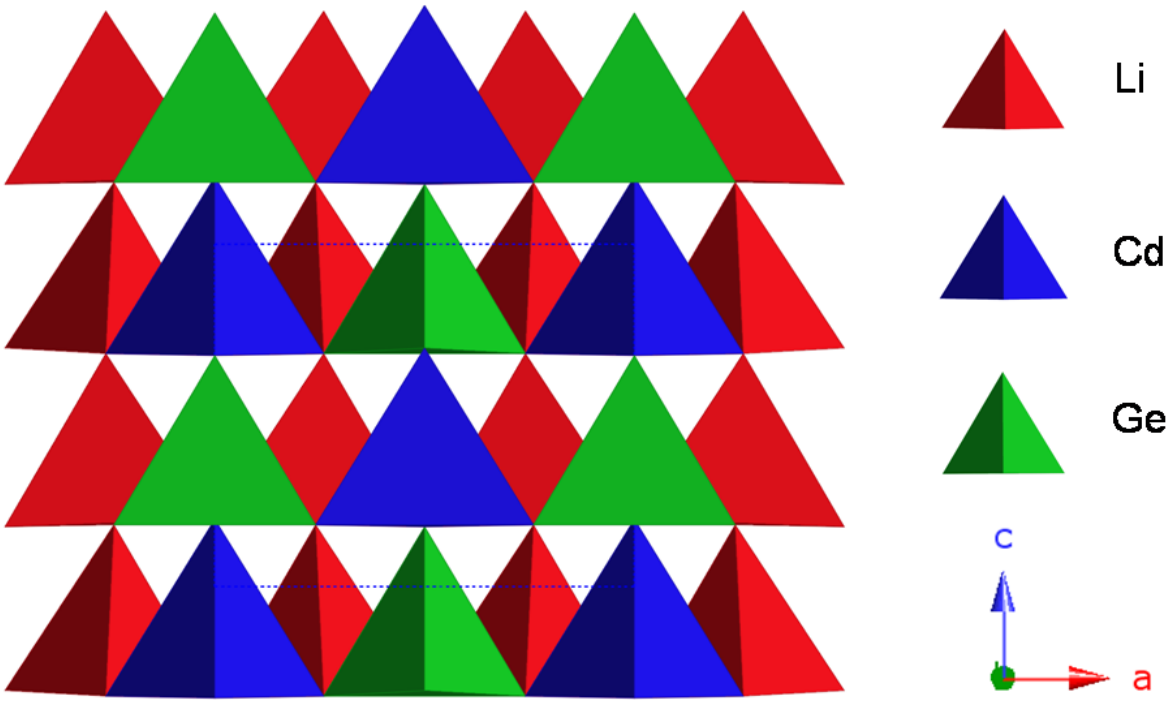

Figure 6.4. Polyhedral representation of the structure of Li_2CdGeS_4 that shows all tetrahedra oriented in the same direction along the *c*-axis, thus demonstrating the lack of an inversion center.

Fourier transform infrared spectroscopy was used to determine that these compounds are transparent in the infrared region, Figure 6.6. Transparency in this region is an additional criterion for practical NLO applications. In addition to infrared spectroscopy, optical diffuse reflectance UV/Vis/NIR spectroscopy was used to determine the band gaps of the compounds. Li_2CdGeS_4, a pale yellow compound, was found to have a band gap of 3.10 eV, while the pale orange Li_2CdSnS_4 was determined to have a band gap of 3.26 eV (Figure 6.7). The result for

Li_2CdSnS_4 is in sharp contrast to the report from Devi et. al. that this compound does not show any absorption edge.[295] These band gaps are significantly larger than those of the analogous Cu-containing compounds, Cu_2CdGeS_4 (2.05 eV)[306] and Cu_2CdSnS_4 (1.38 eV),[307] and the commercially available chalcopyrites used for SHG applications; $AgGaS_2$ (2.73 eV),[291] $AgGaSe_2$ (1.83 eV)[291] and $CuGaS_2$ (2.469 eV).[308] Larger band gaps are important because the laser damage threshold of a material is dependent upon the compound's band gap, with larger gaps leading to increased thresholds.[284] The wide gaps of Li_2CdSnS_4 and Li_2CdGeS_4 coupled with their substantial SHG response makes these and related compounds promising for NLO applications.

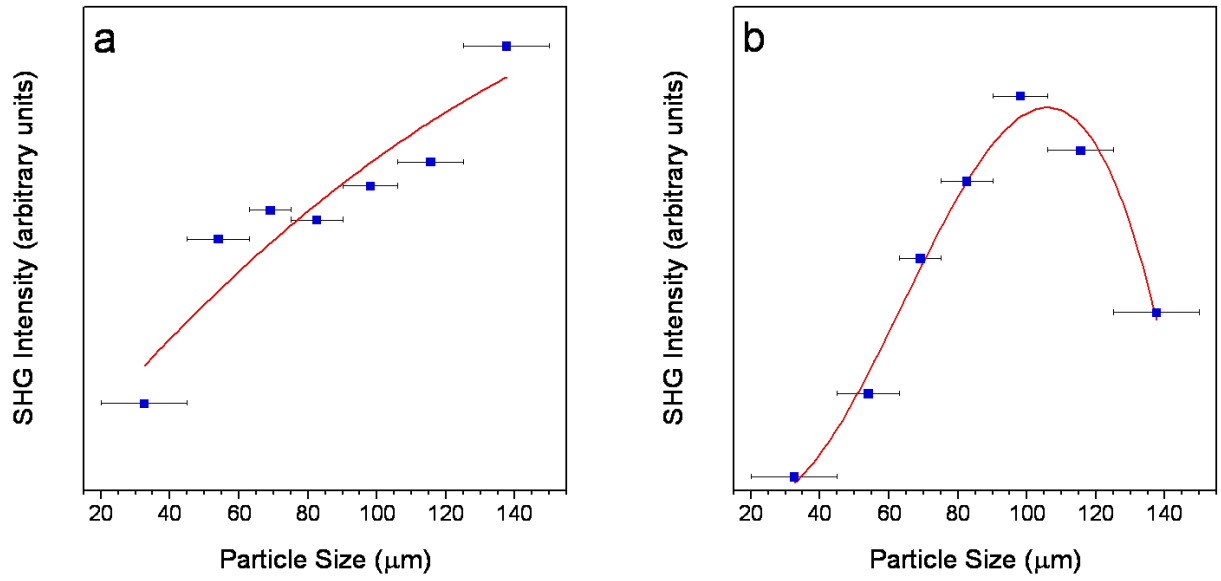

Figure 6.5 SHG measurements of (a) Li_2CdGeS_4 and (b) Li_2CdSnS_4. Li_2CdGeS_4 exhibits a type I, phase-matchable response of approximately 70x α-quartz, while Li_2CdSnS_4 exhibits a type I, non-phase-matchable response of approximately 100x α-quartz. The line in both plots is not a fit to the data but rather a guide for the eye.

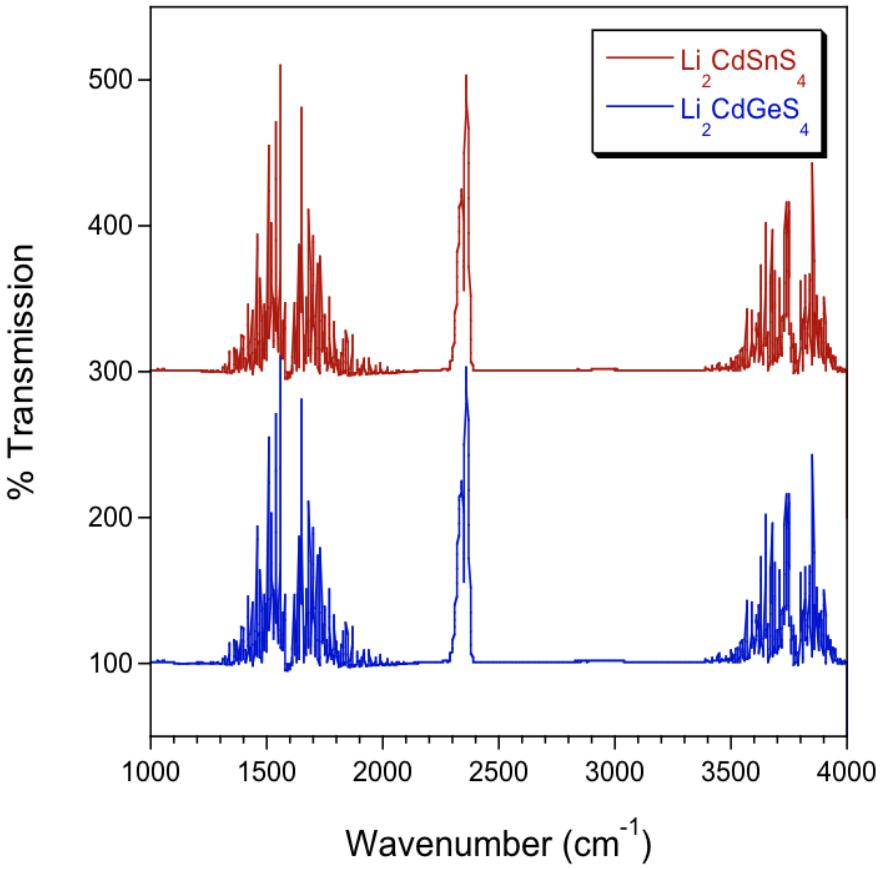

Figure 6.6 Infrared spectra, converted to transmission, of Li_2CdGeS_4 and Li_2CdSnS_4, demonstrating that both compounds are transparent in the infrared region.

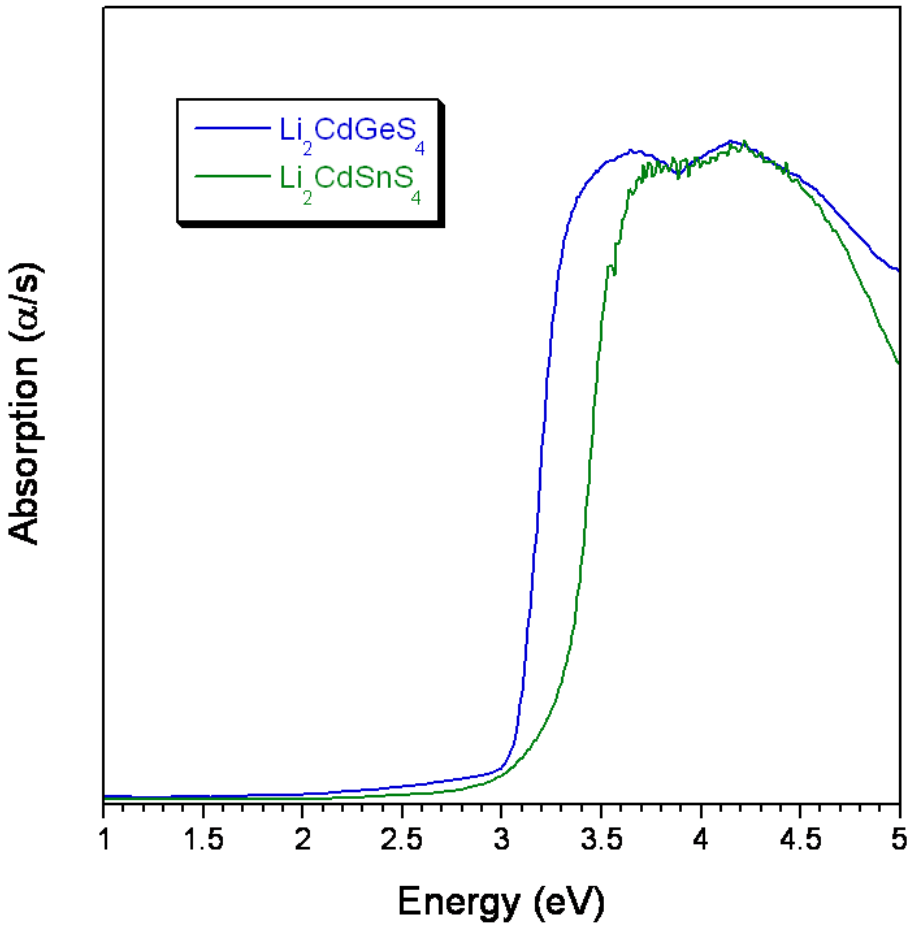

Figure 6.7 Optical diffuse reflectance spectra, converted to absorption, of Li_2CdGeS_4 and Li_2CdSnS_4.

6.4 Conclusion

In conclusion, two DLS, Li_2CdGeS_4 and Li_2CdSnS_4, were synthesized and found to display relatively wide band gaps in addition to significant SHG responses. These properties warrant further investigation of quaternary lithium-containing DLS compounds for nonlinear optical applications. Electronic band structure calculations are being conducted to understand the

origin of the band gaps. Additionally, Li_2ZnSnS_4[296] and Li_2ZnGeS_4 are being synthesized and characterized to expand the library of compounds at our disposal for physical property tuning.

6.5References

[275] Franken, P.A.; Hill, A.E.; Peters, C.W.; Weinrich, G. *Phys. Rev. Lett.* **1961**, *7*, 118.

[276] Kato, K *IEEE J. Quantum Electron.* **1991**, *27*, 1137.

[277] Miller, R.C.; Nordland, W.A. *Phys. Rev.* **1970**, *B2*, 4896.

[278] Brosnan, S.J.; Byer, R.L. *IEEE J. Quantum Electron.* **1979**, *15*, 415.

[279] Dmitriev, V.G.; Gurzadyan, G.G.; Nikogosyan, D.N. *Handbook of Nonlinear Optical Crystals*; Springer: New York, 1999.

[280] Chen, C.; Wu, Y.J. *Opt. Soc. Am.* **1989**, *B6*, 616.

[281] Ruderman, W.; Maffetone, J.; Zelman, D.; Poirier, D. *Mater. Res. Soc. Symp. Proc.* **1998**, *484*, 519.

[282] Bhar, G.C.; Smith, R.C. *Phys. Status Solidi* **1972**, *13*, 157.

[283] Chemla, D.S.; Kupecek, P.J.; Robertson, D.S.; Smith, R.C. *Opt. Commun.* **1971**, *3*, 29.

[284] Jackson, A.G.; Ohmer, M.C.; LeClair, S.R. *Infrared Phys. Technol.* **1997**, *38*, 233.

[285] Catella, G.C.; Burlage, D. *MRS Bull.* **1998**, *23*, 28.

[286] Goryunova, N.A. *The Chemistry of Diamond-Like Semiconductors,* Anderson, J.C. ed.; The M.I.T. Press: Cambridge, 1965.

[287] Parthé, E. *Crystal Chemistry of Tetrahedral Structures,* Gordon and Breach Science Publishers: New York, 1964.

[288] Parthé, E.; Yvon, K.; Dietch, R.H. *Acta Crystallogr. B.* **1969**, *25*, 1164.

[289] Schleich, D.M.; Wold, A. *Mater. Res. Bull.* **1977**, *12*, 111.

[290] Quintero, M.; Barreto, A.; Grima, P.; Tovar, R.; Quintero, E.; Porras, G.S.; Ruiz, J.; Woolley, J.C.; Lamarche, G.; Lamarche, A.M. *Mater. Res. Bull.* **1999**, *34*, 2263.

[291] Ohmer, M.C.; Pandey, R. *MRS Bull.* **1998**, *23*, 16.

[292] Bachmann, K.J.; Buehler, E.; Shay, J.L.; Wernick, J.H. *U. S. Publ. Pat. Appl. B*, **1975**, US 382021.

[293] Goetzberger, A.; Hebling, C.; Schock, H. *Mater. Sci. Eng.* **2003**, *40*, 1.

[294] Davidyuk, G.E.; Parasyuk, O.V.; Semenyuk, S.A.; Romanyuk, Ya. E. *Inorg. Mater.* **2003**, *39*, 919.

[295] Devi, M.S.; Vidyasagar, K. *J. Chem. Soc., Dalton Trans.* **2002**, 2092.

[296] Lekse, J.W.; Leverett, B.M.; Lake, C.H.; Aitken, J.A. *J. Solid State Chem.* **2008**, *181*, 3217.

[297] Kanatzidis, M.G.; Sutorik, A.C. *Progress in Inorganic Chemistry, Vol. 43*, Karlin, K.D. ed.; John Wiley & Sons, Inc.: Hoboken, 1999.

[298] P. Kubelka, F. Munk, Z. Tech. Phys. 12 (1931) 593.

[299] S.K. Kurtz, T.T. Perry, J. Appl. Phys. 39 (1968) 3798.

[300] K.M. Ok, N.S. Bhuvanesh, P.S. Halasyamani, Inorg. Chem. 40 (2001) 1978.

[301] SAINT and SADABS are part of the Apex 2 software package v2.1-4 Program for Data Collection and Reduction on Bruker AXS CCD Area Detector Systems, Bruker Analytical X-ray Systems, Inc., Madison, WI, 2005.

[302] G.M. Sheldrick *Acta Cryst. A* **2008**, *A64*, 112.

[303] Pauling, L. *J. Am. Chem. Soc.* **1929**, *51*, 1010.

[304] Schäfer, W.; Nitsche, R. *Mater. Res. Bull.* **1974**, *9*, 645.

[305] Kurtz, S.K.; Perry, T.T. *J. Appl. Phys.* **1968**, *39*, 3798.

[306] Davidyuk, G.E.; Parasyuk, O.V.; Semenyuk, S.A.; Romanyuk, Ya.E. *Inorg. Mater*+, **2003**, *39*, 919.

[307] Ichikawa, T.; Maeda, T.; Matsushita, H.; Katsui, A. *Journal of Advanced Science*, **2000**, *12*, 99.

[308] Horinaka, H.; Yamamoto, N.; Miyauchi, T. *J. Appl. Phys.* **1978**, *17*, 521.

7 Synthesis and Physicochemical Characterization of Li_2ZnGeS_4 and Trends in Quaternary Lithium-Containing Compounds

7.1 Introduction

Our daily lives are impacted in numerous ways by semiconductors. From the moment we wake (alarm clocks) to the ways we relax before sleep (television, the internet) from the transportation we use (cars, trains, planes, ships) to the devices we use to keep in touch (cell phones, computers) our modern world would not function without semiconductors. One particularly useful class of semiconducting compounds is diamond-like semiconductors (DLS).[309,310] DLS have applications that include photovoltaics[311] and nonlinear optics[312,313] as well as spin-based computing.[314] Silicon, the material that forms the basis of modern computing, can also be considered a DLS.

Diamond-like semiconductors are so named because the structures of these materials are based on that of diamond, either cubic or hexagonal forms. In order to be considered diamond-like a material must follow four guidelines, two valence electron rules and Pauling's first and second rules.[315] The first guideline is that the average number of valence electrons per atom must equal four. The second guideline is that the average valence electron concentration per anion must equal eight. The third guideline is Pauling's first rule, which should be satisfied such that each atom is tetrahedrally coordinated. The final guideline, Pauling's second rule, also known as the electrostatic valence sum rule should also be satisfied to ensure that the valence of each anion is satisfied by the atoms in the local coordination polyhedron.

A large portion of the work with DLS has focused on binary compounds, with less work focusing on ternary compounds and an even smaller portion investigating quaternary compounds.[316,317,318] Therefore, there is a lot of potential for research with quaternary DLS. These compounds are also of interest because increasing the diversity of the elements in the semiconductors also increases the compositional flexibility and the potential for physical property tuning. However, the price to pay for these benefits is an increase in the difficulty of the syntheses of quaternary DLS. Nevertheless, there are a few areas, such as non-linear optics, that could benefit greatly from quaternary DLS if their promise is realized. This is a result of the inherent potential for these compounds to frequency double light due to the lack of an inversion center in these compounds. Additionally, the highly polarizable metal-sulfur bonds are theorized to lead to larger second harmonic generation coefficients.[319] Lithium-containing compounds also have the additional benefit of typically having larger band gap energies than the corresponding copper- or silver-containing compounds. Because band gap energy is proportional to laser damage threshold,[319] larger band gaps are desirable for a material in a real world application. In this work, a new quaternary DLS compound, Li_2ZnGeS_4 was synthesized and compared to several related compounds that were previously reported.

7.2 Experimental

7.2.1 Reagents

Chemicals in this work were used as obtained: 1) lithium sulfide (Li_2S) powder, -200 mesh, 99.9%, Cerac; 2) zinc powder, -140 +325 mesh, 99.9%, Cerac; and 3) sulfur powder, sublimed, 99.5%, Fisher. Germanium pieces, 99.999%, Strem, were ground to a powder prior to use.

7.2.2 Synthetic Procedure

7.2.2.1 Li_2ZnGeS_4 Powder

2 mmol of Li_2ZnGeS_4 was prepared by weighing and grinding stoichiometric amounts of Li_2S, Zn, Ge, and S using an agate mortar and pestle in an argon-filled glovebox. The ground mixture was placed into a graphite crucible inside a 12 mm o.d. fused-silica tube. The tube was sealed under a vacuum of approximately 10^{-3} mbar, heated to 650 °C in 12 h and then held at 650 °C for 72 h. The sample was then slowly cooled to 450 °C in 100 h, heated to 650 °C in 20 h, cooled to 450 °C in 100 h, heated to 650 °C in 20 h, cooled to 450 °C in 100 h and finally cooled to room temperature in 12 h. The graphite crucible is necessary to prevent lithium from reacting with the fused-silica. The tube was opened under ambient conditions and the contents were examined using a light microscope. A white, microcrystalline powder, with a hint of orange, was obtained and used for property measurements.

7.2.2.2 Li_2ZnGeS_4 Crystals

A polychalcogenide flux was used to obtain single crystals of Li_2ZnGeS_4. The reaction mixture consisted of a 2:1:1:8 molar ratio of Li_2S:Zn:Ge:S, which was weighed and ground in an argon-filled glovebox. The ground mixture was placed into a graphite crucible inside a 12 mm o.d. fused-silica tube. The tube was sealed under a vacuum of approximately 10^{-3} mbar, heated to 750 °C in 12 h and then held at 750 °C for 96 h. The sample was cooled slowly to 450 °C in 60 h and then rapidly to room temperature in 3 h. The tube was opened under ambient conditions and the contents were washed with methanol to remove excess flux. A final rinse with diethyl-ether

was used to dry the crystals. An optical light microscope was used to select yellow-orange, plate-like, and orange plate-like crystals for energy dispersive spectroscopy. The orange plates were determined to be ZnS. The yellow-orange plates were identified as the quaternary phase. The yellow-orange crystals were then used for structure determination using single crystal X-ray diffraction.

7.2.3 Physical Property Measurements

7.2.3.1 Scanning Electron Microscopy and Energy Dispersive Spectroscopy (EDS)

A CamScan Series 4 scanning electron microscope was used to image samples and a Princeton Gamma Tech detector was used for EDS. The working distance was 35 mm and the accelerating voltage was set to 22.5 kV. Samples of two distinct kinds of crystals, yellow-orange and orange plates, were mounted onto double-sided carbon tape, which was adhered to an aluminum specimen holder. EDS data were collected for 60 s. The orange plates were found to contain only zinc and sulfur. However, the presence of zinc, germanium and sulfur in each of the yellow-orange crystals was confirmed, though the presence of lithium cannot be determined by this technique. Elemental mapping confirmed that each element was dispersed evenly throughout the yellow-orange crystals.

7.2.3.2 Differential Thermal Analysis (DTA)

DTA was performed using a Shimadzu DTA-50 thermal analyzer calibrated with a three-point calibration curve using indium, zinc and gold. The reference, Al_2O_3, and sample, of comparable masses, were contained in fused-silica ampoules (carbon coated for the sample) and

sealed under a vacuum of ~10^{-3} mbar. The temperature was programmed to increase at a rate of 10 °C/min from 25 °C to 1000 °C. The temperature then decreased to 100 °C at 10 °C/min. To distinguish reversible events from irreversible ones, a second cycle was performed in the same manner.

7.2.3.3 Diffuse Reflectance UV/Vis/NIR Spectroscopy

Optical diffuse reflectance spectra were obtained using a Cary 5000 UV/Vis/NIR spectrometer. Samples were ground and loaded into a Harrick Praying Mantis diffuse reflectance accessory that uses elliptical mirrors. $BaSO_4$ was used as a 100 % reflectance standard. Scans were performed from 2500 nm to 200 nm. Wavelength data were converted to electron volts and the percent reflectance data were converted to absorbance units using the Kubelka-Munk equation.[320] Two methods were used to determine the band gap. The first method was by using a tangent line to extrapolate the absorption edge to determine where it crosses through the baseline. The second method used the first derivative to determine the inflection point of the absorption edge. The inflection point should occur approximately half way between the beginning and the end of the absorption edge.

7.2.3.4 Second Harmonic Generation (SHG) Measurements

SHG of a powdered sample of Li_2ZnGeS_4 was measured using a modified Kurtz NLO system[321] with a Nd:YAG laser, as described elsewhere.[322] The response of Li_2ZnGeS_4 was compared to that of α-quartz, a typical standard for this technique.

7.2.3.5 Powder X-Ray Diffraction

Powder diffraction patterns were collected using a Panalytical X'Pert Pro MPD powder X-ray diffractometer. Data were collected from 5 to 80 °2θ with a sampling interval of 0.083556 °. The scan rate used was 0.010577 °/s. Samples were spun during data collection. The instrument was set to an accelerating voltage of 45 kV and a filament current of 40 mA. Copper K_α radiation with a wavelength of 1.541871 Å was used for measurements. Samples were prepared for analysis by spreading powder onto a piece of double-sided tape adhered to a glass slide placed into the aluminum sample holder.

7.2.3.6 Single Crystal X-Ray Data Collection and Reduction

Single crystal X-ray diffraction data were collected on a Bruker SMART Apex 2 CCD diffractometer at room temperature. Data were collected for 20 s per frame using Mo K_α radiation with a wavelength of 0.71073 Å and a graphite monochrometer. During data collection the instrument was set to 50 kV and 30 mA. A liquid nitrogen cooling system was used to keep the crystal at 175 K during data collection. The unit cell parameters determined using the Bruker software package were unlike previously prepared compounds and did not fit the data well, so the Cell_Now[323] program was used to determine the unit cell parameters that were used for refinement and structure solution. The Bruker SAINT[324] program was used for data integration. After integration, there were a total of 10719 reflections collected with 2191 unique. An empirical absorption correction was performed using the SADABS[255] program. The structure solution and full-matrix least-squares refinement on F^2 were performed using SHELXTL-97.[325] Probable space groups based on systematic absences included *P*nma (centrosymmetric) and *P*na2_1 (noncentrosymmetric). *P*na2_1 was selected, as diamond-like semiconductors should be

noncentrosymmetric based upon the four rules for DLS. The structure that was determined has disorder between zinc and lithium on two sites, Figure 7.1. Important crystallographic data and structure refinement details can be found in Table 7.1.

7.2.4 Electronic Structure Calculations

The DMol3 code within Materials Studio was used to calculate the electronic structure of four lithium-containing DLS. Geometry optimization calculations were performed on each compound. For these calculations, a double numerical potential (DNP) basis set with a Perdew-Wang correction (PWC)[326] local spin density approximation functional was used for Li_2ZnGeS_4, Li_2CdGeS_4, Li_2CdSnS_4 and Li_2ZnSnS_4.

7.3 Results and Discussion

7.3.1 Structure

Known quaternary diamond-like semiconductors have been reported to crystallize in several space groups; *P*mn2_1,[327] *P*na2_1,[328] *P*n[329] and *I*-42m.[330] The differences between these space groups are derived from the arrangement of the cations in the structures. Preliminary structural details were previously determined for Li_2ZnGeS_4 from powder diffraction data. [331] In that report the structure was determined to be orthorhombic with lattice parameters; a=7.83 Å, b=6.53 Å and c=6.21 Å. The lattice parameters found during this study were different than those values. The lattice parameters determined by the Bruker Apex 2 software were a=26.1644 Å, b=7.8282 Å and c=6.2236 Å. Two of the parameters are similar, 7.8 Å and 6.2 Å; however, it

seems as though the third parameter is quadrupled, 6.53 Å compared to 26.1644 Å. Cell_Now was used to check the new lattice parameters and produced a third set of lattice parameters; a=13.0822 Å, b=7.8282 Å and c=6.2236 Å. The lattice parameters obtained from Cell_Now were used for structure refinement and solution. The output from Cell_Now also indicates that the data set could potentially come from a twinned crystal.

The structure of Li_2ZnGeS_4 was solved in the orthorhombic space group $Pna2_1$ with R1, all data, = 2.98 %, Figure 7.1. It possesses the honeycomb arrangement that is observed in all DLS, Figure 7.2. There are eight crystallographically unique atomic sites; one lithium, one germanium, four sulfur and two additional metal sites. In order to refine the structure, the remaining two atomic sites had to be disordered between lithium and zinc. This disorder would lead to violations of Pauling's second rule because, with true disorder, the lithium and zinc cations will be randomly distributed in the structure. For example, this would mean that there are some sulfur anions that would be surrounded by one lithium cation, one germanium cation and two zinc cations, which is too much positive charge around the sulfur and should not occur in a DLS. The opposite is also true and some sulfur anions would be surrounded by too little positive charge. The result of the violation of Pauling's second rule would be distortions of the diamond-like structure. Therefore, we believe that this structure model may be from a twinned crystal as we have observed in Li_2ZnSnS_4.[332]

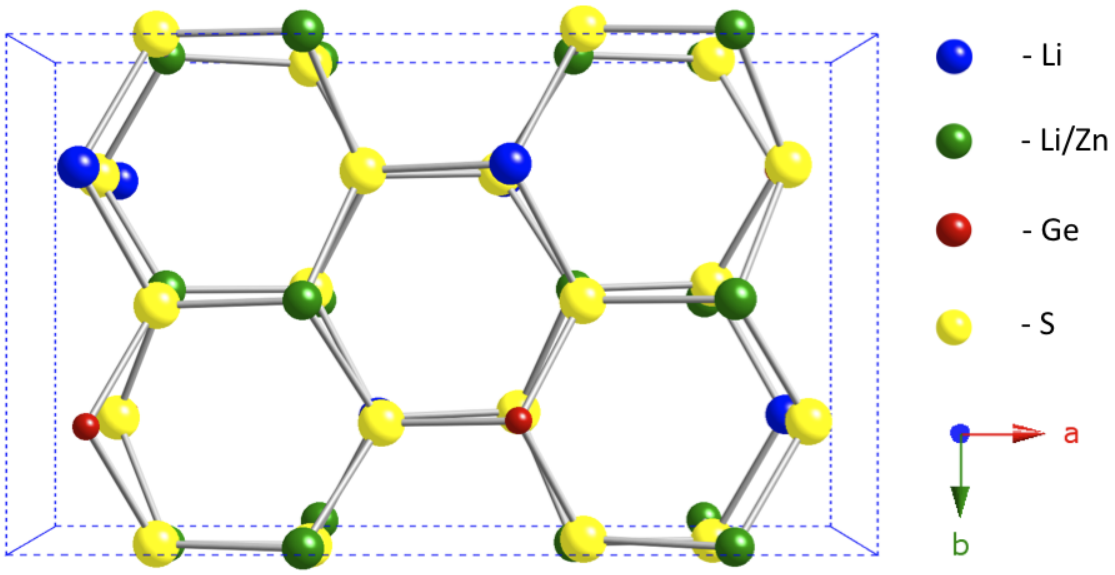

Figure 7.1. The structure of Li_2ZnGeS_4, viewed down the c-axis.

Table 7.1 Selected crystallographic parameters for Li_2ZnGeS_4.

Empirical Formula	Li_2ZnGeS_4
Formula Weight	280.08
Temperature	293(2) K
Wavelength	0.71073 Å
Space Group	*P*na2_1
Unit Cell Dimensions	a = 13.0822(2) Å α = 90.00 °
	b = 7.8282(2) Å β = 90.00 °
	c = 6.2236(1) Å γ = 90.00 °
Volume	637.36 (2) $Å^3$
Z, Calculated Density	4, 2.919 Mg/m^3
Absorption Coefficient	9.648 mm^{-1}
F(000)	528
Reflections Collected / Unique	10719 / 2191
Data / Restraints / Parameters	2191 / 1 / 77
Completeness to theta = 27.06	96.3 %
Goodness of Fit	1.099
Final R indices [I>2sigma (I)]	R1 = 0.0246, wR2 = 0.0750
R indices (all data)	R1 = 0.0298, wR2 = 0.0773

Table 7.2 Atomic coordinates and equivalent isotropic displacement parameters ($Å^2$ x 10^3) for Li_2ZnGeS_4.

	Multiplicity	Wycoff Letter	x	y	z	U(eq)*	SOF
Li(1)	4	*a*	0.1614(1)	0.0117(1)	0.5590(7)	8(1)	0.30614
Zn(1)	4	*a*	0.1614(1)	0.0117(1)	0.5590(7)	8(1)	0.69386
Li(2)	4	*a*	0.1609(1)	0.4909(1)	0.5572(18)	12(1)	0.70515
Zn(2)	4	*a*	0.1609(1)	0.4909(1)	0.5572(18)	12(1)	0.29485
Li(3)	4	*a*	0.0789(5)	0.2530(7)	0.0690(30)	20(2)	1.0
Ge(1)	4	*a*	0.4113(1)	0.2556(1)	0.5576(1)	8(1)	1.0
S(1)	4	*a*	0.3354(1)	0.4891(1)	0.6778(1)	11(1)	1.0
S(2)	4	*a*	0.4064(1)	0.2558(1)	0.2020(2)	10(1)	1.0
S(3)	4	*a*	0.0711(1)	0.2520(1)	0.6736(2)	8(1)	1.0
S(4)	4	*a*	0.3345(1)	0.0214(1)	0.6746(2)	11(1)	1.0

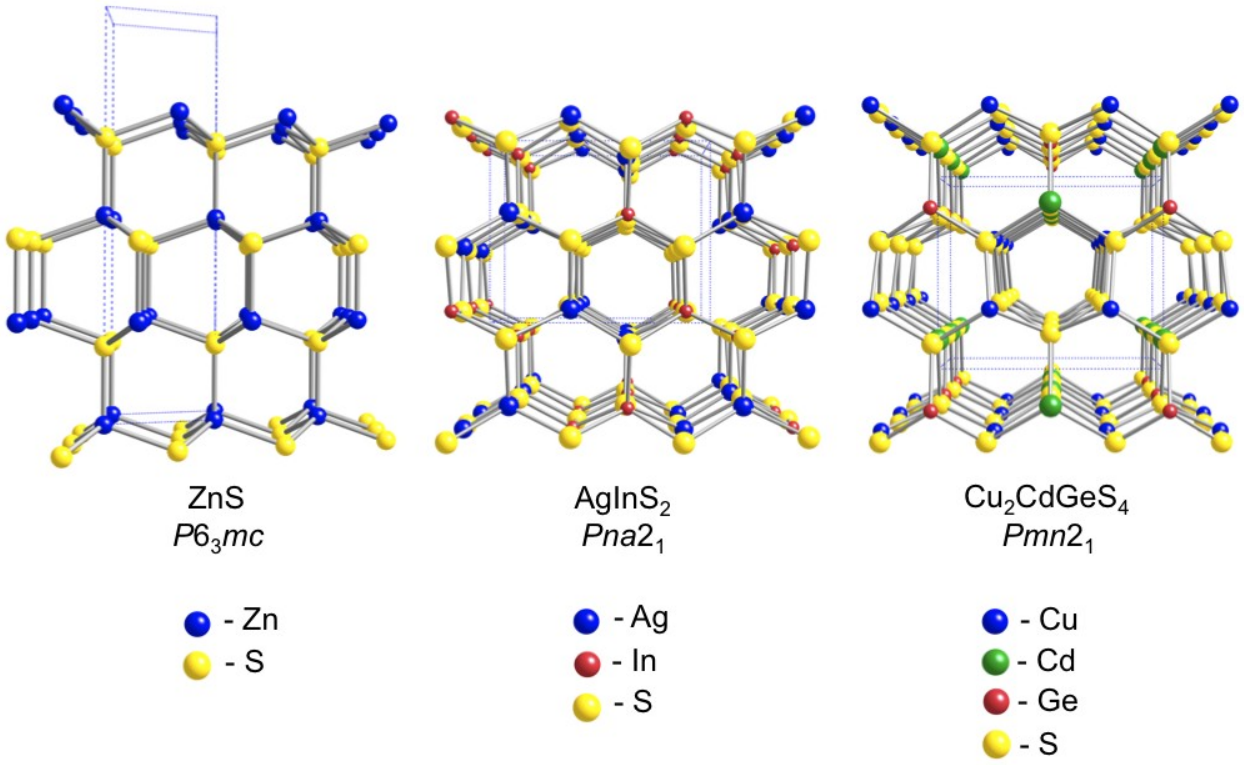

Figure 7.2. The structural progression from binary to ternary and quaternary diamond-like semiconductor based on hexagonal closest packing is demonstrated by three compounds. The honeycomb structure can be seen in each compound.

Comparison of the structures of all four lithium-containing compounds, Li_2ZnGeS_4, Li_2ZnSnS_4, Li_2CdGeS_4 and Li_2CdSnS_4, shows that the structures of the cadmium-containing compounds adopt the space group $Pmn2_1$, which is more prevalent in the DLS literature.[327,328] The zinc-containing compounds crystallize in less encountered space groups, coincidentally, both zinc-containing compounds also have a twinning problem. Both Li_2CdGeS_4 and Li_2CdSnS_4 are of the wurtz-stannite structure type. The structure of Li_2ZnSnS_4 differs from Li_2CdGeS_4 and Li_2CdSnS_4 in the arrangement of the cations, Figure 7.3, which reduces the overall symmetry to monoclinic. Li_2ZnGeS_4 is unique among all four compounds because of the unit cell parameters. Of the four compounds, only Li_2ZnGeS_4 has a unit cell parameter greater than 8 Å, due to a

doubling of one of the unit cell edges. This doubling can also be attributed to the arrangement of the cations, Figure 7.3, though it could also be a result of the twinning problem that was previously mentioned.

Powder X-ray diffraction of the powder obtained from the direct combination reaction was used to determine the validity of the structure model. An experimental pattern was compared to the pattern calculated based on the structure model that contains disorder, Figure 7.4. The two patterns were found to match well. There are two peaks, at 13.3 and 19.7 °, that are unusually broad, the cause of which is unknown at this point in time. Every peak in the calculated pattern is accounted for in the experimental pattern; therefore, we can conclude that the structure model is very close to being correct.

In an attempt to determine a twin law that could explain the single crystal data, the structure was closely examined to determine if the two disordered sites are related by a symmetry element. In the case of Li_2ZnSnS_4, the two problem sites were related by a two-fold rotational axis. Identifying the symmetry element that related the two sites lead to the realization that the compound was a twin and made the eventual structure solution possible. Unfortunately there was no easily observed symmetry element that related the two sites in the Li_2ZnGeS_4 structure. When no symmetry element could be identified, integer twin laws were used systematically to attempt to resolve the twin components. This method was also unsuccessful in resolving the structural issues of this model. Work, including Rietveld refinement, to determine the correct structure model for Li_2ZnGeS_4 is ongoing.

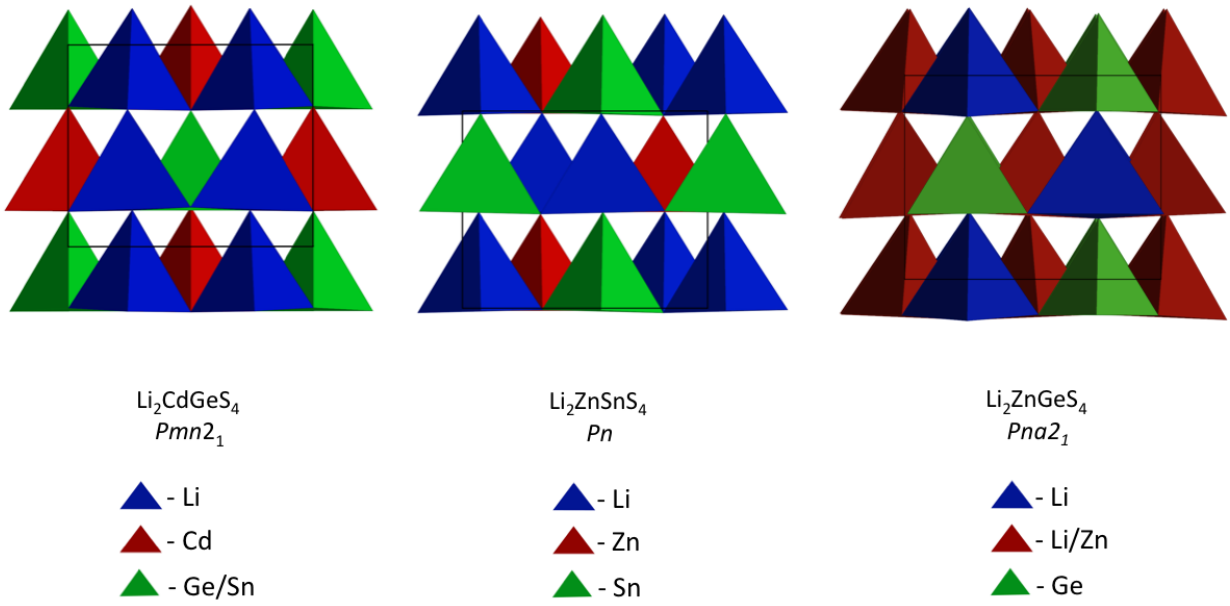

Figure 7.3. A comparison of the polyhedral representations of the three different structures that lithium-containing DLS have been found to adopt. The view is down the corresponding axis for each compound, approximately 6.5 Å in Li_2CdGeS_4 and Li_2ZnSnS_4 and the 13.08 Å axis in Li_2ZnGeS_4.

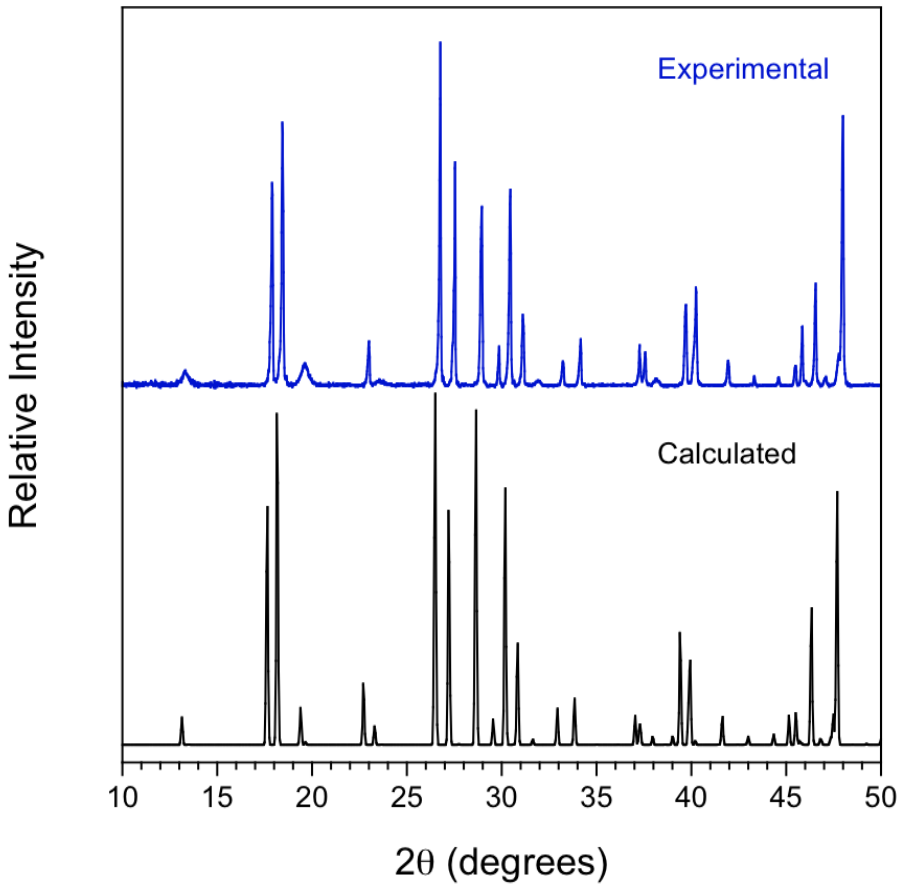

Figure 7.4. Powder diffraction of a sample of Li_2ZnGeS_4 (blue) compared to the powder pattern calculated from the crystal structure model containing disorder (black).

7.3.2 Second Harmonic Generation

Previous research has shown that lithium-containing DLS are promising materials for non-linear optical applications.[333] Li_2CdGeS_4 and Li_2CdSnS_4 were found to be second harmonic generating in the infrared region. Li_2CdGeS_4 demonstrated a Type I phase-matchable SHG response approximately 70x α-quartz and Li_2CdSnS_4 exhibited a Type I non-phase-matchable SHG response approximately 100x α-quartz. Due to these promising results, the second

harmonic response of Li_2ZnGeS_4 was measured and found to be Type I non-phase-matchable with a response approximately 100x α-quartz, Figure 7.5,comparable to Li_2CdSnS_4.

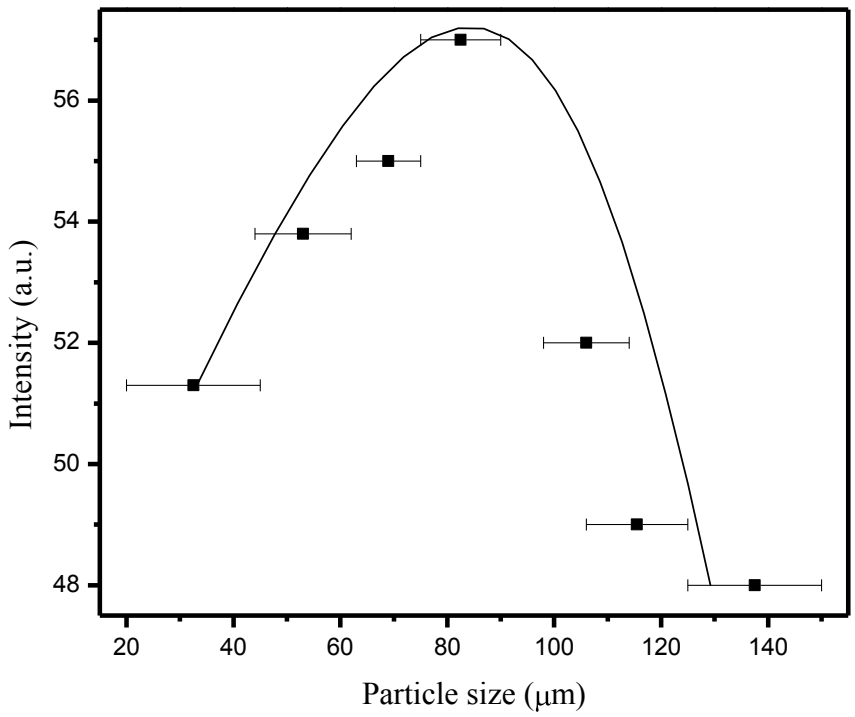

Figure 7.5. SHG measurement of Li_2ZnGeS_4 which exhibits a type I, non-phase-matchable response of approximately 100x α-quartz. The line in the plot is not a fit to the data but rather a guide for the eye.

7.3.3 Differential Thermal Analysis

Differential thermal analysis was used to determine the thermal behavior of all four diamond-like compounds. It was found that the germanium-containing compounds, Li_2ZnGeS_4 and Li_2CdGeS_4, had lower melting points compared to the tin analogs. Li_2ZnGeS_4 was found to

have only one thermal event, at 846 °C, upon heating and one corresponding thermal event upon cooling, Figure 7.6. This event was identified as a melting point. The melting points of the other lithium-containing compounds have been previously reported, Table 7.3. The compound appears to melt congruently which could have implications for crystal growth. To determine if the compound truly melts congruently, an experiment with a slower heating and cooling rate need to be performed and a PXRD pattern of the product obtained. This is problematic because the sample reacts with the ampoule during the second cycle in spite of the carbon coating. If the heating and cooling rates are slowed the sample will have more time to react with the ampoule during the first cycle. To account for this an experiment could be conducted using a furnace with the sample in a graphite tube.

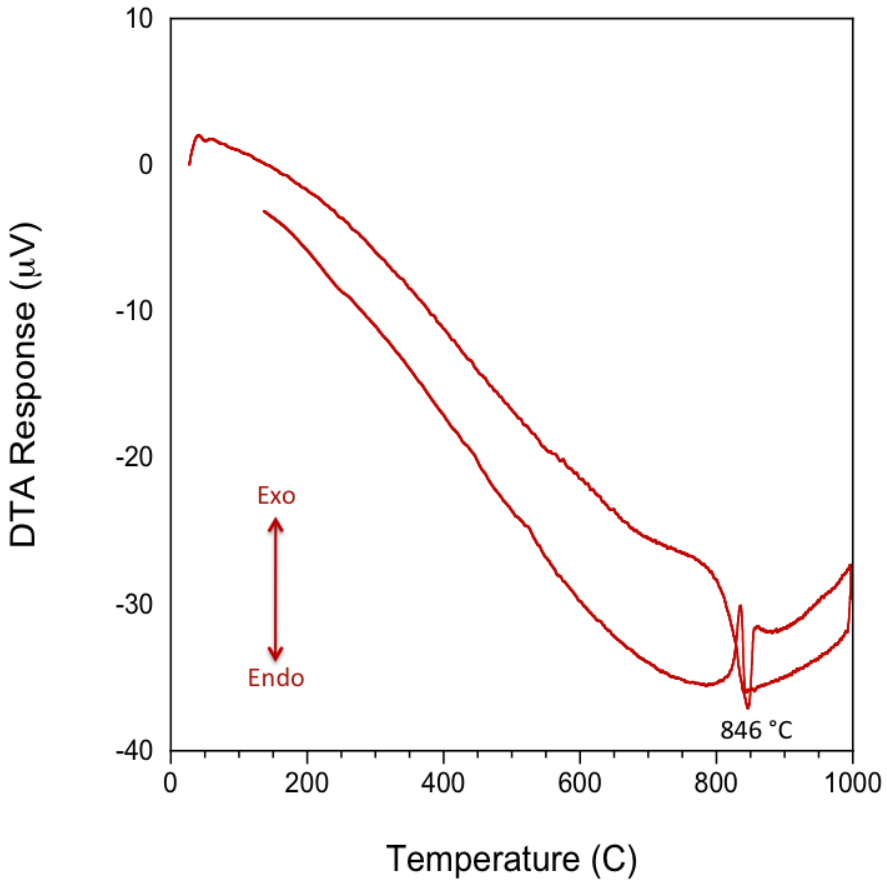

Figure 7.6. Differential thermal analysis was used to characterize the thermal properties of Li_2ZnGeS_4. The one thermal event, at 846 °C, observed upon heating is attributed to the compound melting and the corresponding event upon cooling is the subsequent recrystallization.

Table 7.3 Melting points of quaternary lithium-containing DLS

Compound	Melting Point (°C)
Li_2CdGeS_4	817
Li_2ZnGeS_4	846
Li_2ZnSnS_4	919
Li_2CdSnS_4	923

7.3.4 Diffuse Reflectance

New materials for non-linear optical applications need to outperform existing materials in order to be viable for device applications. One way to achieve increased performance is to have a greater SHG response than currently used materials. An alternative route is to have an increased laser damage threshold. The laser damage threshold of a material is a measure of the intensity of light that is required for a material to begin to degrade. The band gap of a material is directly proportional to the laser damage threshold of a material; therefore, new materials with large band gaps are desirable.[334] Diffuse reflectance UV/Vis/NIR spectroscopy was used to determine that the band gap of Li_2ZnGeS_4 is 3.92 eV, Figure 7.7. This value is greater than the band gaps of Li_2ZnSnS_4, Li_2CdGeS_4 and Li_2CdSnS_4, Table 7.4. All of these new compounds have wider band gaps than materials that are currently in use for nonlinear optical device applications, providing further evidence of the promise of these compounds for non-linear applications.

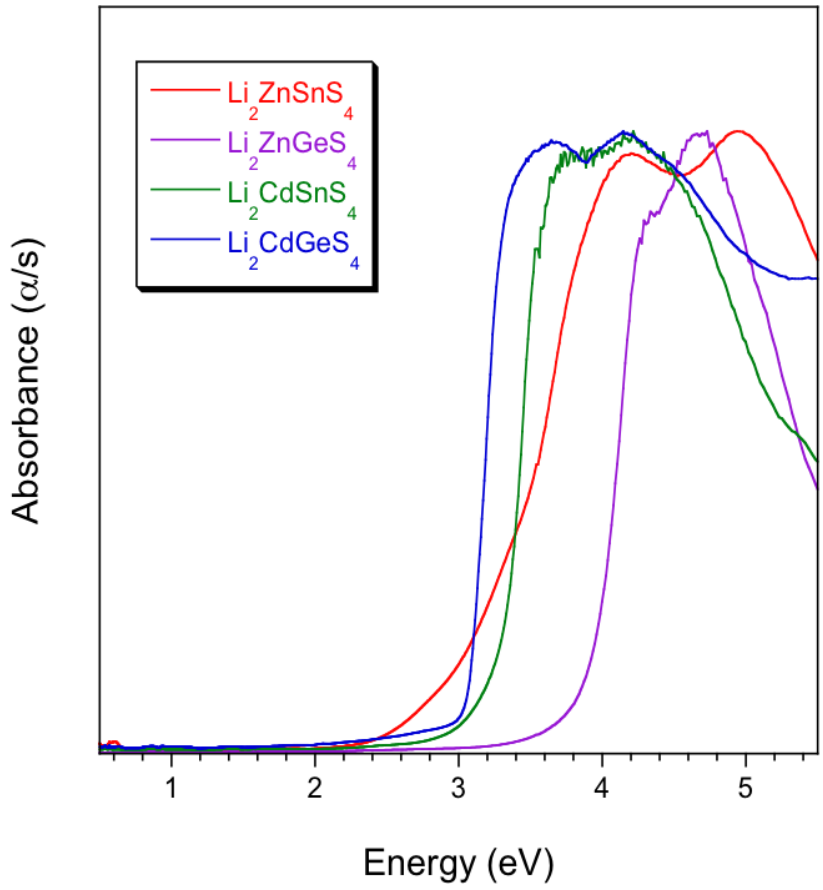

Figure 7.7. A comparison of the diffuse reflectance spectra of four lithium-containing DLS. Li_2ZnGeS_4 has the largest band gap energy, 3.92 eV.

Table 7.4. Band gap energies of quaternary lithium-containing DLS

Compound	Experimental Band Gap Energy by Extrapolation (eV)	Experimental Band Gap Energy by First Derivative (eV)	Computational Band Gap Energy (eV)
Li_2ZnGeS_4	3.92	4.14	1.96
Li_2CdSnS_4	3.25	3.45	2.18
Li_2CdGeS_4	3.05	3.29	2.45
Li_2ZnSnS_4	2.87	3.75	2.37

7.3.5 Electronic Structure Calculations

In an attempt to explain the trend in the experimentally obtained band gap energies, electronegativity differences between atoms and bond distances in the structures were examined. Pauling electronegativities,[335,336] Table 7.5, were used to calculate the electronegativity difference between sulfur and each other element. The average electronegativity difference for each compound was found by averaging the four electronegativity differences for the bonding atoms, Table 7.6. in simple binary DLS, band gap energies are found to increase for compounds containing atoms where $\Delta\chi$ increases, for example Ge<GaAs<ZnSe<CuBr.[337,338] An increase in the electronegativity difference results in an increase in the ionic character of the bonding in these compounds. As the bonding in these compounds becomes more ionic the band gap energies of the compounds increase. Based upon the values in Table 7.6, the band gap trend in order of increasing energy is Li_2CdGeS_4, Li_2ZnGeS_4, Li_2CdSnS_4 and Li_2ZnSnS_4. Li_2ZnGeS_4 and Li_2CdSnS_4 have approximately the same value for overall electronegativity difference; however, when additional decimal places are included the difference for Li_2CdSnS_4 is slightly larger. This differs from the observed trend in that, experimentally, Li_2ZnGeS_4 has the largest band gap energy, but only the second largest average electronegativity difference. It should also be noted that the range of the electronegativity differences in these four compounds is small, 1.17-1.19, which could contribute to the discrepancy in the predicted band gap trend. It appears that electronegativity, by itself, is not sufficient to explain the observed trend as a result bond distances in the four compounds were examined.

Table 7.5. Pauling electronegativity value for selected elements

Element	Electronegativity (χ)
Li	0.98
Cd	1.69
Zn	1.65
Ge	2.01
Sn	1.96
S	2.58

Table 7.6. Average electronegativity differences for lithium-containing DLS

Compound	Average Electronegativity Difference
Li_2ZnGeS_4	1.18
Li_2ZnSnS_4	1.19
Li_2CdSnS_4	1.18
Li_2CdGeS_4	1.17

Bond distances in the four compounds were also examined in order to attempt to explain the observed trend in band gap energy. In simple elemental DLS, band gaps widen with shorter atomic distances, for example Si>Ge>Sn with respect to band gap but Si<Ge<Sn with respect to bond distances.[337,338] The shorter the bond distance the more overlap there is between atomic orbitals. It is this additional overlap that results in stronger bonds and an increase in the band gap energy. The average bond distances can be found in table 7.7. The length of the cadmium-sulfur

bonds is longer than the average length of the zinc-sulfur bonds and the average length of the tin-sulfur bonds is greater than the germanium-sulfur bonds. Neither of these observations seems to explain the observed band gap trend. The trend in the total average bond distances is also different than the observed trend in the experimental data. One compound is out of order; Li_2CdGeS_4, which should have the longest bond distances, because it has instead has the second shortest average bond distance. However, the length of the lithium-sulfur bond, between sites that are exclusively lithium and sulfur, follows the same trend as the experimental band gap energies, i.e. the band gap energy increases with increasing bond length. This correlation is likely not enough, by itself, to fully explain the origin of the trend in band gap energy, but could be a useful starting point for future studies that incorporate both bond distance and electronegativity among other properties.

Table 7.7. Average bond distances in four lithium-containing DLS

Li_2ZnGeS_4		**Li_2ZnSnS_4**		**Li_2CdSnS_4**		**Li_2CdGeS_4**	
Li-S	2.45(1) Å	Li-S	2.44(3) Å 2.43(5) Å	Li-S	2.42(1) Å 2.42(1) Å	Li-S	2.42(1) Å 2.42(1) Å
Li/Zn-S	2.364(2) Å 2.387(7) Å	Zn-S	2.352(8) Å	Cd-S	2.540(1) Å	Cd-S	2.546(1) Å
Ge-S	2.213(1) Å	Sn-S	2.391(7) Å	Sn-S	2.386(1) Å	Ge-S	2.212(1) Å
Average	2.354(6) Å	Average	2.40(3) Å	Average	2.442(7) Å	Average	2.340(7) Å

In previous research, electronic structure calculations have been used to gain an understanding of the origin of the trends observed in the physical properties of materials. For example, electronic structure calculations have been used to determine the elements and in particular which orbitals contribute to the states around the band gap. This can then guide

researchers as to which elements to replace in order to affect the band gap. To our knowledge there are no examples of electronic structure calculations being used as a predictive tool, where the calculated predictions are then followed and reinforced by experimental evidence. However, there are experimental groups that use calculations to rationalize experimentally obtained data. There are also computational groups using calculations to make predictions, but there is rarely any follow through that corroborates the predictions. In an ideal scenario, a group would synthesize several compounds, then use calculations to model trends in those compounds. These compounds would then be used to predict which compounds show the most promise and then synthesize those compounds, which would ideally posses the predicted properties. In this way experiments and calculations are used synergistically to support and enhance each other, greatly furthering research in both areas. This is the ultimate vision for this work, however we are only beginning to embark upon a path that will lead to this goal. For this work, the DMol3 code in the Materials Studio[339] package was used to calculate the electronic structure of the four lithium-containing diamond-like semiconductors; Li_2ZnGeS_4, Li_2CdGeS_4, Li_2CdSnS_4 and Li_2ZnSnS_4. In order to perform a calculation, a basis set and a functional must be selected. The basis set is used to determine the electron density which the functional then converts to energy.

Geometry optimization calculations were performed on each compound. For these calculations, a double numerical potential (DNP) basis set with a Perdew-Wang correction (PWC)[326] local spin density approximation functional was used for the four compounds. Though this combination did not result in the same trend as that obtained from the experimental data, Table 7.4, it was an important step that will begin our group's study of the electronic structure of these materials. The calculations provided the density of states and band structure plots for each compound, an example of which can be found in Figure 7.8. These plots show that the orbitals

with the largest contribution near the Fermi level are germanium s and d orbitals and sulfur p orbitals. Lithium p orbitals also contributes slightly, while zinc appears to contribute very little, to the electronic structure near the Fermi level. This work can expand to include the use of other basis sets, functional and even other programs. Initial work with other combinations of the available basis sets and functionals was performed in an attempt to reproduce the trend observed in the experimental band gap energies. The most promising options, those with the highest levels of theory, were examined; unfortunately, no combination of basis set and functional, that was tested in the DMol3 package, produced the same trend as that observed experimentally. Though the testing was thorough, it was not exhaustive and the remaining options, though of lower levels of theory, should also be tested to determine if they can produce a trend identical to that observed in the experimental data. There are indications that DMol3 may not be the ideal code to perform these calculations. An examination of the literature revealed that while DMol3 is often used to model molecular solids, it is rarely found in the literature where the electronic structures of extended solids are calculated. In order to better model these compounds a different program, such as WIEN2K,[340] should be used in the future. WEIN2K is the code that is most commonly found in the solid-state literature and may provide electronic structures that more closely correspond with the trend observed in the experimental band gaps.

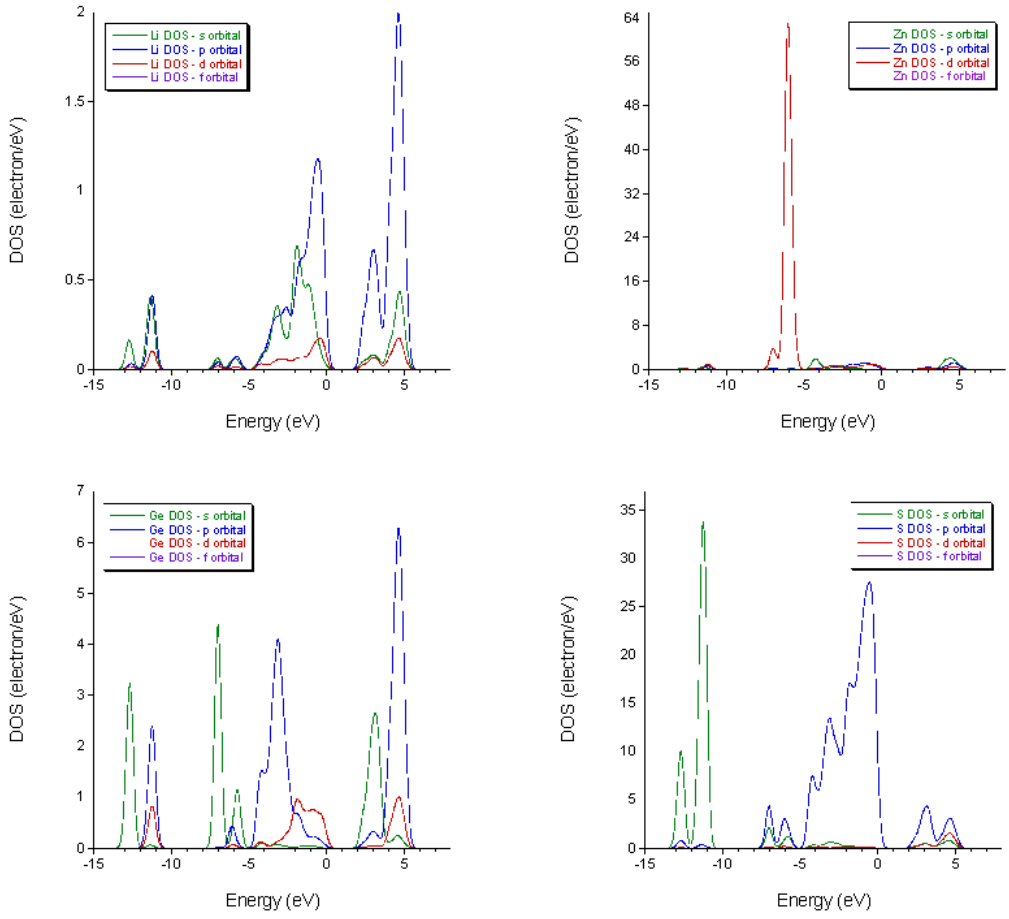

Figure 7.8. Density of states plots showing the contribution of each orbital in each element of Li_2ZnGeS_4, created based on the electronic structure calculations.

7.4 Conclusions

Li_2ZnGeS_4 was synthesized and characterized. The structure of the compound was proposed, but contains disorder, which should not be present in a true diamond-like

semiconductor. Future investigations should be made into the structure of Li_2ZnGeS_4, because the disorder is likely an indicator of a twinning problem. The properties of Li_2ZnGeS_4 were compared to three other diamond-like semiconductors, Li_2CdGeS_4, Li_2CdSnS_4 and Li_2ZnSnS_4, that were also synthesized and characterized by our laboratory. Three of the four compounds were found to possess interesting nonlinear optical properties, specifically second harmonic generation. The compounds also have larger band gap energies than materials that are currently in use for SHG applications. The nonlinear optical properties coupled with wide band gaps means that these compounds are promising for real-world applications. Additionally, electronic structure calculations were used in an attempt to understand the origin of the band gaps of the four compounds. The calculations did not result in the same trend in band gap as that observed experimentally, but provide a good starting point for future electronic structure calculations from our lab. In conclusion, it does not seem that any individual property of the elements or their bonds determines the band gap energies in the compounds. Therefore, it is most likely the overall structural differences (i.e. ordering of the cations) which dictate the band gap in these materials. Consequently, band structure calculations which take into account the entire structure and its symmetry should eventually provide an answer.

7.5 References

[309] N.A. Goryunova *The Chemistry of Diamond-like Semiconductors*, J.C. Anderson, ed., The M.I.T. Press; Cambridge, 1965.

[310] E. Parthé, *Crystal Chemistry of Tetrahedral Structures*, Gordon and Breach Science Publishers; New York, 1964.

[311] A. Goetzberger, C. Hebling, H. Schock *Mater. Sci. Eng.* **2003**, *40*, 1.

[312] M.C. Ohmer, R. Pandey *MRS Bull.* 1998, *23*, 16.

[313] G.C. Catella, D. Burlage *MRS Bull.* **1998**, *23*, 28.

[314] S.J. Pearton, C.R. Abernathy, D.P. Norton, A.F. Hebard, Y.D. Park, L.A. Boatner, J.D. Budai *Mater. Sci. Eng.* **2003**, *40*, 137.

[315] Pauling, L. *J. Am. Chem. Soc.* **1929**, *51*, 1010.

[316] Parthé, E.; Yvon, K.; Dietch, R.H. *Acta Crystallogr. B.* **1969**, *25*, 1164.

[317] Schleich, D.M.; Wold, A. *Mater. Res. Bull.* **1977**, *12*, 111.

[318] Quintero, M.; Barreto, A.; Grima, P.; Tovar, R.; Quintero, E.; Porras, G.S.; Ruiz, J.; Woolley, J.C.; Lamarche, G.; Lamarche, A.M. *Mater. Res. Bull.* **1999**, *34*, 2263.

[319] Jackson, A.G.; Ohmer, M.C.; LeClair, S.R. *Infrared Phys. Technol.* **1997**, *38*, 233.

[320] P. Kubelka, F. Munk *Z. Tech. Phys.* **1931**, *12*, 593.

[321] S.K. Kurtz, T.T. Perry *J. Appl. Phys.* **1968**, *39*, 3798.

[322] K.M. Ok, N.S. Bhuvanesh, P.S. Halasyamani *Inorg. Chem.* **2001**, *40*, 1978.

[323] Cell_Now is a program for unit cell determination, George M. Sheldrick, Göttingen University, http://shelx.uni-ac.gwdg.de/SHELX/.

[324] SAINT and SADABS are part of the Apex 2 software package v2.1-4 Program for Data Collection and Reduction on Bruker AXS CCD Area Detector Systems, Bruker Analytical X-ray Systems, Inc., Madison, WI, 2005.

[325] G.M. Sheldrick *Acta Cryst. A* **2008**, *A64*, 112.

[326] J.P. Perdew, Y. Wang *Phys. Rev. B.* **1992**, *B45*, 13244.

[327] E. Parthé, K. Yvon, R.H. Deitch *Acta. Crystallogr.* **1969**, *B25*, 1164.

[328] W. Schäfer, R. Nitsche *Mater. Res. Bull.* **1974**, 645.

[329] J.W. Lekse, B.M. Leverett, C.H. Lake, J.A. Aitken *J. Solid State Chem.* **2008**, *181*, 3217.

[330] L.O. Brockway *Z. Kristallogr. Krist.* **1934**, *89*, 434.

[331] R. Kanno, T. Hata, Y. Kawamoto, M. Irie *Solid State Ionics* **2000**, *130*, 97.

[332] Lekse, J.W.; Leverett, B.M.; Lake, C.H.; Aitken, J.A. *J. Solid State Chem.* **2008**, *181*, 3217.

[333] J.W. Lekse, M.A. Moreau, K.L. McNerny, J. Yeon, P.S. Halasyamani, J.A. Aitken *Inorg. Chem.* **2009**, *48*, 7516,

[334] M.C. Ohmer, R. Pandey *MRS Bull,* **1998**, *23*, 16.

[335] L. Pauling *The Nature of the Chemical Bond, Third Edition*, Cornell University Press; Ithaca, 1960.

[336] A.L. Allred *J. Inorg. Nucl. Chem.* **1961**, *17*, 215.

[337] G.C. Lisensky, R. Penn, M.J. Geselbracht, A.B. Ellis *J. Chem. Ed.* **1992**, *69*, 151.

[338] A.B. Ellis, M.J. Geselbracht, B.J. Johnson, G.C. Lisensky, W.R. Robinson *Teaching General Chemistry: A Materials Science Companion* American Chemical Society; Washington, D.C. 1993.

[339] Materials Studio v4.4.0.0 is a registered trademark of Accelrys Software, Inc.

[340] P. Blaha, K. Schwartz, G. Madsen, D. Kvasnicka, J. Luitz *WIEN2K*, An Augmented Plane Wave + Local Orbitals Program for Calculating Crystal Properties (Karlheinz Schwartz, Techn. Universität Wien, Austria) 2001 ISBN 3-9501031-1-2.

Appendix I Ag_2MnSnS_4

AI.1 Introduction

In addition to quaternary lithium containing diamond-like semiconductors (DLS), we also began to explore silver-containing compounds with Ag_2MnSnS_4. This compound is predicted to form based on the selection criteria for DLS and was chosen because 1) it has not been previously reported, 2) it incorporates Mn and 3) it could potentially display interesting magnetic properties. Ideally, the compound would be a ferromagnetic semiconductor of potential interest for spintronic applications; however, the effect of "replacement" of lithium with silver is also of interest in order to study the trends in physicochemical properties such as second harmonic generation.

AI.2 Experimental

AI.2.1 Reagents

Chemicals in this work used as obtained: 1) silver powder, -325 mesh, 99.99%, Cerac; 2) tin powder, -100 mesh, 99.999%, Strem; and 3) sulfur powder, sublimed, 99.5%, Fisher. Manganese, 0.8-3mm, 99.99%, Cerac, was ground using an impact mortar and pestle prior to addition to the reaction mixture.

AI.2.2 Synthetic Procedure

AI.2.2.1 Ag_2MnSnS_4 powder

Stoichiometric amounts of Ag:Mn:Sn:S to prepare 2 mmol of Ag_2MnSnS_4 was prepared by weighing and grinding, using an agate mortar and pestle, in an argon-filled glovebox. The ground mixture was placed into 9 mm o.d. fused-silica tube. The tube was sealed under a vacuum of approximately 10^{-3} mbar, heated to 800 °C in 12 h and then held at 800 °C for 72 h. The sample was then slowly cooled to 450 °C in 100 h and then cooled to room temperature in 6 h. The tube was opened under ambient conditions and the contents, a grey mass with hints of red, were examined using a light microscope. Grinding of the sample produced a dark red, microcrystalline powder that was used for property measurements.

AI.2.2.2 Ag_2MnSnS_4 crystals

Stoichiometric amounts of Ag, Mn, Sn and S to prepare 1 mmol of Ag_2MnSnS_4 were weighed and ground in an argon-filled glovebox. The ground mixture was placed into a 9 mm o.d. fused-silica tube and sealed under a vacuum of approximately 10^{-3} mbar. The sample was heated to 650 °C in 12 h and then held at 650 °C for 72 h. The sample was slowly cooled to 450 °C in 100 h and then cooled to room temperature in 12 h. The tube was opened under ambient conditions and the contents were examined using a light microscope. Deep red, X-ray-quality single crystals of the product were obtained and used for structure determination.

AI.2.3 Physical Property Measurements

AI.2.3.1 Scanning Electron Microscopy and Energy Dispersive Spectroscopy (EDS)

A CamScan Series 4 scanning electron microscope was used to image samples and a Princeton Gamma Tech detector was used for EDS. The working distance was 35 mm and the accelerating voltage was set to 22.5 kV. Samples were mounted onto double-sided carbon tape, which was adhered to an aluminum specimen holder. EDS data were collected for 60 s. The presence of silver, manganese, tin and sulfur in each of the dark red crystals was confirmed and elemental mapping revealed that each element was dispersed evenly throughout the crystals.

AI.2.3.2 Differential Thermal Analysis (DTA)

DTA was performed using a Shimadzu DTA-50 thermal analyzer calibrated with a three-point calibration curve using indium, zinc and gold. The reference, Al_2O_3, and sample, of comparable masses, were contained in fused-silica ampoules (carbon coated for the sample) and sealed under a vacuum of ~10^{-3} mbar. The temperature was programmed to increase at a rate of 10 °C/min from 25 °C to 1000 °C. The temperature then decreased to 100 °C at 10 °C/min. To distinguish reversible events from irreversible ones, a second cycle was performed in the same manner.

AI.2.3.3 Diffuse Reflectance UV/Vis/NIR Spectroscopy

Optical diffuse reflectance spectra were obtained using a Cary 5000 UV/Vis/NIR spectrometer. Samples were ground and loaded into a Harrick Praying Mantis diffuse reflectance accessory that uses elliptical mirrors. $BaSO_4$ was used as a 100 % reflectance standard. Scans

were performed from 2500 nm to 200 nm. Wavelength data were converted to electron volts and the percent reflectance data were converted to absorbance units using the Kubelka-Munk equation.[341]

AI.2.3.4 Powder X-Ray Diffraction

Powder diffraction patterns were collected using a Panalytical X'Pert Pro MPD powder X-ray diffractometer. Data were collected from 5 to 80 °2θ with a sampling interval of 0.083556 °. The scan rate used was 0.010577 °/s. Samples were spun during data collection. The instrument was set to an accelerating voltage of 45 kV and a filament current of 40 mA. Copper K_α radiation with a wavelength of 1.541871 Å was used for measurements. Samples were prepared for analysis by spreading powder onto a piece of double-sided tape adhered to a glass slide placed into the aluminum sample holder.

AI.2.3.5 Single Crystal X-Ray Data Collection and Reduction

Single crystals were mounted onto a glass fiber using Krazy® glue. Over a hemisphere of data were collected using 0.3 ° steps in omega and phi on a Bruker SMART Apex 2 diffractometer with a CCD detector at room temperature. Data were collected for 35 s per frame using Mo K_α radiation with a wavelength of 0.71073 Å and a graphite monochrometer. During data collection the instrument was set to 50 kV and 30 mA. The Bruker SAINT[342] program was used for data integration. After integration of the data, there were a total of 6664 reflections collected with 1406 unique. An empirical absorption correction was performed using the SADABS[342] program. The structure solution and full-matrix least-squares refinement on F^2 were performed using SHELXTL-97.[343] Probable space groups based on systematic absences for both

compounds included *P*mmn (centrosymmetric) and *P*mn2$_1$ (noncentrosymmetric). *P*mn2$_1$ was selected, as diamond-like semiconductors should be noncentrosymmetric based upon the four rules for DLS. Important crystallographic data and structure refinement details can be found in Table A.1.

AI.3 Results and Discussion

AI.3.1 Synthesis

A number of attempts were made to synthesize single crystals and a phase-pure powder by stoichiometric combination of elemental starting materials. Initial stoichiometric reactions did not contain X-ray quality single crystals, so chemical vapor transport using iodine was attempted. These reactions yielded crystals, but not of the intended 2:1:1:4 phase. SEM/EDS was used to verify that all four elements were present with a formula of approximately $Ag_{13}Mn_{9.5}Sn_{28.5}S_{48}$. Single crystal diffraction was performed and structure solution was attempted but was unsuccessful.

Additional stoichiometric reactions were then attempted and eventually resulted in single crystals and a nearly phase-pure powder. The first reaction temperature, 500 °C, was chosen based on differential thermal analysis of a stoichiometric mixture of silver, manganese, tin and sulfur. The reaction temperature was lowered in subsequent reactions and the phase purity seemed to decrease with decreasing temperature. Several reactions were then attempted with increasing reaction temperatures; 450 °C, 650 °C, 700 °C and then 800 °C. Single crystals were obtained from the 650 °C reaction, but the 800 °C reaction was found to be the most phase-pure

sample. More promising crystals for X-ray diffraction were to be obtained with a slower cooling rate. Reactions with extremely slow cooling rates could potentially result in a phase-pure powder. Another alternative to prepare a phase-pure sample is to attempt to cycle the reaction through multiple heating and cooling steps. This proved a successful technique to obtain a phase-pure powder of Li_2ZnGeS_4.

AI.3.2 Structure

Ag_2MnSnS_4 adopts a diamond-like structure and was found to crystallize in the orthorhombic space group *P*mn2_1, Figure A.1. This space group has previously been reported for other DLS compounds including Li_2CdGeS_4 and Li_2CdSnS_4.[344] The model refines to $R1_{(all)}$ of 6.28 % indicating that there is a potential problem with this model. One potential problem is that in this model the compound exhibits disorder between one of the silver atoms and the tin atom. This is an indicator of crystal twinning. The twin law still needs to be identified and then applied to the model.

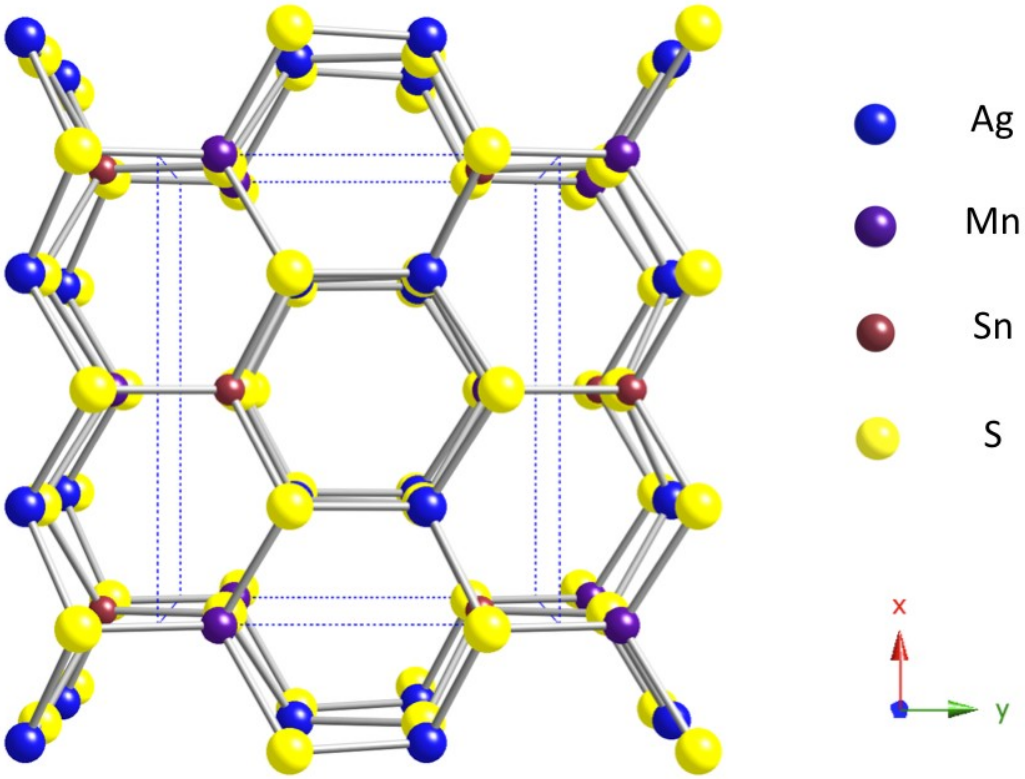

Figure A.1. The structure of Ag_2MnSnS_4 viewed down the *z*-axis.

Powder diffraction was also performed on samples of Ag_2MnSnS_4. The pattern calculated for Ag_2MnSnS_4 based on the single crystal structure corresponds with the experimentally obtained patterns, Figure A.2. This is an indication that the structure solution is close to being correct, with only a minor problem. There also appears to be a small SnS impurity in most samples that precludes performing magnetic measurements on these samples.

Table A.1 Crystallographic data and experimental details for Ag_2MnSnS_4

Empirical Formula	Ag_2MnSnS_4
Formula Weight	517.61
Temperature	296(2) K
Wavelength	0.71073 Å
Space Group	$Pmn2_1$
Unit Cell Dimensions	a = 8.159(1) Å α = 90 °
	b = 6.9654(9) Å β = 90.00(3) °
	c = 6.6511(8) Å γ = 90.00 °
Volume	377.99 (8) $Å^3$
Z, Calculated Density	2, 4.548 Mg/m^3
Absorption Coefficient	10.994 mm^{-1}
F(000)	466
Reflections Collected / Unique	6664 / 1406
Data / Restraints / Parameters	1406 / 1 / 46
Completeness to theta = 32.81	96.6 %
Goodness of Fit	0.988
Final R indices [I>2sigma (I)]	R1 = 0.0592, wR2 = 0.1211
R indices (all data)	R1 = 0.0631, wR2 = 0.1228

Table A.2 Atomic coordinates and equivalent isotropic displacement parameters ($Å^2$ x 10^3) for Ag_2MnSnS_4.

	x	y	z	U(eq)
Ag(1)	1.0000	0.8224(2)	0.4316(5)	19(1)
Ag(2)	0.7490(1)	0.6679(1)	-0.594(1)	26(1)
Sn(1)	0.7490(1)	0.6679(1)	-0.594(1)	26(1)
Mn(1)	1.0000	1.1519(5)	-0.802(9)	35(1)
S(1)	1.0000	0.8123(6)	0.659(6)	18(1)
S(2)	1.0000	1.1541(5)	0.5551(7)	15(1)
S(3)	0.7566(4)	0.6672(6)	0.5638(6)	28(1)

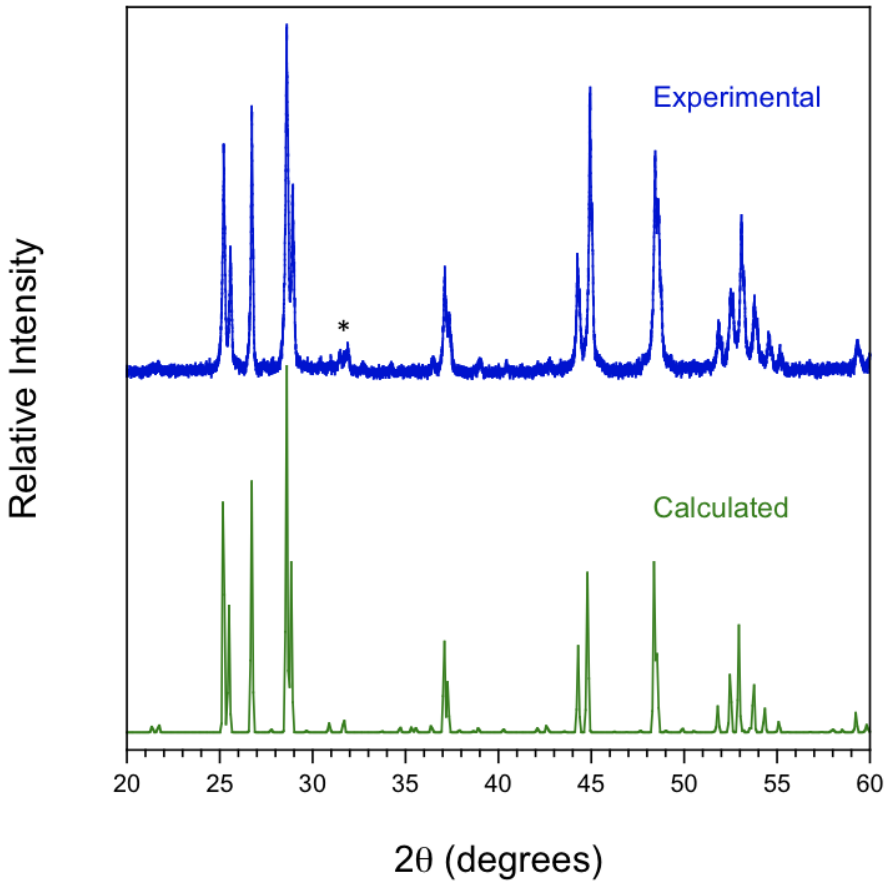

Figure A.2. An experimental X-ray powder diffraction pattern compared to the pattern calculated from our single crystal structure model in *P*mn2$_1$. Peaks denoted by the asterisk are due to the presence of a small amount of the secondary phase SnS.

AI.3.3 Physical Property Measurements

AI.3.3.1 Differential Thermal Analysis

Differential thermal analysis was used to determine the thermal properties of Ag_2MnSnS_4. The sample exhibited two reversible events upon both heating and cooling, endothermic events at 652 °C and 711 °C upon heating and two corresponding exothermic

events at 677 °C and 632 °C upon cooling, Figure A.3. The events at 652 °C and 632 °C are probably due to a phase change, while the events at 711 °C and 677 °C are probably melting and subsequent recrystallization of the sample. The thermal event at 652 °C upon heating is difficult to distinguish in the first cycle, but can be seen upon close examination. There were no noticeable events at 880 °C, the melting point of SnS. This could be because SnS is such a small portion of the sample.

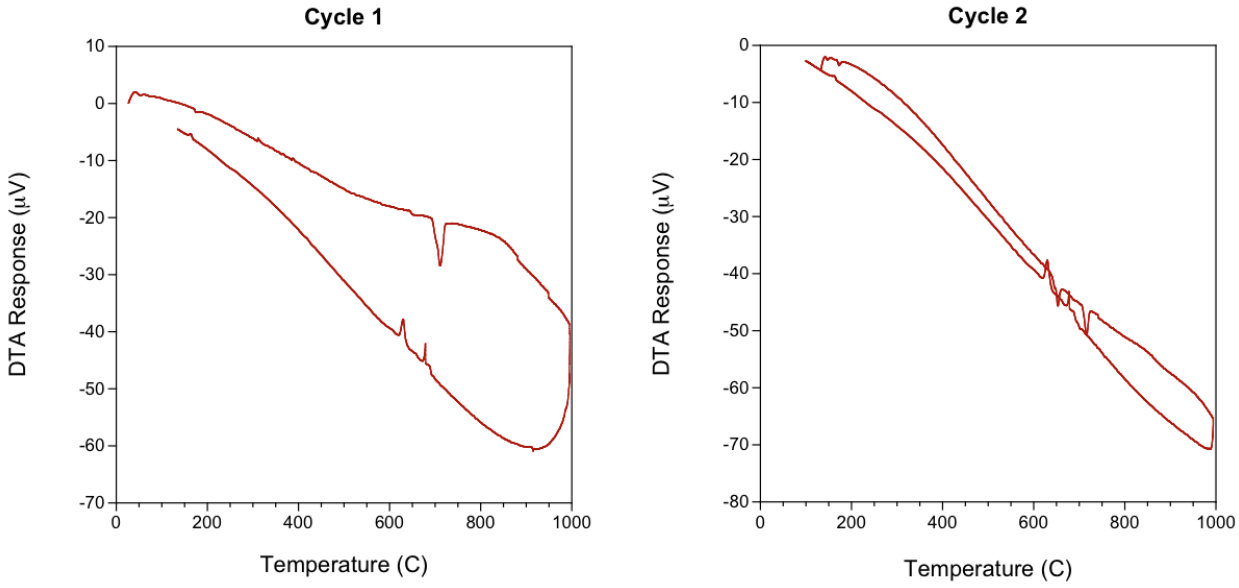

Figure A.3. Differential thermal analysis of a sample of Ag2MnSnS4. There are two reproducible thermal events upon both heating and cooling indicating the possibility that this compound experiences a phase change.

AI.3.3.2 Diffuse Reflectance Spectroscopy

Diffuse reflectance spectroscopy was used to determine that the compound was a semiconductor with a band gap of 1.98 eV, Figure A.4. A second absorption edge can be seen at lower energy. This is most likely due to the presence of SnS, which has a band gap of 1.1 eV.[345] This reinforces the conclusion derived from the powder X-ray diffraction data.

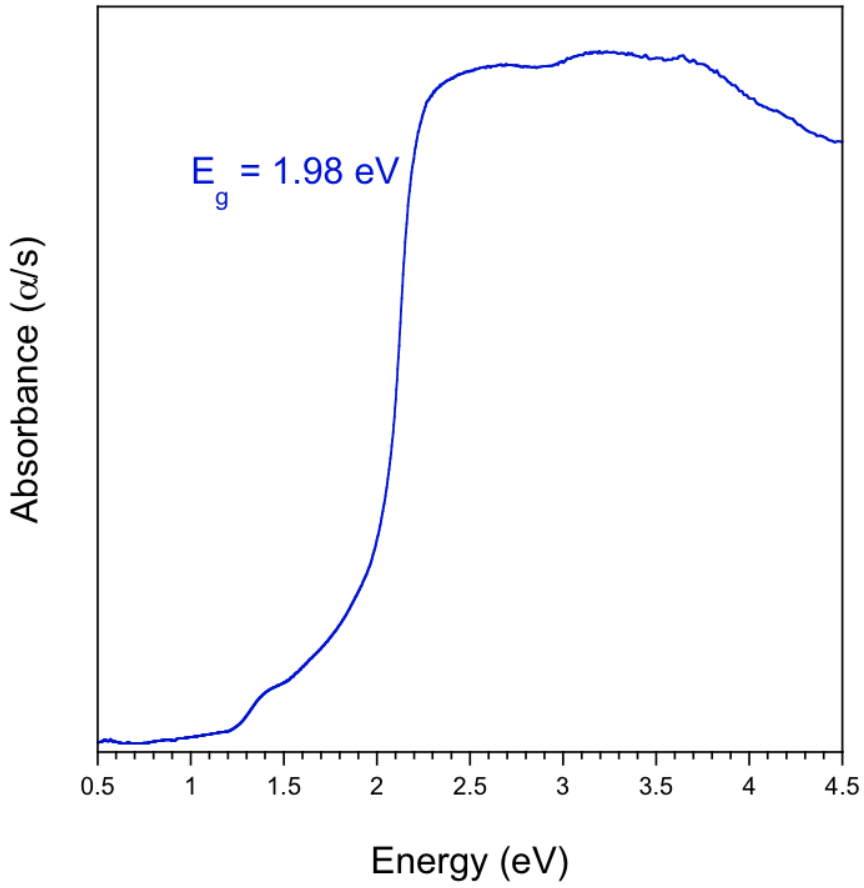

Figure A.4. Diffuse reflectance spectrum, converted to absorbance, of Ag_2MnSnS_4. The compound has a band gap of approximately 1.98 eV.

AI.4 Conclusions and Future Work

The diamond-like semiconductor Ag_2MnSnS_4 was synthesized and a preliminary structure determined for the first time. The structure is suspect, due to the presence of disorder, which should not occur in a true diamond-like semiconductor because it will lead to violations of Pauling's second rule, and needs to be carefully examined. A phase-pure powder needs to be synthesized so that both magnetic and second harmonic generation measurements can be performed. The band gap energy of the compound and the melting point have already been determined to be 1.98 eV and 715 °C, respectively.

AI.5 References

[341] P. Kubelka, F. Munk *Z. Tech. Phys.* **1931**, *12*, 593.

[342] SAINT and SADABS are part of the Apex 2 software package v2.1-4 Program for Data Collection and Reduction on Bruker AXS CCD Area Detector Systems, Bruker Analytical X-ray Systems, Inc., Madison, WI, 2005.

[343] G.M. Sheldrick *Acta Cryst. A* **2008**, *A64*, 112.

[344] J.W. Lekse, M.A. Moreau, K.L. McNerny, J. Yeon, P.S. Halasyamani, J.A. Aitken *Inorg. Chem.* **2009**, *48*, 7516.

[345] A.M. Elkorashy *Chemtronics* **1986**, *1*, 76.

Appendix II Materials Studio Input and Output Files

AII.1 Introduction

A second appendix containing all input and output files from the calculations performed using the DMol3 code in Materials Studio and discussed in Chapter 7. Due to the length of the document, the second appendix can only be found as an electronic download available through ProQuest.